arXiv:cond-mat/0506708v1 [cond-mat.dis-nn] 27 Jun 2005

The Microscopic Quantum Theory of Low Temperature Amorphous Solids

Vassiliy Lubchenko* and Peter G. Wolynes

Department of Chemistry and Biochemistry and Department of Physics, University of California at San Diego, La Jolla, CA 92093-0371

(Dated: December 17, 2004)

The quantum excitations in glasses have long presented a set of puzzles for condensed matter physicists. A common view is that they are largely disordered analogs of elementary excitations in crystals, supplemented by two level systems which are chemically local entities coming from disorder. A radical revision of this picture argues that the excitations in low temperature glasses are deeply connected to the energy landscape of the glass when it vitrifies: the excitations are not low excited states built on a single ground state but locally defined resonances, high in the energy spectrum of a solid. According to a semiclassical analysis, the two level systems involve resonant collective tunneling motions of around two hundred molecular units which are relics of the mosaic of cooperative motions at the glass transition temperature T_g. The density of states of the TLS is determined by T_g and the mosaic's length scale, which is a weak function of the cooling rate. The universality of phonon scattering in insulating glasses is explained. The Boson Peak and the plateau in thermal conductivity, observed at higher temperatures, are also quantitatively understood within the picture as arising from the same cooperative motions, but now accompanied by thermal activation of the mosaic's vibrational modes. The dynamics of some of the local structural transitions have significant quantum corrections to the semiclassical picture. These corrections lead to a deviation of the heat capacity and conductivity from the standard tunneling model results and explain the anomalous time dependence of the heat capacity. Interaction between tunneling centers contributes to the large and negative value of the Grüneisen parameter often observed in glasses.

Contents

I. Introduction 1

II. Overview of the Classical Theory of the Structural Glass Transition 5

III. The Intrinsic Excitations of Amorphous Solids 14
- A. The Origin of the Two Level Systems 14
- B. The Universality of Phonon Scattering 18
- C. Distribution of Barriers and the Time Dependence of the Heat Capacity 22

IV. The Plateau in Thermal Conductivity and the Boson Peak 24
- A. Introduction: Classification of Excitations in Glasses 24
- B. The Multilevel Character of the Entropic Droplet Excitations 25
- C. The Vibrational Spectrum of the Domain Wall Mosaic and the Boson Peak 26
- D. The Density of Scatterers and the Plateau 29
- E. Phonon scattering off frictionless ripplons 29
- F. The effects of friction and dispersion 32
- G. The Relaxational Absorption 34

V. Quantum Effects beyond the strict Semi-Classical Picture 35
- A. Quantum Mixing of a Tunneling Center and the Black-Halperin Paradox 35
- B. Mosaic Stiffening and Temperature Evolution of the Boson Peak 41

VI. The Negative Grüneisen Parameter: an Elastic Casimir Effect? 42

VII. Conclusions 48

Acknowledgments 49

A. Rayleigh Scattering of the Phonons due to the Elastic Component of Ripplon-Phonon Interaction 49

B. Frequency Cutoff in the Interaction Between the Tunneling Centers and the Linear Strain 52

References 53

I. INTRODUCTION

During the past several decades, it has been gradually recognized in the condensed matter and materials science community that amorphous materials, while sharing many characteristics with the more common crystalline solids, represent a distinct solid state of matter. On the one hand, glasses exhibit rigidity and elastic response on humanly relevant time scales, thus qualifying them as solids for many practical purposes. In fact, until the relatively recent advent of systematic studies of the materials' response to mechanical and electromagnetic perturbation, as well as of their detailed microscopic structure, the only commonly known distinct attributes of amorphous substances had been their optical properties and the low magnitude and isotropic character of their thermal expansion. Those properties still undergird the main technological importance of amorphous materials. On the other hand, there are many ways in which glasses

*Current Address: Department of Chemistry, Massachusetts Institute of Technology, Cambridge, MA 02139.

are fundamentally different from crystals. This is most noticeable in their properties at cryogenic temperatures.

We presently know very well that an amorphous solid is in reality a liquid caught *locally* in a small set of metastable free energy minima (Xia and Wolynes, 2000), each of which are separated from the much lower free energy crystalline arrangement by high barriers. Therefore, the glass transition, as manifest in the laboratory, is not strictly speaking a phase transition in the regular thermodynamic sense and is not accompanied by a symmetry change or appearance of a free energy singularity. In contrast, a liquid that was cooled below its melting point fast enough so as to avoid crystallization - i.e. has become supercooled - experiences a crossover to (highly viscous) activated transport. As the temperature is lowered further, the relaxation barriers grow in a very dramatic fashion thus confining the molecules in their metastable arrangements long enough to give the appearance of shear elasticity in the sample on the technologically relevant frequency scales. A quantitative understanding of the physics behind the glass transition has recently been achieved with the random first order transition (RFOT) theory of glasses (Kirkpatrick *et al.*, 1989; Xia and Wolynes, 2000). This theory has provided a microscopic picture of molecular motions in supercooled liquids, such as first principle predictions of the length scales of these motions and the cooperativity lengths and the barrier heights of the activated transport. At any given time, a supercooled liquid is a mosaic of cooperatively rearranging regions, whose size becomes larger as the temperature is lowered. This article describes how the RFOT theory also provides the necessary microscopic input to understand the cryogenic anomalies observed in glasses.

In spite of the absence of periodicity, glasses exhibit, among other things, a specific volume, interatomic distances, coordination number and local elastic modulus comparable to those of crystals. Therefore it has been considered natural to consider amorphous lattices as nearly periodic with the disorder treated as a perturbation, often-times in form of defects, so such a study is not futile. This is indeed a sensible approach, as even the crystals themselves are rarely perfect, and many of their useful mechanical and other properties are determined by the existence and mobility of some sort of defects as well by interaction between those defects. Nevertheless, a number of low temperature phenomena in glasses have persistently evaded a microscopic model-free description along those lines. A more radical revision of the concept of an elementary excitation on top of a unique ground state is necessary (Lubchenko, 2002; Lubchenko and Wolynes, 2001, 2003a).

Let us give a brief historical overview of some of the most outstanding issues in low temperature amorphous state physics. It was already noted in the 1960s that the thermal conductivity of amorphous solids is significantly lower than that of crystals. A low-temperature experimentalist using epoxy in his apparatus knew that its thermal conductivity at liquid helium temperatures went roughly as $\texttt{constant}\times T^2$, where the `constant` was practically the same for other amorphous substances as well (Anderson, 1999). Surprisingly, this had not particularly alarmed anyone, even though one would not *à priori* expect low temperature properties of disordered solids to be different from crystals, as the appropriate thermal phonon length is much larger than the molecular scale which was presumed to characterize the relevant heterogeneity scale. It was not until Zeller and Pohl published their classic paper (Zeller and Pohl, 1971) that it became generally known that both the heat capacity and thermal conductivity of glasses were significantly different from those of crystals, and that these anomalies were correlated. The heat capacity turned out to be approximately linear in temperature and larger than the T^3 phononic contribution up to temperatures ~ 10 K. The challenge to the theorists was soon met by the so called Standard Tunneling Model (STM) (Anderson *et al.*, 1972; Phillips, 1972), in which one assumes that due to a disordered pattern of molecular bonds in glasses, there are a number of defects in the lattice (something like "loose" atoms or "dangling bonds"), which have two alternative positions in space separated by a sufficiently low tunneling barrier. At low temperatures, the dynamics of such a system is described well by a two-level system (TLS) hamiltonian. If one assumes that the spectral density of these TLS's is flat, one recovers the linear heat capacity. One also finds that the inverse mean free path of a thermal phonon due to resonant scattering off the TLS's is equal to $l_{\rm mfp}^{-1} \propto T$, which implies thermal conductivity $\kappa \simeq \frac{1}{3}\sum_\omega C_{\rm ph}(\omega)\, l_{\rm mfp}(\omega)\, c_s \propto T^2$. Here, $C_{\rm ph}(\omega)$ is the heat capacity of a phonon mode of frequency ω and c_s is the speed of sound (one assumes here that heat is carried primarily by phonons, which was experimentally demonstrated explicitly four years later by Zaitlin and Anderson (Zaitlin and Anderson, 1975)). Note that the resonant character of phonon scattering implies that the scattering cross-section of low-frequency phonons would be independent of the scatterer size, but would scale with the phonon wavelength (squared) itself. Therefore no knowledge of scatterer's microscopic details are needed. Rather, only a single coupling parameter is needed to estimate the magnitude of scattering at low temperatures. The STM did prove to be very successful (Phillips, 1981), as it predicted, among other things, nonlinear sound absorption due to the saturation of the resonant absorption and the phonon echo, both of which were later observed (Golding and Graebner, 1976; Hunklinger *et al.*, 1976). In spite of these successes, the microscopic nature of these defects had remained unknown, although there later appeared several indications in the literature that the tunneling centers are not single atom entities but rather involve motions within larger groups of atoms (Guttman and Rahman, 1986; Mon and Ashcroft, 1978). On the experimental front, there had been a growing amount of evidence that the number of these additional excitations and their coupling to the phonons are correlated and also depend on T_g (Raychaudhuri and Pohl,

1981; Reynolds, Jr., 1979, 1980), which culminated in the observation made by Freeman and Anderson (Freeman and Anderson, 1986), that the heat conductivities of all studied insulating glasses, if scaled by elastic constants, fall onto the same line in two regions, connected by a non-universal flat piece corresponding to the so called "plateau". In Fig.1 we show a facsimile of Fig.2 from (Freeman and Anderson, 1986) that demonstrates this heat conductivity universality. The lower tempera-

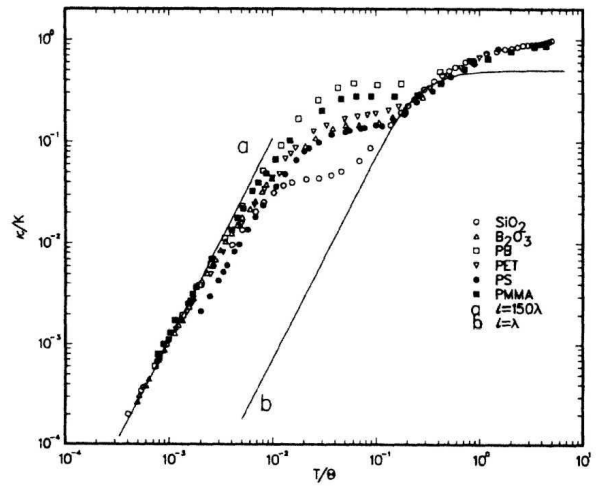


FIG. 1 Scaled thermal conductivity (κ) data for several amorphous materials is shown. The horisontal axis is temperature in units the Debye temperature T_D. The vertical axis scale $K \equiv \frac{k_B^3 T_D^2}{\pi \hbar c_s}$. The value of T_D is somewhat uncertain, but its choice made in (Freeman and Anderson, 1986) is strongly supported by that it yields universality in the phonon localization region. The solid lines are calculated using $\kappa \simeq \frac{1}{3}\sum_\omega C_{\rm ph}(\omega) l_{\rm mfp}(\omega) c_S$ with $l_{\rm mfp}/\lambda = 150$ and $l_{\rm mfp}/\lambda = 1$ respectively (Freeman and Anderson, 1986).

ture straight line corresponds to the value $\simeq 150$ of the ratio of the thermal phonon mean free path $l_{\rm mfp}$ to the thermal Debye wave-length $\lambda \equiv \hbar c_s/k_B T$. This region spans roughly 1.5 decades in temperature between several mK (lowest T accessed so far for the heat conductivity measurements) and to 1-10 K, depending on the substance. The short linear region at higher temperatures (20-60 K) corresponds to $l_{\rm mfp}/\lambda \simeq 1$, which actually implies complete phonon localization (Graebner *et al.*, 1986) according to the heuristic Ioffe-Riegel criterion. This implies, among other things, that one can no longer use kinetic theory expressions for heat transfer at these temperatures, as a diffusive mechanism must prevail [1]. The intermediate region ("plateau") is usually observed between 1 and 30 K, and does not scale with the Debye temperature and speed of sound. The standard tunneling model of non-interacting two-level systems mentioned above is normally applied to the region where $l_{\rm mfp}/\lambda \simeq 150$, that is generically below 1 K. The universality of $l_{\rm mfp}/\lambda$ can be boiled down (Phillips, 1981) to the universality of the following combination of parameters: $\bar{P}\frac{g^2}{\rho c_s^2}$, where $\bar{P}$ is the spectral and spatial density of the TLS's (empirically $\sim 10^{45\pm1} J^{-1} m^{-3}$), g is coupling to the elastic strain on the order of eV, ρ is the mass density (for reference, $\sim \frac{g^2}{\rho c_s^2 r^3}$ would be the interaction strength between such TLS's at distance r from each other). Now, if the defects involved the motion of only a single atom, one would reasonably assume that the value of their spectral density and coupling to the lattice or their combination would be very strongly material dependent. Even though $\bar{P}$ and g^2 vary within almost two orders of magnitude (still surprisingly little), the combination $\bar{P}\frac{g^2}{\rho c_s^2}$ is constant within 50% for different materials (ρ and c_s^2 vary considerably as well). It certainly takes a stretch of imagination to think that this is merely a coincidence, as pointed out in (Leggett, 1991). In 1988, Yu and Leggett proposed (Yu and Leggett, 1988) that the density of states of the TLS might itself be a result of dipole-dipole interactions between some original non-renormalized excitations. In short, this idea is motivated by the observation that for TLS coupled to the phonons with strength g, the coefficient at the dipole-dipole interaction term $g^2/\rho c_s^2$ has dimensions energy times volume. Therefore the interaction induced renormalized density of states $\bar{P}$ has to be the inverse of $g^2/\rho c_s^2$ with a coefficient, hence the universality of $\bar{P} g^2/\rho c_s^2$ for different materials. However, it so far has not proved possible to use their approach to justify the value of that coefficient to yield the experimental $l_{\rm mfp}/\lambda \simeq 150$. This is surprising, since one expects such a simple dimensional argument to be very robust. (Several other studies of the universality (Coppersmith, 1991; Meissner and Spitzmann, 1981) were undertaken at the time, that followed the paper by Freeman and Anderson (Freeman and Anderson, 1986).) There has been subsequent work applying a renormalization group style calculation to a system of interacting TLS (Burin and Kagan, 1996), but it seems from the results that renormalizations are relevant only at ultra-low temperatures (μK's and below) (Neu *et al.*, 1997). In spite of the difficulties in justifying the strong interaction scenario (Caruzzo, 1994; Lubchenko and Wolynes, 2000), the works (Leggett, 1991; Yu and Leggett, 1988) that first challenged the standard TLS paradigm remain the main conceptual motivation behind the present pa-

[1] This idea that the heat was transfered by a random walk was used early on by Einstein (Einstein, 1911) to calculate the thermal conductance of crystals but, of course, he obtained numbers much lower than those measured in the experiment. As we now know, crystals at low enough T support well defined quasiparticles - the phonons - which happen to carry heat at these temperatures. Ironically, Einstein never tried his model on the amorphous solids, where it would be applicable in the $l_{\rm mfp}/\lambda \sim 1$ regime.

per. One stresses however that the idea that the observed coupling constant, which is quite small, could be a result of some original "bare" strong interaction, is consistent with the microscopic theory if we argue it is the molecular interactions behind the glass transition itself which become "renormalized" in a somewhat unexpected fashion. This microscopic theory suggests (Lubchenko and Wolynes, 2001) that the phenomenological two-level systems are discrete energy levels representing resonantly accessible local degrees of freedom that exist in glasses due to the possibility of collective transitions between alternative structural configurations of compact regions encompassing roughly 200 molecular units. The theory of glassy ergodicity breaking shows the spectrum of these excitations is nearly flat and the density of states scales with the inverse glass transition temperature T_g, echoing the excitation spectrum of a random energy model (REM) with that glass transition temperature. Furthermore, the transitions are an alternative mode of motion that must be in equilibrium with phononic excitations at T_g. This equilibrium requirement makes one realize that TLS-phonon coupling g, T_g and the material's elastic constants are intrinsically related. The universality of the $l_{\rm mfp}/\lambda$ ratio is a consequence of this relationship reflecting the non-equilibrium character of the glassy state. The structural transitions, that become tunneling two-level systems at cryogenic temperatures, exist because a glassy sample, when it falls out of equilibrium, resides in a metastable configuration chosen from a very high density of states. The sample is broken up into a mosaic of dynamically cooperative regions. Alternatively speaking, the energy landscape is local in nature; that is rearrangements of compact regions will not change the structural state of the rest of the sample, but only deform the surrounding regions weakly and purely elastically. A (small) fraction of these rearrangements requires overcoming only a very low barrier and can therefore occur even down to sub-Kelvin temperatures. The tunneling occurs by consecutive molecular displacement within the cooperativity length established at T_g. The consecutive motion of atoms is conveniently visualized as a domain wall separating the two alternative local structural states, moving through the local region.

The thermal conductivity plateau has traditionally been considered by most workers a separate issue from the TLS. In addition to the rapidly growing magnitude of phonon scattering at the plateau, an excess of density of states is observed in the form of the so called "bump" in the heat capacity temperature dependence divided by T^3. The plateau is interesting from several perspectives. For one thing, it is non-universal if scaled by the elastic constants (say ω_D and c_s). It is, however, located between two universal regions and it is important to understand which *other* scales in the problem determine its location and shape. The excitations that give rise to the dramatically increased phonon absorption at the corresponding frequencies have been circumstantially associated with the excitations observed as the so called Boson Peak (BP), directly seen in the inelastic X-ray and neutron scattering experiments, also observed in the optical Brillouin and Raman scattering measurements. These experimental developments date well into 90-s and became possible, in the neutron spectroscopy case, due to the improved resolution in the neutrons' velocity detection, combined with the ability to generate higher energy incident beams (Foret *et al.*, 1996). Similarly, meV resolution was needed to utilize the X-ray scattering technics to discern the small inelastic wings on the sides of the strong elastic peak (Benassi *et al.*, 1996). The term "Boson Peak" comes from the fact that its intensity scales roughly according to the Bose-Einstein statistics. The extraction of the density of states from the spectra is unfortunately model dependent, and those models can be roughly divided (Pilla *et al.*, 2000) into the ones where the Boson peak signifies the energy scale on the edge of phonon localization, as promoted in (Foret *et al.*, 1996), and those following the other school of thought which asserts that these modes are propagating even well above the frequency of the BP, as supported by the interpretation in (Pilla *et al.*, 2000). As far as theoretical interpretation is concerned, it is our impression that most of theories of the Boson Peak, existing until recently, have postulated a sort of spatial heterogeneity in an otherwise perfectly elastic medium (see a partial list of references in (Grigera *et al.*, 2001)), with the notable exception of the soft-potential model (SPM) (Buchenau *et al.*, 1992; Karpov *et al.*, 1983). It is, of course, always possible to recover the observed magnitude of the heat capacity excess at the BP temperatures by a particular choice of parameters. While a contribution of the lattice disorder to the density of states undoubtedly exists and can be very significant (see, for example, simulations of silica's heat capacity by Horbach at el. (Horbach *et al.*, 1999)), we must note that if amorphous lattices were purely harmonic, the phonon absorption at the BP frequencies would be of the Rayleigh type and should be significantly lower than observed in the experiment (Anderson, 1981; Joshi, 1979). There must be internal resonances present in the bulk, that scatter phonons inelastically. Though phenomenologically introduced, this feature is present, for example, in the soft-potential model. An analysis of the higher temperature behavior of the tunneling transitions that give rise to the TLS at subKelvin energies was provided in the RFOT approach in (Lubchenko and Wolynes, 2003a). When these transitions occur at high enough temperature, the domain wall separating the two alternative states can have its surface vibrations thermally excited. The large degeneracy of these vibrational states, characteristic of a two dimensional membrane, that accompany the underlying structural transition, is sufficient to account for the enhancement of phonon scattering at the plateau, as compared to the TLS regime. Finally, the superposition of the domain wall vibrations on the underlying tunneling transition leads to an excess of density of states that reproduces well the bump in the heat capacity (these com-

pound excitations we call "ripplons"). We therefore arrive at a unified physical picture that allows a unified quantitative explanation of previously seemingly unrelated mysteries in the TLS regime and at the higher, plateau energies.

The paper is organized as follows: the first section outlines the basics of the RFOT theory and then proceeds in applying that theory to understanding the origin of the tunneling centers in amorphous solids. The spectrum of the two-level systems, their coupling to the phonons and the origin of the universality of phonon scattering are then discussed. Additionally, we show how details of the derived TLS' tunneling amplitude distribution lead to a deviation of T dependence of the heat capacity from a strict linear form. The second section explains how the high energy vibrational excitations (ripplons) of the tunneling interfaces gives rise to an excess of states which exhibits itself as the heat capacity bump and yields the rapidly rising phonon scattering at these higher energies. A short discussion of the *relaxational* absorption from these excitations is given and its frequency dependent part is derived. The contents of these first two sections are, for the most part, a detailed account of the calculations underlying two earlier brief letters (Lubchenko and Wolynes, 2001, 2003a) that have reported our explanation of the low temperature anomalies in glasses within a semiclassical approach. The third and fourth chapters are comprised of new results. There, we establish that, while not altering the main conclusions of the semiclassical picture, a purely quantum phenomenon of level mixing and repulsion has an observable effect on the density of states of the tunneling centers at low T. Finally, the interaction between tunneling centers, mediated by phonons, is estimated and this is argued to make a significant contribution to the negative thermal expansivity (and thus a negative Grüneisen parameter) observed in many amorphous materials.

II. OVERVIEW OF THE CLASSICAL THEORY OF THE STRUCTURAL GLASS TRANSITION

From a physicist's perspective, a theory of the glass transition describes what happens to a liquid when it is cooled down sufficiently but is not observed to crystallize. To a mathematician, this is a generalized problem of packing compact interacting objects of comparable size given a specific constraint on the density distribution (it is not periodic) and total energy of the system. A nearly complete conceptual, microscopic picture of the amorphous state has emerged in the course of the two last decades (Stoessel and Wolynes, 1984) (Singh *et al.*, 1985) (Kirkpatrick and Wolynes, 1987a,b) (Kirkpatrick and Thirumalai, 1987a,b; Kirkpatrick *et al.*, 1989) (Xia and Wolynes, 2000, 2001a,b) (Lubchenko and Wolynes, 2001, 2003a,b, 2004). This framework has lead to a unified, quantitative understanding of many seemingly unrelated phenomena in supercooled liquids above and below the glass transition. The glasses we consider form at temperatures where quantum effects are small so classical statistical mechanics is used. We review such a classical glass transition in what follows.

First, we make several comments on the phenomenology of supercooled liquids. Strictly speaking, these are nonequilibrium systems: When cooled sufficiently slowly, most simple liquids will crystallize at a temperature just below the melting temperature T_m. Randomly atactic polymers become glassy but presumably never crystallize. The melting point is defined as the temperature at which the liquid and crystal free energies are equal. Cooling the liquid at least a bit below T_m is necessary to create a free energy driving force so as to make the nucleation barrier finite and to allow the system to equilibrate. The crystal, once formed is different from the liquid in several ways, e.g. it scatters X-rays at precise angles and it is anisotropic. Crucially for us, a crystal supports transverse sound waves, at *all* frequencies (including $\omega = 0$, thence the crystal retains its shape). In contrast, the supercooled liquid is a finite lifetime state since crystallization will eventually occur by nucleation. However, the growth of crystalline nuclei, inside the liquid, is subject to the slowing of all motions in liquids. Owing to this dramatic slowing of liquid motions upon lowering the temperature, one can supercool the liquid substantially below its melting point, which is the key to forming glasses. The extra nucleation barrier ensures there is adequate time to study the properties of the supecooled noncrystalline state. Local structures in supecooled liquids persist for some time, call it $1/\omega_c$. This time is longer than the time it takes to establish a Maxwell distribution of velocity, which is at most a few vibrational periods. Such an amorphous system will support transverse waves at frequencies $\omega > \omega_c$, just as a crystal would, but will in contrast exhibit a liquid like, equilibrium response to time dependent perturbations at frequencies $\omega < \omega_c$. As we have said, ω_c drops rapidly upon cooling. If one is intent on observing equilibrium response at *some* frequency range, one must prepare the sample by cooling it more slowly than ω_c. Conversely, for any given cooling rate, no matter how slow, the liquid will fall out of equilibrium on *all* time scales and the sample will appear to be mechanically solid. We say the liquid has undergone the glass transition. (The corresponding ω_c usually ranges between 10^2 and 10^5 sec, depending on the experimenter's patience.) The liquid just below the glass transition temperature T_g is only subtly different from the liquid just above T_g. Structurally, first of all, the two are nearly identical. Even dynamically, both can flow, although the T-dependences of the corresponding transport coefficients are distinct in the two forms of the "equilibrium" supercooled liquid and the nonequilibrium glassy state (Lubchenko and Wolynes, 2004). The residual dynamics below T_g is referred to as "aging". Aging is at least as slow as the motions just above T_g, but can be much slower when the sample is studied well below

T_g. This requires a greater amount of the experimenter's patience in studying system properties than even needed for sample preparation. Finally, when the sample falls out of equilibrium at T_g, a jump in the heat capacity is measured by differential calorimetry, thus resembling, crudely, a phase transition.

The dramatic slowing down of molecular motions is explicitly seen in a vast area of different probes of liquid local structures. Slow motion is evident in viscosity, dielectric relaxation, frequency dependent ionic conductance, as well as in the speed of crystallization itself. In all cases, the temperature dependence of the generic relaxation time obeys to a reasonable, but not perfect approximation the empirical Vogel-Fulcher law:

$$\tau_{\rm rlxn} \propto e^{DT_0/(T-T_0)} \tag{1}$$

For a review, see (Angell *et al.*, 2000; Böhmer *et al.*, 1993). A specific example of a $\tau(T)$ dependence is shown in the l.h.s. panel of Fig.7. In the expression above, T_0 is a material dependent temperature at which the relaxation times would presumably diverge, if the experimenter had the patience to equilibrate the liquid at the corresponding temperatures. Needless to say, measurements of equilibrium dynamics near T_0 are essentially nonexistent. The coefficient D is often called "fragility", with larger values of D corresponding to "stronger" substances, while smaller values are associated with "fragile" liquids. This terminology apparently refers to the degree of covalent networking in the material (Angell, 1985), a qualitative trend later rationalized by a density-functional study of (Hall and Wolynes, 2003). Fragility appears to correlate with the Poisson ratio, at least for non-polymeric glasses (Novikov and Sokolov, 2004). At any rate, the value of coefficient D is directly related to what glassblowers refer to as "short glasses" and "long glasses", (Pfaender, 1996): (molten) glass can be worked or shaped in the range of viscosities $10^4 - 10^9$ Poise. If the corresponding temperature range is short, the glass is called "short", and vice versa for the "long"glass. The former and the latter obviously correspond to a small and large value of the parameter D respectively.

The non-equilibrium character of a supercooled liquid is exhibited in the entropy of the liquid which is considerably larger at T_g than that of the corresponding crystall at this temperature. This additional entropy corresponds to all the molecular translations, that would have otherwise frozen out at crystallization. In crystallization, this would appear as the latent heat of the liquid-to-crystal transition. In a supercooled liquid, the molecular structure is dense enough to define a lattice locally. Vibrations around lattice sites are small. The excess entropy associated with the locations of these lattice sites has traditionally been designated as the "configurational" entropy. This excess entropy, s_c, is temperature dependent. It refers to all possible liquid configurations that could be surveyed by the liquid if we wait long enough for molecular translations to occur. Experimentally, we determine the configurational entropy by relying on the third law of thermodynamics. Using the third law, we know the total entropy of the liquid at T_m by integrating the crystal's heat capacity (over T) and adding the entropy of melting. Now for the supercooled liquid, we integrate the heat capacity difference between the liquid and the crystal. To do this we, of course, assume the vibrational entropies of the ordered and aperiodic lattices are close. The heat capacity measured by differential calorimetry above the glass transition depends on the rate of the configurational and vibrational entropy decrease with temperature right above T_g. Below T_g the structure of the liquid remains the same as of the moment of vitrification, apart from some (normally insignificant) aging. The vibrational entropy decreases as it did above T_g, but there is no component from configurational change. Thus one observes a non-zero heat capacity jump at T_g. Above T_g, the s_c decreases and the density increases with lowering the temperature. This is expected because there are fewer ways to mutually arrange the molecules at higher densities. When extrapolated past T_g, as was done by Simon (Simon, 1937) and notably by Kauzmann in his review (Kauzmann, 1948), the configurational entropy vanishes at a temperature T_K, which is securely above the absolute zero. This suggests that only a non-extensive number of low energy aperiodic, liquid arrangements could be found at T_K and the entropy of the liquid is thus equal to the corresponding crystal (correcting for differences in their vibrational spectrum). This phenomenon is sometimes referred to as the "entropy crisis", which, again, would presumably occur only under completely equilibrium cooling. Such an entropy crisis strictly occurs in several mean-field spin glass models with infinite interactions (Gross *et al.*, 1985; Gross and Mézard, 1984; Kirkpatrick and Wolynes, 1987b). There are many sound arguments suggesting a strict singular vanishing of configurational entropy at T_K is unlikely for real liquids (Eastwood and Wolynes, 2002; Stillinger, 1988). Nevertheless, T_K is a useful fiducial point for the analysis. None of the results of the present theory in the experimentally accessible regime depend on the configurational entropy truly vanishing at any point. As we shall see, the configurational entropy is macroscopic but decreases with temperature. s_c is typically $\sim .8k_B$ per movable unit at the conventional glass transition temperature corresponding to cooling rate of inverse hour and decreases at a rate proportional to $\Delta c_p/T_g$. For simplicity, we will assume s_c extrapolates so as to scale linearly with the proximity to the entropy crisis (see (Richert and Angell, 1998)): $s_c = \Delta c_p(T - T_K)/T_K$.

Before our formal discussion, let us make several qualitative statements about molecular transport above T_g. The motions of a supercooled liquid are much slower than the local vibrations. The potential felt by an individual molecule comforms to a local "cage". This local "cage" is formed by the neighboring molecules, of course. In order to translate irreversibly a given molecule, as opposed to vibrating about the current position, the cage must be destroyed. In other words, a number of sur-

rounding molecues must be translated as well. Upon lowering the temperature, the density increases and s_c decreases, therefore fewer alternative states are available to any given group of molecules. Thus it is clear that conforming the liquid to an arbitrary translation of a given molecular unit will require readjusting the positions of more and more surrounding molecules at the same time. This leads to a larger cooperative region size, leading in turn to higher barriers for relaxation processes and higher viscosity. At a crude level, this picture underlies the arguments from (Adam and Gibbs, 1965), but those arguments fail to relate the size of the moving regions to the energy landscape itself. In contrast, the Random First Order Transition (RFOT) theory (Kirkpatrick *et al.*, 1989; Xia and Wolynes, 2000) explicitly shows how these reconfigurational motions occur and thus establishes intrinsic connection between the kinetic properties and the thermodynamics of supercooled liquids. Our account is based on (Lubchenko and Wolynes, 2004) which also discusses the intrinsic connection between cooperative, activated motions in the supercooled liquid both above and the classical aging dynamics below the glass transition. These arguments also pave the way for understanding the quantum dynamics at cryogenic temperatures.

The main prerequisite of the RFOT theory is the existence of time scale separation between vibrational thermalization and equilibrating structural degrees of freedom that involve crossing saddle points on the free energy surface. This only occurs below a crossover temperature T_A which is predicted by the theory itself. The existence of local trapping in cages is well established by experiment: there is a long plateau in the time dependent structure factor as measured by the inelastic neutron scattering (Mezei, 1991). In RFOT, such trapping was first established theoretically using a density functional theory (DFT) in (Singh *et al.*, 1985): This paper shows there are aperiodic free energy minima by computing the free energy of an aperiodic variational density distribution function: $\rho(\mathbf{r}) \equiv \rho(\mathbf{r}, \{\mathbf{r}_i\}) = \sum_i \left(\frac{\alpha}{\pi}\right)^{3/2} e^{-\alpha(\mathbf{r}-\mathbf{r}_i)^2}$. The set of coordinates $\{\mathbf{r}_i\}$ denotes a particular aperiodic lattice. The typical lattice spacing is a. A zero value for the parameter α would correspond to a completely delocalized, uniform liquid state, such as just below the liquid-vapor transition. $\alpha \to \infty$ would imply freezing into an infinitely rigid lattice. α can also be interpreted as the spring constant of an equivalent Einstein oscillator forcing each molecule to remain near its proper location in the aperiodic lattice. $F(\alpha)$ develops a metastable minimum, at non-zero $\alpha = \alpha_0 \neq 0$, only below some temperature T_A. This minimum has higher free energy than than the lowest minimum at $\alpha = 0$ (see Fig.2). In the mean field limit, the appearance of such minimum would lead a lattice stiffness and would represent a state with a divergent viscosity. This localization transition and the viscosity catastrophe of mode-coupling theories are essentially identical as was established in (Kirkpatrick and Wolynes, 1987a). A single such high lying free energy minimum would be thermodynamically irrelevant, but one must recall that this $F(\alpha)$ is computed for a *single*, particular aperiodic lattice, which is actually only one of many possibilities. Taking into acount the thermodynamically large number of alternative aperiodic packings increases the entropy of the (set of) localized, aperiodic state(s) and thus lowers the metastable free energy minima just the right amount to make them competitive with the mean-field uniform, delocalized state. The correspondence between the free energy difference in mean field theory and the configurational entropy was rigorously shown for the Potts Glass by (Kirkpatrick and Wolynes, 1987b) who argued such systems have similar symmetry properties to structural glasses. For structural glasses this correspondnce may also be shown more formally using a replica formalism (Mézard and Parisi, 1999). The localization transition at T_A is accompanied by a discontinuous change in the order parameter α. This is why the transition is called "Random First Order". Although there is a discontinuity in α, the actual structure in which the system freezes is chosen at random out of a multitude of possibilities (given by the configurational entropy) At the same time, such an ordered phase will persist only for finite times, therefore this is a true transition only for high-frequency motions, comparable at first to the vibrational time scale. This transition at T_A only signifies a soft cross-over, as far as the *whole* dynamical range is concerned. We emphasize, there are many different "phases" below T_A, all of which are random packings. The number of random packings, thermally available to a region of size N, $e^{s_c N}$, decreases *gradually* with temperature. (This corresponds to gradual freezing out the translational degrees of freedom with lowering the temperature, as signified by the decreasing ω_c.) Because the decrease is gradual, the *random* first order transition does

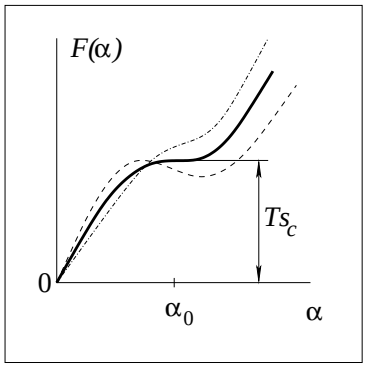


FIG. 2 This is a schematic of the free energy density of an aperiodic lattice as a function of the effective Einstein oscillator force constant α (α is also an inverse square of the localization length used as input in the density functional of the liquid. Specifically, the curves shown characterize the system near the dynamical transition at T_A, when a secondary, metastable minimum in $f(\alpha)$ begins to appear as the temperature is lowered. This figure is taken from (Lubchenko and Wolynes, 2003b).

not exhibit a latent heat. In a finite range system, different minima can interconnect by barrier crossing. (Such barriers would be infinite in mean field.) Even though the transition at T_A is a crossover, the temperature T_A itself is a useful parameter characterizing material properties.

The resulting time scale separation at and below T_A has two important consequences. First, one may perform canonical averaging over the vibrations within a particular structural state. This gives a free energy of a particular structural state: $\Phi = E - TS_{\rm vibr}$, where $S_{\rm vibr}$ is the vibrational entropy. Note the vibrations are not necessarily harmonic. To define Φ, all that matters is that the local vibrations equilibrate much faster than the structural degrees of freedom. As a consequence, Φ can be termed the bulk, *microcanonical* energy of a given *structural* state. To any value of this energy one may associate a bulk, microcanonical *entropy* $S_c(\Phi)$ counting states with similar contributions from energy and vibrational entropy; both Φ and $S_c(\Phi)$ scale linearly with the size of the system. One may thus to work with morphologically distinct, globally defined aperiodic phases without actually specifying their precise molecular constitution, so long as we know their spectrum, i.e. their number as a function of the microcanonical free energy. These statistics are directly measurable by calorimetry just as in our discussion of the Kauzmann paradox.

Having established the transitory existence of a global aperiodic structure, we may next enquire into how molecular motions allow the system to escape such a phase [2]. This occurs by replacing locally one part of the aperiodic packing by a different local packing. This will be an activated event. The RFOT theory allows one to compute the mean activation barrier and its distribution. Also, the theory determines critical region size and the spatial extent of the excitations corresponding to the cooperative rearrangement. The magnitude of an individual molecular displacement during the transition is determined by α. To estimate the activation free energy, let us make the following construct. Considering a library of possible local aperiodic arrangements at a particular location, as illustrated in Fig.3. This *local* library of states can be constructed based on the existence of the *global* library of states introduced earlier that we described by the energy variable Φ and the corresponding entropy $S_c(\Phi)$ reflecting the spectrum. Clearly, the energy density $\exp[S_c(\Phi)]$ is extremely high and grows rapidly with Φ. We might perform a full survey of local states by mentally carving out a small region of size N, while freezing in place the lattice sites surrounding the region. One can then heat the local region and then allow that region to equilibrate. Unless the new local arrangement is exactly the same as the original one, its energy will likely be significantly

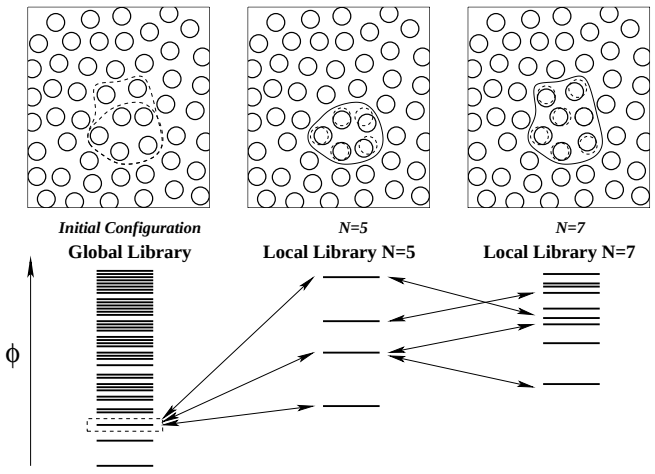


FIG. 3 This figure is taken from (Lubchenko and Wolynes, 2004). In the upper panel on the left a global configuration is shown, chosen out of a global energy landscape. A region of $N = 5$ particles in this configuration is rearranged in the center illustration. The original particle positions are indicated with dashed lines. A larger rearranged region involving $N = 7$ particles is connected dynamically to these states and is shown on the right. In the lower panel, the left most figure shows the huge density of states that is possible initially. The density of states found in the local library originating from a given initial state with 5 particles being allowed to move locally is shown in the second diagram. These energies are generally higher than the original state owing to the mismatch at the borders. The larger density of states where 7 particles are allowed to move is shown in the right most part of this panel. As the library grows in size, the states as a whole are still found at higher energies but the width of the distribution grows. Eventually with growing N, a state within thermal reach of the initial state will be found. At this value of N^* we expect a region to be able to equilibrate.

higher: A local substitution statistically must cost free energy, stemming from a structural mismatch between two randomly chosen aperiodic packings of a given energy Φ. This mismatch energy corresponds to the usual surface energy, such as that between two different crystal forms or at a liquid-crystal interface. The free energy cost of locally replacing the initial phase (labelled as "in") by another phase, call it j, can therefore be written as

$$\phi_j^{lib}(\mathbf{R}) - \phi_{\rm in}^{lib}(\mathbf{R}) = \Phi_j(N) - \Phi_{\rm in}(N) + \Gamma_{j,in}, \qquad (2)$$

where $\Gamma_{j,in}$ is the mismatch energy and $\mathbf{R}$ is the location of the local region. As before, the capital Φ denotes the *bulk* energy, corresponding to a distinct aperiodic packing, with the vibrational entropy already included. To compute the likelihood of such a local rearrangement, substitute for the specific surface energy $\Gamma_{j,in}$ its average value which should scale with size: γN^x. γ depends on the material and on temperature. Naively, the usual surface energy scaling is $N^{(d-1)/d}$, expected in d dimensions. One can argue however that x will actually turn out to equal $1/2$. Such a surface tension renormalization was first conceived by Villain (Villain, 1985), in the context

[2] Of course, the issue of producing the aperiodic state in the *laboratory* would also involve estimating whether corresponding quenching rates can be experimentally achieved.

of the random field Ising model (RFIM). In RFIM, the Ising spins, in addition to their coupling, are subjected to a random static magnetic field obeying certain fluctuation statistics. A flat interface, or domain wall, between spin-up and spin-down domains will distort so as to conform to the local variation of the field. An RG argument incarnating this distortion on a hierarchy of length scales yields a scale dependent renormalization of the surface tension, giving a surface free energy exponent $x = 1/2$ (Villain, 1985). The structure-structure interface in a supercooled liquid resembles the RFIM, owing to the fluctuations of local energies of the various aperiodic packings. The statistics of these fluctuating local energies require that $\delta\Phi(\delta N) \sim \Phi_0\sqrt{\delta N}$, where Φ_0 is δN-independent, echoing the fluctuation statistics of the frozen random field of the RFIM. Thus, as (Kirkpatrick *et al.*, 1989) suggest, the originally thin flat interface will become diffuse yielding $x = 1/2$. In the liquid case, a vivid interpretation of the surface energy renormalization is possible: Since the interface is distorted down to the smallest scale (allowed by the material's discretness), the region occupied by the now diffuse wall is neither of the two original structures it separates. Instead it may be interpreted as accommodating *other* structures. These intermediate packings interpolate structurally two randomly chosen, and thus *à priori* energetically disagreeable packings. In other words, the original thin interface separating two given packings, is "wetted" by other packings thus lowering the overall interface energy. As we shall see, real liquids have only modest size regions of rearrangement, so it is hard to argue about the exact value of the exponent. Nevertheless, we note two felicitous observations: With $x = 1/2$, the usual scaling argument will give precisely a discontinuity in Δc_p at any ideal transition, to be seen at T_K. Also, while the RFIM itself remains the subject of discussion, Villain's argument does give a length scale exponent agreeing with the majority of experiments and numerical studies (Belanger, 1998; Nattermann, 1998).

The role of the interface mismatch energy in the reconfiguration process can be beneficially understood from a statistical point of view, as illustrated in Fig.3. It costs free energy to reconfigure a small number N of molecules because considering a small region severely limits the number of available liquid configurations. The interface energy grows with N, however the available density of states, too, grows with N, both in terms of its absolute value and the distribution's *width*. At some size N^*, that will be computed shortly, all relevant liquid states become available. The rate of escape of a group of N molecules to another structural state can be determined by a canonical type sum accounting for the multiplicity of the final states at energy ϕ_j:

$$\begin{aligned} k &= \tau_{\rm micro}^{-1} \int (d\phi_j^{lib}/c_\phi) e^{S_c(\Phi_j)/k_B} e^{-(\phi_j^{lib}-\phi_{\rm in}^{lib})/k_B T} \\ &\simeq \tau_{\rm micro}^{-1} e^{S_c(\Phi_{\rm eq})/k_B} e^{-(\phi_{\rm eq}-\phi_{\rm in}^{lib})/k_B T}. \end{aligned} \quad (3)$$

In the second step, a steepest descent evaluation is made where $\phi_{\rm eq}$ maximizes the integrand. c_ϕ is some constant of units energy that reflects the local curvatures of the energy landscape. The quantities ϕ_j^{lib} and Φ_j are related through Eq.(2). The time scale $\tau_{\rm micro}$ is the time scale of a molecular scale non-activated process, typically of the order a picosecond. The value $\phi_{\rm eq}$ that maximizes the integrand above will be the internal (equilibrium) free energy characteristic of the system at the ambient (i.e. vibrational) temperature T. In other words, the greatest kinetically accessibility of a state, as embodied in the optimization in Eq.(3), implies that the state will be most frequently visited by the system, therefore it must be the *equilibrium* state. The integration in Eq.(3) is similar to a canonical sum; yet it is different in an important way: The summation in Eq.(3) is far more general than the usual expression for the partition function because when relaxation times are continuously distributed, one must *explicitly* weigh the contribution of a state (to the canonical sum) by its kinetic accessibility. The latter, in general, will depend on the spatial extent of the excitation corresponding to a transition between two states; in this regard, the integration variable ϕ_j is, in a sense, a local *microcanonical* energy. Consequently, the energy $\phi_{\rm eq}$ corresponds to a *canonical* energy. Yet, ϕ_j and $\phi_{\rm eq}$ would strictly become a microcanonical and canonical energy, in their conventional sense, only in the large N limit, when the boundary effects are small. In contrast, the very thermodynamic relevance of the glassy state is due to the locality of the landscape and non-smallness of the surface term. Finally, since the bulk entropy $S_c(\Phi_{\rm eq})$ corresponds to the equilibrium energy, it will be given by the equilibrium configurational entropy $S_c(T)$, measured by calorimetry. Thus given $\phi_{\rm eq}$, one can compute the value of the typical escape rate to a structure where N particles have moved. This gives:

$$k(N) = \tau_{\rm micro}^{-1} \exp\left\{ S_c(N,T) - \frac{\phi_{\rm eq} - \phi_{\rm in}^{lib}}{k_B T} \right\}. \quad (4)$$

The number of particles that must be moved for complete equilibration is determined by the minimum of this expression over N. We thus determine an activation free energy profile

$$\begin{aligned} F^\ddagger(N) &= \phi_{\rm eq} - \phi_{\rm in}^{lib} - T S_c(N,T) \\ &= \Phi_{\rm eq}(N) - \Phi_{\rm in}(N) + \gamma\sqrt{N} - T S_c(N,T), \end{aligned} \quad (5)$$

where we used Eq.(2) in the second equality. The maximum of the $F(N)$ curve defines the bottleneck location. This equation is suitable for finding the rate of structural rearrangement both in the equilibrated supercooled liquid (before it crystallizes!) and in the nonequilibrium glass, which ages below T_g.

Let us first consider equilibrium liquid rearrangements. In this case typically $\Phi_{\rm eq} = \Phi_{\rm in}$, apart from fluctuations. Thus one arrives at the following simple expression,

$$F(N) = \gamma\sqrt{N} - T s_c N, \quad (6)$$

where we have used the thermodynamic scaling of the configurational entropy, $S_c(N) = s_c N$. In the supercooled equilibrated liquid, molecular transport is driven

by only the multiplicity of mutual molecular arrangements. For this reason, the reconfigurations following the activation profile from Eq.(6) have been called "entropic droplets". The graph of the function in Eq.(6) is shown in Fig.4. The transition state configuration will

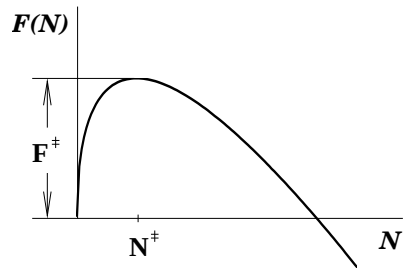


FIG. 4 The droplet growth free energy profile from Eq.(6) is shown.

satisfy $\partial F/\partial N = 0$, corresponding to an unstable saddle point of this free energy. This gives for fixed γ a rearranging region size $N^\ddagger$ that grows as s_c diminishes: $N^\ddagger = (\gamma/2s_cT)^2$. The resulting barrier also scales inversely proportionally to s_c:

$$F^\ddagger = \frac{\gamma^2}{4s_cT}. \tag{7}$$

An inverse scaling of the barrier with the configurational entropy was arrived at by Adam and Gibbs (Adam and Gibbs, 1965) in a different (and inequivalent) way. Notice if γ, as function of temperature, is smooth around T_K and s_c is described by the linear law $s_c \propto (T - T_K)$, the resulting activation barrier is exactly of the Vogel-Fulcher law form (1), which, as we have said, fits data well. Many arguments can lead to increasing relaxation times at low temperatures and with enough adjustable parameters, can fit data. What is different about the RFOT theory is that it establishes an intrinsic link between the rate law and the entropy crisis. In addition, if the entropy of the equilibrated fluid can be estimated, the density functional theory allows the vibrational entropy and thus, by substraction, the configurational entropy to be determined. Therefore T_K can be estimated from the microscopic force laws. This has been done for simple soft spheres by Mezard and Parisi (Mézard and Parisi, 1999), giving reasonable results. Hall and Wolynes (Hall and Wolynes, 2003) have also calculated T_0 and T_A for a simplified model of a network fluid. Their study is consistent with known chemical trends for T_A and T_K as the network becomes more thoroughly crosslinked.

The idea of the configurational entropy itself driving liquid rearrangements still appears to generate some confusion. One possible reason for this is that s_c is totally unambiguously defined only in the mean field limit. In the latter limit, rearrangements are infinite so dynamics driven by s_c do not arise. This is a good place to emphasize that the RFOT theory is not mean-field! Only the local landscape, within an entropic droplet, is actually well described by a mean-field, Random Energy Model like approximation. We took advantage of this in extracting the energy spectrum of low energy structural excitations in a frozen glass (Lubchenko and Wolynes, 2001), as explained in detail in the following Section. We wish to point the reader to the recent elegant treatment of (Bouchaud and Biroli, 2004) re-analyzing the RFOT conclusions for rearrangements in an equilibrated fluid from the viewpoint of Derrida's Random Energy Model (REM) (Derrida, 1981).

Now, calculations of T_A and T_K are plagued by the usual difficulties of liquid state structure theory and the accuracy of approximations some of which are hard to control. Still, even in the face of such approximations, such microscopic considerations lead us to expect a universal value of γ/T_g at T_g as we shall discuss below.

The RFOT theory allows the coefficient γ in the mismatch energy to be estimated from a microscopic argument. It turns out to be proportional to T_K and to depend logarithmically on the inverse square of the so called Lindemann ratio. Early in the 20th century, Lindemann argued that the thermal fluctuations of an atom's position could only be a fraction of the lattice spacing a in a solid, if the packing is to be mechanically stable (Lindemann, 1910). Since the threshold value of the vibrational amplitude of an atom in the lattice is finite, the transition in which the lattice disintegrates must be first order. For crystals, the Lindemann ratio of this threshold displacement d_L to the lattice spacing is about 1/10. For amorphous materials, the d_L/a ratio can be obtained from the plateau in the self correlation functions measured by neutron scattering experiments (Mezei, 1991). Again, this ratio turns out to be approximately one-tenth (universally!). This number is reproduced in several microscopic calculations consistent with the RFOT theory, such as the self-consistent phonon theory and density functional theories (Singh *et al.*, 1985; Stoessel and Wolynes, 1984), and dynamical mode coupling theory (Bengtzelius *et al.*, 1984; Kirkpatrick and Wolynes, 1987a,b; Wolynes, 1992), with modest quantitative variations. The meaning of $\alpha \simeq 0.1$ as a mechanical stability criterion has been also corroborated within the replica formalism (Mézard and Parisi, 1999). In terms of the DFT calculation dicussed earlier, α_L corresponds with the metastable minimum that the free energy $F(\alpha)$ develops below the dynamical transition temperature T_A (see Fig.2). It has a relatively weak temperature dependence. The logarithmic scaling of the surface tension coefficient with the Lindemann length follows from a detailed calculation by (Xia and Wolynes, 2000), but can be rationalized in a simple way: Below T_A, motions span only the length d_L, while in the liquids, they can move a distance a before losing their identity with a neighboring molecule. The entropy of the "caged" fluid is less and thus the free energy cost of confining a molecule within length d_L, as opposed to a, can be assessed by recalling the free energy expression for an ideal monatomic gas: $-f = \frac{3}{2}k_BT \ln\left[\left(\frac{eV}{N}\right)^{2/3}\frac{mT}{2\pi\hbar^2}\right]$, written

deliberately here so as to have a length scale squared in the logarithm.

γ is proportional to T_K and only logarithmically depends on a nearly universal quantity, the Lindemann ratio. If T_g is near T_K, i.e. for slow quenches, γ/T_g is thus nearly material independent and calculable: $\gamma = \frac{3}{2}\sqrt{3\pi}k_B T_g \ln(\alpha_L a^2/\pi e)$. Quantifying the mismatch energy this specifically leads to many predictions about the dynamics near T_g, for a range of substances. First, the coefficient in the Vogel-Fulcher law D is predicted to follow from the measured thermodynamics. Using the γ value above, we find not only the VF dependence of the relaxation times on the temperature, $\propto e^{DT_0/(T-T_0)}$, but also a remarkably simple formula relating D and the heat capacity jump: $D = 32.R/\Delta c_p$ (Xia and Wolynes, 2000). The coefficient 32. is nearly universal and, as we see, follows numerically from the microscopic theory since the universal value of the Lindemann ratio enters only logarithmically in the localization entropy cost. The numerical relation between D and Δc_p from this simple explicit calculation is in rather remarkable agreement with experiment. In Fig.5, we plot the so called fragility index m, as computed from calorimetry and extracted from direct relaxation measurements. m is proportional to the slope of the $\log\tau$ vs. $1/T$ relation at T_g and thus is directly related to D if the VF law is valid. (D values in the literature are obtained from global fits of $\log\tau$ vs. $1/T$ and depend somewhat on the fitting procedure.)

Two other remarkable universalities emerge from the value of γ. First, at a reference laboratory time scale of 1 hr $\sim 10^{17}\tau_0$ we have a universal value of $s_c \simeq 0.8k_B$. This implies $s_c(T_g)/s_c(T_m) \simeq 0.7$, where $s_c(T_m)$ is, of course, also the fusion entropy. This relation is independent of question of what is the moving subunit. The relation holds very well. A second important universal feature emerges from the universal value of γ/T_g: the cooperative size at T_g is nearly universal.

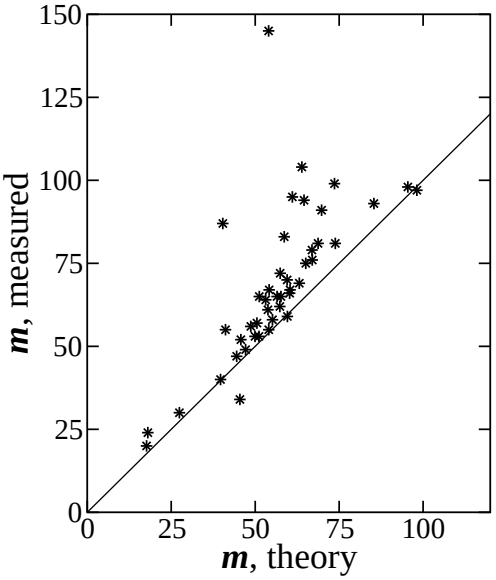


FIG. 5 The horisontal axis shows the value of fragility as computed from the thermodynamics by the RFOT theory, and the vertical axis contains the fragility directly measured in kinetics exoeriments. Here m is the so called fragility index, defined according to $m = T[d\log_{10}\tau(T)/d(1/T)]$. m is somewhat more useful than the fragility D, because deviations from the strict Vogel-Fulcher law, $\tau = \tau_0 e^{DT_K/(T-T_K)}$, are often observed, see text. m essentially gives the apparent activation energy of relaxations at T_g, in units of T_g, it is roughly an inverse of D. This figure is taken from (Stevenson and Wolynes, 2004). In evaluating m theoretically, one needs to know the size of the moving unit, or "bead", in each particular liquid. The latter can be estimated using the entropy loss at crystallization (Lubchenko and Wolynes, 2003b), resulting in $m_{\rm theor} \propto \frac{\Delta c_p(T_g)T_g}{\Delta H_m s_c^2(T_g)} \propto \frac{\Delta c_p(T_g)T_g}{\Delta H_m}$, in view of the near universality of $s_c(T_g)$ (see text).

Let us now consider in greater detail the pattern of cooperative structural rearrangements in a supercooled liquid. These turn out to presage the existence of the residual degrees of freedom in a glass below T_g. Within a period of time shorter than the typical relaxation time τ, the molecular motions within regions of size ξ^3 will be highly correlated and, at the same time, approximately decoupled from the surrounding. That is, the liquid is broken up in to a (flickering) mosaic pattern of cooperative regions. This mosaic structure is directly manifested in the dynamical heterogeneity recently observed in supercooled liquids using single molecule experiments (Russel and Israeloff, 2000), nonlinear relaxation experiments (Silescu, 1999) and non-linear NMR experiments (Tracht *et al.*, 1998). (These experimental tools became available only a decade after the RFOT theory was first formulated.) The size of a typical mosaic cell is found from the thermodynamic condition $F(N^*) = 0$. Unlike the regular nucleation of one distinct phase within another (as in crystal growth in the liquid), by crossing the barrier from Eq.(6) the local region arrives at a statistically similar but an alternative solution of the free energy functional, thus that solution still represents a typical liquid state! An informal analogy here is that distinct low energy dense local liquid packings are like the fingerprints of different individuals - different in detail, yet generically equivalent liquid states. Since we have agreed that $F = 0$ is the liquid *equilibrium* free energy at this temperature (the crystalline state is assumed to be hidden behind a high enough crystal nucleation barrier), the condition $F(N^*) = 0$ specifies the size of region to which an arbitrary liquid configuration is available. Therefore, a region of size N^* is able to reconfigure on the experimental time scale characterized by $F^\ddagger$. In terms of physical length, $F(N^*) = 0$ implies $\xi \equiv N^{*1/3}a = a\left[\frac{8}{3\sqrt{3\pi}}\ln\left(\frac{\tau}{\tau_0}\right)/\ln\left(\frac{\alpha_L a^2}{\pi e}\right)\right]^{2/3} \simeq 5.8\,a$ ($N^* \simeq 190$). The critical radius r^* at T_g is a multiple of ξ. Droplets of size $N > N^*$ are thermodynamically unstable and will break up into smaller droplets, in contrast to what prescribed by $F(N)$, if used naively beyond size N^*. This is because $N = 0$ and $N = N^*$ repre-

sent thermodynamically equivalent states of the liquid in which every packing typical of the temperature T is accessible to the liquid on the experimental time scale, as already mentioned. In view of this "symmetry" between points $N = 0$ and N^*, it may seem somewhat odd that $F(N)$ profile is not symmetric about $N^{\ddagger}$. Droplet size N, as a one dimensional order parameter, is not a complete description. The profile $F(N)$ is a projection onto a single coordinate of a transition that must be described by $e^{s_c N^*}$ order parameters - the effective number of distinct aperiodic packings explored by the liquid. At the point N^*, the free energy functional actually has a minimum as a function of the (multi-component) order parameter. A more detailed discussion of this can be found in Ref.(Lubchenko and Wolynes, 2003b), where we compute the softening of the barrier $F^{\ddagger}$ near T_A due to order parameter magnitude fluctuations that are important near T_A.

We thus see that the length scale of the mosaic and number density of the mosaic domain walls is determined by the competition between the energy cost of a domain wall and the entropic advantage of using the large number of configurations. We emphasize again, the relative domain size ξ/a depends only on the logarithms of the relaxation rate and the Lindemann ratio, nearly universal parameters themselves, and is therefore the same for different substances. This high temperature phenomenon of universality at T_g has direct consequences for the universality of the *ultra-low* temperature glassy anomalies.

We have seen that the cooperative region, which represents a nominal dynamical unit of liquid, is of rather modest size, resulting in observable fluctuation effects. Xia and Wolynes computed the relaxation barrier distribution (Xia and Wolynes, 2001a). The configurational entropy must fluctuate, with the variance given by the usual expression: $\left\langle (\delta S_c)^2 \right\rangle = C_p \propto 1/D$ (Landau and Lifshitz, 1980). The barrier height for a particular region is directly related to the local density of states, and hence to the configurational entropy itself by Eq.(6), $F^{\ddagger} \propto 1/s_c$. As a result, the barrier distribution width must correlate with the fragility. A gaussian approximation leads to a simple formula $\delta F^{\ddagger}/F^{\ddagger} = 1/2\sqrt{D}$ (Xia and Wolynes, 2001a). There are also calculable deviations from gaussianity. The barrier distribution gives rise to non-exponentiality of relaxations. These are well fitted by a *stretched* exponential $e^{-(t/t_0)\beta}$. The measured β correlates with the fragility, in good agreement with the theory, see Fig.6.

We have so far presented a simplified picture of activated relaxation in liquids, which is more accurate at temperatures close to T_K, and thus sufficiently lower than T_A - the temperature at which activated processes emerge. The transition at T_A where metastable minima emerge, along with a mosaic structure with intermediate tense regions, i.e. domain walls, is in many respects similar to a spinodal for an ordinary first order transition, except that the number of alternative phases is very large ($e^{s_c N}$ for a region of size N). The

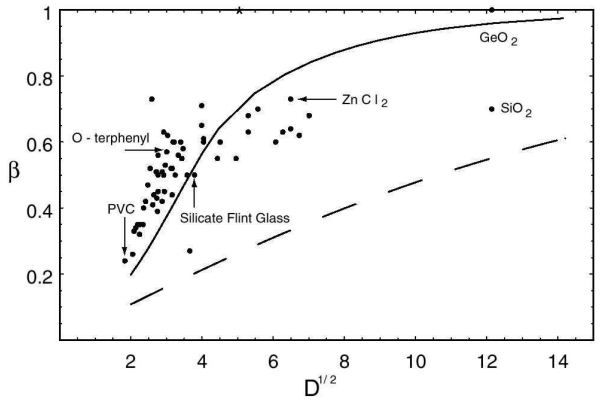


FIG. 6 Shown is the correlation between the liquid's fragility and the exponent β of the stretched exponential relaxations, as predicted by the RFOT theory, superimposed on the measured values in many liquids taken from the compilation of (Böhmer *et al.*, 1993). The dashed line assumed a simple gaussian distribution with the width mentioned in the text. The solid line takes into account the existence of the highest barrier by replacing the barrier distribution to the right of the most probable value by a narrow peak of the same area; the peak is located at that most probable value. This figure is taken from (Xia and Wolynes, 2001a).

proper treatment of this transition must include fluctuations of the order parameter and consequent softening of the droplet surface tension at temperatures close to T_A. As a result of this, closer to T_A the structural relaxation barriers are lowered from what would be expected extrapolating from near T_K - this gives deviations from the VF law. The corresponding length scales $r^{\ddagger}$ and ξ also should be smaller than would be predicted by the "vanilla", T_K-asymptotic version of the RFOT theory. These barrier "softening" effects were quantitatively estimated in (Lubchenko and Wolynes, 2003b). They demonstrated that softening effects do vary between different substances and are more pronounced for fragile liquids. As a result, the value of the configurational entropy at T_g, as predicted by the RFOT theory with softening varies somewhat, within a factor of two or so among different substances. This is in contrast to the universal $s_c(T_g) = .82$ of the vanilla RFOT. Nonetheless, the value of ξ at T_g is much less sensitive and seems to be always within 5% of the simple estimate above. This is shown in the r.h.s. panel of Fig.7. Understanding of the softening effect has allowed us to compute the activation barrier for liquid rearrangements in the full temperature range, including the high T part near T_A, where the barriers become low, and the transport is dominated by activationless, collisional phenomena. Consistent with this predicted softening, the T dependence of relaxation times, $\tau = \tau_{\rm micro} e^{\gamma^2/4T^2 s_c(T)}$, as predicted by the RFOT (see Eq.(6)), fits well the experimental dependences in the low frequency range, but underestimates the viscosity near boiling. After softening is included, one can compute the activation component of the molecular trans-

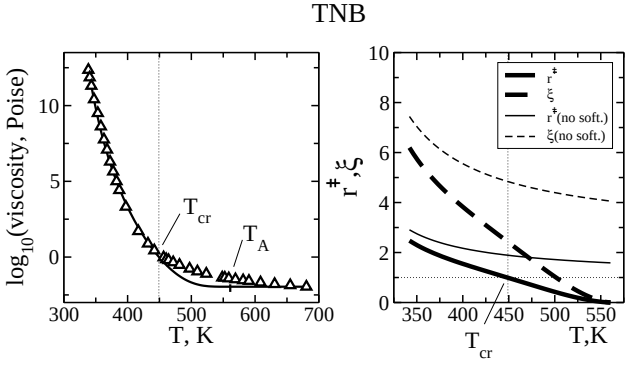


FIG. 7 Experimental data (symbols) for TNB's viscosity (Plazek and Magill, 1968), superimposed on the results of the fitting procedure (line) from (Lubchenko and Wolynes, 2003b) are shown. T_A is shown by a tickmark. The temperature $T_{\rm cr}$ signifies a cross-over from activated to collisional viscosity, dominant at the lower and higher temperatures respectively (see text). The temperature is varied between the boiling point and the glass transition. The r.h.s. pane depicts the temperature dependence of the length scales of cooperative motions in the liquid. The thick solid and dashed lines are $r^{\ddagger}$ and ξ respectively. This figure is taken from (Lubchenko and Wolynes, 2003b).

port, with the temperature T_A as a fitting parameter of the theory (Lubchenko and Wolynes, 2003b). Fitting the viscosity was performed using the following obvious constraints: (a) at low temperatures, the order parameter α fluctuations are negligible, the barriers are fully established and high, and the transport is thus fully activated; (b) near boiling, the barrier vanishes, and the viscosity (known to be around a centipoise for all liquids) gives the value of $\tau_{\rm micro}$. The fit, shown in Fig.7, demonstrates that of the 16-17 orders of the total dynamical range, about three orders, on the low viscosity side, are dominated by collisions. The experimental and activation-only theoretical curve differ from each other above a temperature $T_{\rm cr}$. The three order of magnitude time scale separation, arising *internally* in the theory, is indeed consistent with the prerequisite of the transport being fully activated at $T_{\rm cr}$ and below. The discussion above indicates that samples quenched (sufficiently fast) from a temperature $T > T_{\rm cr}$ may exhibit somewhat distinct detailed molecular motions, also implying quantitative deviations form the RFOT predictions. At any rate, these sample, being caught in a very high energy state, are expected to have small cooperative regions, and also be very brittle and in general mechanically unstable. Such rapid quenches would be extremely difficult to produce in a lab, because $T_{\rm cr}$ corresponds to relaxation times of the order $10^{-8...9}$ sec. On the other hand, it is these ultra fast quenches, that must be currently employed by simulations owing to the limitations of computer power. We speculate that the thin "amorphous" films made by vapor deposition on a cold substrate also may sometimes correspond to such ultra-quenches. While one may expect a number of behaviors in the *bulk* that are qualitatively distinct from what we have discussed here, various *surface* effects are likely to be important too: For one thing, such films are thin, have a large free surface, and strongly interact with the substrate. Further, there is a good reason to believe these films undergo local cracking, and spontaneous crystallization (Perry, 2004).

The present article deals with phenomena in glasses at temperatures much much lower than the temperatures at which the samples form. If a sample, upon vitrification, is cooled significantly below T_g, its lattice remains practically the same as of the moment of freezing. Indeed, the typical reconfiguration barrier is at least $\ln(10^{15}) \sim 35 k_B T_g$, as already mentioned. If, on the other hand, the sample in maintained at some temperature T close enough to T_g, exceedingly slow structural relaxations take place. These attempts of the sample to equilibrate to a structure characteristic of temperature T can be detected. Achieving quantitative accuracy in such experiments is difficult. Consistent with the notion that the lattice, and the barrier distribution, freeze in at the glass transition, the relaxation below T_g, obeys approximately the following temperature dependence:

$$k_{\rm n.e.} = k_0 \exp\left\{ -x_{\rm NMT} \frac{\Delta E^*}{k_B T} - (1 - x_{\rm NMT}) \frac{\Delta E^*}{k_B T_g} \right\}, \tag{8}$$

where E^* is the equilibrated apparent activation energy at T_g and $x_{\rm NMT}$ lies between 0 and 1. This equation is part of the Nayaranaswany-Moynihan-Tool (NMT) empirical description of aging (Moynihan *et al.*, 1976; Narayanaswamy, 1971; Tool, 1946). The difference in the apparent activation energy above and below T_g, as expressed by the parameter $x_{\rm NMT}$, will depend on how fast the barrier itself was changing, with cooling, above T_g, under "equilibrium" cooling conditions. Since the rate of that change depends on the fragility, $m = \frac{1}{T_g} \frac{\partial \log_{10} \tau}{\partial (1/T)}\Big|_{T_g} = \frac{\Delta E^*}{k_B T_g} \log_{10} e$, one expects that $x_{\rm NMT}$ and m are correlated. The RFOT based theory of aging in (Lubchenko and Wolynes, 2004) analyzes structural rearrangements in a non-equibrium glassy sample by means of Eq.(5), where the initial state is not equilibrium, but instead corresponds to the structure frozen-in at T_g. The predicted correlation between $x_{\rm NMT}$ and m is very simple: $m \simeq 19/x_{\rm NMT}$, and is consistent with experiment, see Fig.8.

For some of the comparison of theory and experiment it is necessary to be specific about the molecular length scale a (a very detailed discussion of this quantity can be found in (Lubchenko and Wolynes, 2003b)). The molecular scale denotes the lattice spacing between molecular units (or "beads") that act as idealized spherical objects at the ideal glass transition at T_K. The determination of a, though approximate, is rather unambiguous and can be done using the knowledge of chemistry to give values accurate within 15%. For example, the number of beads in a chain molecule, that interacts with the surrounding only weakly, is always close to the number of monomers. Highly networked substances, such as

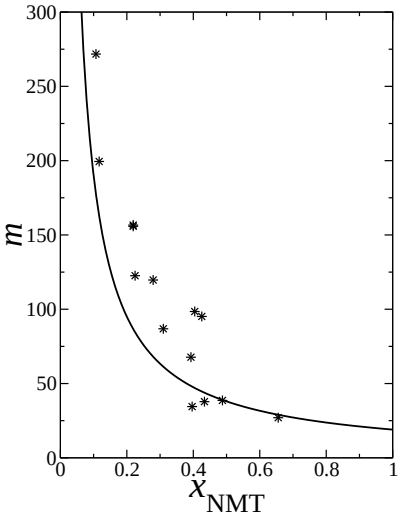


FIG. 8 The fragility parameter m is plotted as a function of the NMT nonlinearity parameter $x_{\rm NMT}$. The curve is predicted by the RFOT theory when the temperature variation of γ_0 is neglected. The data are taken from Ref. (Angell *et al.*, 2000). The disagreement may reflect a breakdown of phenomenology for the history dependence of sample preparation. The more fragile substances consistently lie above the prediction, which has no adjustable parameters. This discrepancy may be due to softening effects.

amorphous silica, present a more difficult case, because it is not clear how covalent the intermolecular bonds in these substances are. Since melting also involves freeing up molecules, with encreased entropy, an independent check on the soundness of a particular bead number assignment can be done by comparing the fusion entropy of the substance (if it exists in crystalline form) with the known entropy of fusion of a hard sphere liquid or Lennard-Jones liquid, equal to $1.16k_B$ and $1.68k_B$ respectively (Hansen and McDonald, 1976). Note, however, the knowledge of the absolute value of a is not required for most of the numerical predictions the theory will make in the quantum regime.

We thus see that the RFOT theory provides a rather complete picture of vitrification and the microscopics of the molecular motions in glasses. The possibility of having a complete chart of allowed degrees of freedom is very important, because it puts strict limitations on the range of *à priori* scenarios of structural excitations that can take place in amorphous lattices. This will be of great help in the assessment of the family of strong interaction hypotheses mentioned in the introduction. To summarize, the present theory should apply to all amorphous materials produced by routine quenching, with quantitative deviations expected when the sample is partially crystalline. The presence and amount of crystallinity can be checked independently by X-ray. It is also likely that other classes of disordered materials, such as disordered crystals, will exhibit many similar traits, but of less universal character.

III. THE INTRINSIC EXCITATIONS OF AMORPHOUS SOLIDS

A. The Origin of the Two Level Systems

In this section we discuss how phenomena near the glass transition temperature, described in the previous subsection, dictate the existence and character of the quantum excitations in glasses at liquid helium temperatures and below. As mentioned earlier, a dynamical pattern of cooperative regions forms in a supercooled liquid below T_A. Each cooperative region is defined by the existence of at least *two* distinct configurations mutually accessible within the time scale τ, which chatacterizes the life-time of the local mosaic pattern. Conversely, a molecular transport event is made possible by rearranging molecules within the cooperative length scale. The mosaic pattern "flickers" on the time scale τ; this process slows down dramatically upon vitrification and, below T_g is referred to as "aging", as it corresponds to (very slow) structural changes. At T_g, the existent pattern of transitions (with distributed energy changes and reconfiguration barriers) freezes in because each cell is now surrounded by a rigid lattice (this is because the rearrangements of the neighboring domains were uncorrelated at T_g). Each region of the material can now explore the phase space as prescribed by the environment at the time of freezing. Below T_g, the mosaic is spatially defined by the molecular motions that were not arrested at T_g, and is thus strictly speaking only *dynamically* detectable. It is true that the weaker walls will probably be the site of (unstable) instantaneous normal modes in the fluid state with imaginary frequencies. This dynamical correlation pattern does not necessarily imply any easily discernible spatial heterogeneity in the atomic locations. In fact, there has been no direct evidence for any static type of heterogeneity of the appropriate scale in glasses so far, which definitely contributes to the (underappreciated) mystery of glasses [3]. But can the *dynamical* heterogeneity be seen directly? We will claim later that this is done for us by thermal phonons: the magnitude of scattering at the plateau can only be explained by presence of *dynamical* heterogeneities. The latter are signified by structural transitions that scatter the phonons *inelastically*. Apart from aging (which we will ignore in the rest of the work), a particular pattern of flipping regions, as frozen-in at T_g, will persist down to the lowest temperature. The apparent size of each cell in this mosaic of flippable regions will depend on the observation time. The longer this time is, the more structural relaxation degrees of freedom (from the high barrier tail of the barrier distribution) one should observe. Even-

[3] We note, however, that there have been instances of mistaking polycrystalline samples for truly amorphous ones.

tually, in fact, the glass should crystallize[4]. In order to estimate the number of tunneling centers that are thermally active at low temperatures we will have to find the size of the regions that allow for a rearrangement accompanied by a small energy change and, at the same time with a low barrier. It may reasonably seem that typically such barriers for multiparticle events would be very high. Nevertheless, the lattice is arrested in a high energy state. We can thus foresee the possibility of stagewise barrier crossing (or tunneling) events, when the width of the barrier for each consecutive atomic movement is only a small fraction of a typical interatomic distance, thus rendering individual atomic movements nearly barrierless. This is as if one could define an instantaneous mode of nearly zero frequency, at each point along the tunneling trajectory. (Yet at no point is the motion harmonic per se!) The presence of such low frequency modes should be expected given the high number of configurational states available to the sample as the moment of freezing, as reflected in the high value of the configurational entropy at T_g. After all, the material is unstable, both globally and locally! (Note, the extent of bond deformation during an individual atomic movement is low - within the Lindemann length - actually affording a few "hard" places along the tunneling trajectory, where the "instantaneous" frequencies are not necessarily low.) One may contrast the situation above with, say, tunneling of a substitutional impurity in a crystal, a system which is indeed near its true ground state. Such tunneling would not contribute to the very low T thermal properties owing to a large barrier. Also, we note that multiparticle barrier crossing events *have* been seen in computer simulations of amorphous systems (Guttman and Rahman, 1986), anticipated theoretically (Heuer and Silbey, 1993; Mon and Ashcroft, 1978), and recently inferred from simulations of dislocation motions in copper (Vegge *et al.*, 2001).

We summarize the discussion so far by noting that the preceding Section has demonstrated that the possible atomic motions in a supercooled liquids are either purely vibrational excitations or structural rearrangements. Any possible motions *below* T_g, in terms of the *classical* basis set must be a subset of the motions above T_g, although the dynamics of these events become quantum-mechanical at low enough temperatures. Even after the system is cooled to an arbitrarily low temperature, it remains essentially in the configuration in which it got stuck at the glass transition. The density of directly accessible states at that high energy configuration is rather high; the *total* density of states is, of course, exponentially larger, but inaccessible on realistic time scale without other regions of the glass rearranging. Since the *typical* rearrangements near T_g span about a length ξ across, we may make the following, preliminarily conclusion: The non-equilibrium character of the glass transition necessarily dictates the existence of intrinsic additional non-elastic degrees of freedom in a glass, tentatively one per region of roughly size ξ, in addition to the usual vibrations of a stable lattice. The universality of ξ, in a sense, is the main clue to the cryogenic universality that is observed. A schematic of a cooperative region is shown in Fig.9.

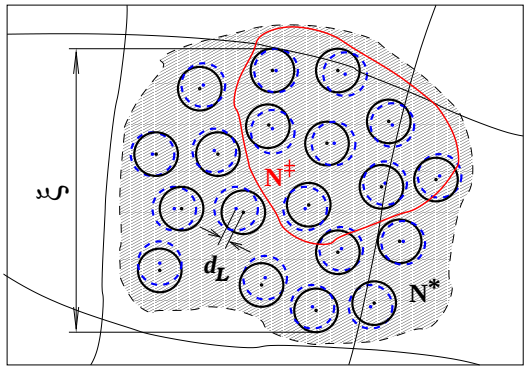


FIG. 9 A schematic of a tunneling center is shown. ξ is its typical size. d_L is a typical displacement of the order of the Lindemann distance. The doubled circles symbolize the atomic positions corresponding to the alternative internal states. The internal contour, encompassing N^* beads, illustrates a transition state size, to be explained later in the text.

Note that showing the existence of low energy tunneling paths is really a mathematically problem of finding hyper-lines, connecting two points of particular latitude on a high-dimensional surface, that meander within a certain latitude range. Visualizing high-dimensional surfaces is prohibitively difficult, while the field of topology, at its present stage of development, is of little help. Yet, a completely general argument is not required here: We only need to consider a very small subset of all surfaces, such that they satisfy the (very severe) constraint on the liquid density distribution above T_g, namely such that conforms to an "equilibrated" liquid at T_g. Because (and with the help) of this constraint, it is possible to put forth a formal argument showing that there are indeed enough low energy structural transitions in a frozen glass: This argument will follow (albeit in the reverse order, in a sense) the argument from the preceding Section, where we found the *typical* trajectory for rearrangement. The key point of the microcanonical-like library construction from Section II is that the distribution width of energies of a region increases with region size. A region is guaranteed to have a state at some low energy, call it $E_{\rm GS}(N)$, as found by integration in Eq.(3). Past a certain critical size, this energy decreases as N grows larger, giving rise to the existence of a resonant state at a large enough N. One must bear in mind, however, that $E_{\rm GS}(N)$ reflects the typical freezing energy. It really gives an *upper bound*

[4] Note that there are, in principle, other ways to move molecules in a glass, in addition to the cooperative rearrangements: for example by creating defects such as vacancies (the corresponding barriers are prohibitively high, of course)

on the lowest energy level. The *actual* lowest energy state fluctuates and always lies *below* $E_{\rm GS}(N)$, although most likely not much below. Here we will look in detail the statistics of these energy states below the typical reconfiguration profile, with the aim to find the probability of a low energy trajectory for reconfiguring a region size N.

We will make several preliminary, quite general notions that will guide us in constructing an adequate approximation for the local statistics of the energy landscape of a frozen lattice. First, we give a general argument of the density of frozen-in excitations, valid, as we will see shortly, in the limit of infinitely slow aging: Since the atomic arrangement does not change upon freezing, the *classical* density of states of a frozen glass is that of the supercooled liquid at T_g. Those states correspond to configurations in which the system could have frozen at T_g and in principle can explore, provided they are thermally accessible and have a sufficiently low barrier separating them from a given configuration. Take a generic liquid state at T_g as the reference state. Then the Boltzmann probability to switch to a conformation higher in energy by amount ϵ is $\propto e^{-\epsilon/T_g}$. That a configuration with that energy was one of the allowed configurations upon freezing means there must have been $n(\epsilon) = \frac{1}{T_g} e^{\epsilon/T_g}$ of them. The factor $1/T_g$ arises because the energy spectrum by construction is continuous, while the actual *local* spectrum is discrete and $\epsilon = 0$ gives the upper bound on the location of the actual ground state. The latter must be somewhere between 0 and $-\infty$: $\int_{-\infty}^{0} d\epsilon\, n(\epsilon) = 1$. This argument, however, is silent as to what the *spatial* characteristics of such excitations or their time scale are.

This inverse "Boltzmann" density of states has been computed explicitly in frustrated mean-field spin systems (Mézard *et al.*, 1985), but is of more general nature. Indeed, such distributions arise *universally* when describing the statistics of the lowest energy state of a wide class of energy distributions (Bouchaud and Mézard, 1997), including the random energy model (Derrida, 1981), that will be used later on. Kinetic considerations did not explicitly enter our heuristic derivation above (or, the mean-field estimates in (Bouchaud and Mézard, 1997; Mézard *et al.*, 1985)). This is directly seen by differentiating $\partial \log n(\epsilon)/\partial\epsilon = 1/T_g$. Clearly, $n(\epsilon)$ is the microcanonical density of states corresponding to the translational (liquid-like) degrees of freedom, and the system is assumed to be completely ergodic within that set of states. This corresponds to an approximation where we consider all degrees of freedom which are faster than a given time scale as *very* fast, and everything slower than that chosen time scale is regarded to be *much* slower than can be detected in the experiment. By using this same density $n(\epsilon)$, as it was at T_g, also at $T < T_g$, we formally express the fact that this subset of the total density of states no longer thermally equilibrates but stays put where it was at T_g - the subsystem of the translational degrees of freedom has undergone an entropy crisis, a glass transition. Everywhere in the discussion above, we have been ignoring the contribution of the purely vibrational excitations to the total free energy. We thus assume that the spectrum of those elastic excitations is independent of precisely where on the glassy landscape the liquid is.

We now give the argument, first laid out in (Lubchenko and Wolynes, 2001), that allows one to estimate the classical density of states and will also simultaneously yield the size of the region where the excitation takes place. First we address the question of how many structural states are available to a compact fragment of lattice of size N, regardless of the barrier that separates those alternative states from the initial ones. This corresponds to the assumption of time scale separation mentioned just above. Within this assumption, the low energy limit of the spectrum must obey e^{E/T_g} so as to give a glass transition at T_g. Next, the spectrum, when integrated, must give $e^{s_c N}$ for the total number of states available to the region. Notice further that we expect the reconfiguring regions to be relatively small. The atomic motions within these small regions are directly coupled and so a mean-field, gaussian density of states, that only describes lowest order fluctuations around the mean, should be accurate enough. An energy density satisfying the requirements above actually corresponds to the well known Random Energy Model (REM) (Derrida, 1981), which also describes the pure state free energy in mean field frustrated spin models:

$$\Omega_N(E) \sim \exp\left\{ s_c N - \frac{[E - (N\Delta\epsilon + \gamma\sqrt{N})]^2}{2\delta E^2 N} \right\}, \quad (9)$$

where δE^2 is the variance to be determined shortly. Here, the factor $e^{s_c N}$ gives the correct total number of states, the term $\gamma\sqrt{N}$ takes into account the interface energy cost of considering distinct atomic arrangements with the region. Note the fluctuations in the surface term are expected but are automatically included in the fluctuation of the microcanonical energy E itself.The term $N\Delta\epsilon$ is a bulk energy necessary to account for the observed excess energy of the frozen structure relative to the energy of the ideal structure at T_K. It is easy to relate to measured quantities: To do this, recall that the system freezes in its "ground state", with energy $E_{\rm GS}$, when its entropy becomes non-extensive:

$$\Omega_N(E_{\rm GS}) = 1. \quad (10)$$

We take the energy E_g of the liquid state at T_g as the *reference* energy. Next note that in the *absence* of the surface energy term $\gamma\sqrt{N}$, the lowest available energy state is that of the liquid at T_K: $(E_K - E_g)/N = -\int_{T_K}^{T_g} dT \Delta c_p(T) \simeq -\Delta c_p(T_g - T_K) \simeq -T_g s_c$. (The two latter equalities are accurate for T_g close to T_K. The corrections would be observable (Lubchenko and Wolynes, 2003b, 2004), but small.) One immediately gets from Eqs.(9) and (10) that $\Delta\epsilon = \sqrt{2\delta E^2 s_c} - T_g s_c$ ($\gamma = 0$ must be used in this estimate, but nowhere else!). Further, using the microcanonical $\partial \ln \Omega_N(E)/\partial E|_{E=E_{\rm GS}} = 1/T_g$ fixes the value of the variance $\delta E^2 = 2T_g^2 s_c$. The resultant density of states is proportional to $e^{(E-E_{\rm GS})/T_g}$ at

T_g, as already shown above by a general argument. Now that we have determined the thermodynamical quantities entering Eq.(9), we can find how the excess energy of an alternate ground state depends on the size N:

$$E_{\rm GS}(N) = \gamma\sqrt{N} - T_g s_c N, \qquad (11)$$

where $E_{\rm GS}$ is defined by Eq.(10). Only low energy excitations will be thermally active at the lowest temperatures. Therefore, we are looking for excitations that are nearly isoenergetic with the reference state. This imposes an additional condition $E_{\rm GS}(N) = 0$ thus prescribing the minimal size N_0 of a region such that has $\Omega_N(0) \geq 1$ for $N \geq N_0$. A region of this size has at least one alternative structural state at the same energy. One obtains from Eq.(11) that $N_0 = (\gamma/T_g s_c)^2 = N^*$, consistent with our previous argument that any region of size N^* has a spectral density of states equal to $\frac{1}{T_g}e^{E/T_g}$. Note that Eq.(11) echoes the free energy profile of droplet growth from Eq.(6), but unlike Eq.(6), it can be used for $N > N^*$ as well. Eq.(11) explicitly shows that a droplet of size larger than N^* has an exponentially increasing number of available configurations corresponding to lattices typical of T_g, consistent with the instability of droplets larger than N^* at temeperatures above T_g mentioned earlier.

The microcanonical argument above is basically a gedanken experiment in which we had the demon-like ability to browse through all possible atomic arrangements, given the total number of allowed states equal to e^{Ns_c}. The total sample is thus comprised of regions of the type considered in the argument (the interface energy has been taken into account by the term $\gamma\sqrt{N}$, this energy may be viewed as the penalty for considering the states of a given compact region as if this region were totally independent from the rest of the sample; c.f. our earlier comments on the locality of the liquid's energy landscape). Therefore, if the rate of conversion between the alternative glassy states can be ignored, the argument immediately yields the density of residual excitations in a frozen glass: $\simeq \frac{1}{N^* a^3 T_g} e^{\epsilon/T_g}$ ($N^* a^3 \equiv \xi^3$, of course). However, even though each of these imaginary regions has an alternative resonant state, there is so far only an undetermined chance to reach it within any particular time. In fact, the typical *classical* barrier for the excitations available to the regions of size $\leq N^* \simeq 190$ is $F^\ddagger \simeq 39 k_B T_g$. Such a barrier would seem to exclude the possibility for tunneling for a typical domain of size N^*. But to account for kinetics issues, we should repeat the argument for the critical size, but also simultaneously include the life-time of each considered configuration as a selection criterion. In other words, one should compute the *combined* distribution of the excitation energies, their spatial extent and the corresponding tunneling amplitudes. Later in the paper, we will discuss one source of correlation between the excitation energy and the tunneling amplitude owing to level repulsion effects. Nonetheless here, we present a simpler argument, given in (Lubchenko and Wolynes, 2001), in which the tunneling rate distribution is assumed to be independent from that of ϵ. Simpler yet, we will look for the density of regions that allow for a rearrangement with a *zero*-height barrier. As vindicated *post factum*, all of these simplifications can lead only to at most a 10% error in the resulting density of states.

Imagine the process of conversion to another state as a step-wise process where the "nucleus" of this new state is increased by adding one atom at a time, as signified by the horisontal axis in Fig.10. Such addition involves moving the atom a distance of the order of the Lindemann distance d_L. It follows then that the path connecting the two states is likely to encounter a high barrier of the order $F^\ddagger$, which effectively disconnects those two states. However, the possible configurations through which one can pass and therefore the barrier heights are *distributed* and there is a chance even for a region of size N^* to have an arbitrarily low barrier. What would such a distribution be? We first have to decide whether the tunneling probability is a sum of contributions of many (interfering) paths or, whether it is dominated by a single path, which has the lowest barrier. The first scenario would be realized in a highly quantum glass, where Debye temperature rivals or exceeds the glass transition temperatures (Schmalian and Wolynes, 2000). Such a highly quantum glass could in fact melt due to quantum fluctuations. In our case, freezing is a completely classical process, which is signified by the fact that the barriers are proportional to a classical energy scale T_g. We now assume more specifically that the contribution of a tunneling path is proportional to $e^{-\pi V^\ddagger/\hbar\omega^\ddagger}$, where $\omega^\ddagger$ is a quantum frequency scale, a multiple of ω_D, and barrier $V^\ddagger$ scales with T_g, as mentioned earlier. This would be an accurate assignment in the case of a parabolic barrier. The form of the tunneling amplitude $e^{-\pi V^\ddagger/\hbar\omega^\ddagger}$ conforms to our expectation that the tunneling trajectory is dominated by a single path with the lowest barrier, as $V^\ddagger$ and $\hbar\omega^\ddagger$ are taken from distributions characterized

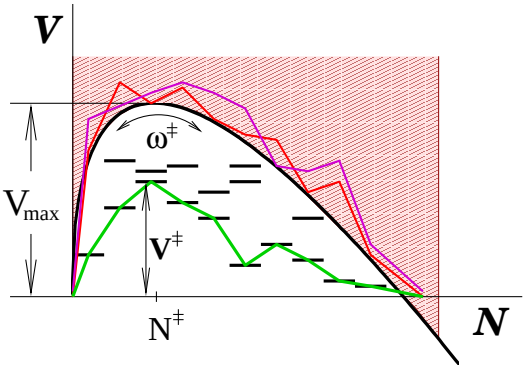


FIG. 10 The black solid line shows the barrier along the most probable path. Thick horizontal lines at low energies and the shaded area at energies above the threshold represent energy levels available at size N. The red and purple line demonstrate generic paths, green line shows the actual (lowest barrier) path, which whould be followed if $\hbar\omega^\ddagger < k_B T/2\pi$.

by scales $k_B T_g$ and $\texttt{const}\times\hbar\omega_D$ respectively, the former one generally much larger than the latter (the const self-consistently will turn out to be less than one in subsection IV.B). Since the energy profile along the tunneling trajectory has a complicated shape formed by *many* intermediate states separated by *small intermediate* barriers (see below), it is fair to say that the state of the system at the highest barrier corresponds to the highest energy intermediate state (the "transition" state). The statistics of energy states have already been found earlier. We therefore use distribution (9) with only one difference: we must double the variance because the barrier height is actually the difference between two fluctuating quantities: the energy of the final (or initial) energy and the highest energy along the path. As a result,

$$\Omega_N(V) \sim \exp\left\{ s_c N - \frac{[V-(T_g s_c N + \gamma\sqrt{N})]^2}{4\delta E^2 N} \right\}. \quad (12)$$

Distribution (12) thus gives the typical value of the barrier for the (quantum) growth of a droplet. It is easy to see from (12) that the highest barrier corresponds to rearranging a region of size $N^\ddagger \simeq 14$ and is equal to

$$V_{max} = F^\ddagger/(2\sqrt{2}-1) \simeq 26 T_g s_c. \quad (13)$$

Since this is the hardest place to get through, we must take it as the transition state. Hence, the final distribution of (transition state) barriers is the density of pure states corresponding to Eq.(12) with $N = N^\ddagger$ (similar to the e^{ϵ/T_g}, obtained above). Thus,

$$\Omega(V^\ddagger) \sim \exp\left\{ \frac{V^\ddagger - V_{max}}{\sqrt{2}T_g} \right\} = \exp\left\{ -18\cdot s_c + \frac{V^\ddagger}{\sqrt{2}T_g} \right\}. \quad (14)$$

As one can see, the probability to have a small barrier path is exponentially suppressed. Nevertheless, owing to the large value of the energy parameter in distribution (12) the fraction of zero barrier paths per mosaic cell $\sim e^{-18 s_c} \simeq 3\cdot 10^{-7}$ is actually not prohibitively small. A region larger by only 18 molecules (less than a single layer) will have $e^{18 s_c}$ more final states (and therefore paths) to go to. We therefore conclude, any region of size $\simeq 200$ molecules will have an accessible alternative state with spectral density $1/T_g$. Finally, we stress a remarkable feature of the tunneling paths statistics in glass. Mark the very rapid - exponential - scaling of the number of paths leading out of a particular local structural state on the size of the respective region. This means that the final estimate of the density of structural transitions that have low enough barriers to be thermally relevant is rather insensitive to the details of correlation between the energy of the transition and its tunneling amplitude. Consequently, even a very simple estimate of this density, such as the one above, is very robust. Finally, note that the tunneling argument above is, again, a microcanonical argument, such as the one leading to Eq.(9), that also takes into account (in a rather crude manner) the mutual accessibility between alternative energy states.

As we will see later, the tunneling barriers, and hence the relaxation times of the tunneling centers, are distributed. This would lead to a time dependent heat capacity. Ignoring this complication for now, the *classical*, long time heat capacity is easy to estimate already (assuming it exists): Since our degrees of freedom span a volume ξ^3 and their spectral density is $1/T_g$ at low energy, one obtains for the low T heat capacity per unit volume: $T/T_g\xi^3$, up to an insignificant coefficient. The coefficient at the linear heat capacity dependence is often denoted $\bar{P}$. For silica, T_g =1500 K and realistic $\xi = 20\mathring{A}$ yields $\bar{P} \simeq 6\cdot 10^{45}\mathrm{m}^{-3}\mathrm{J}^{-1}$ in agreement with the experiment (we took $a = 3.5\mathring{A}$ - a length scale appropriate for a tetrahedron formed by four oxygens around a silicon atom. These tetrahedra appear to be moving units in a-Silica (Trachenko *et al.*, 2000)). The assumption of the existence of the long-time heat capacity is empirically justified (within logarithmic accuracy), but is also consistent with the present theory, see Subsection III.C and Section V.

In conclusion, the main result of this Subsection is that the non-equilibrium nature of the glass transition results in the existence of residual motional degrees of freedom, a significant fraction of which remain thermally active down to the lowest temperatures. These degrees of freedom are collective highly anharmonic atomic motions within compact regions of size ξ^3, determined mainly by the length scale of the entropic droplet mosaic determined at T_g. The energy scale in the spectrum of these excitations is set by the glass temperature T_g itself. We now turn to the question of what determines the *strength* with which these entropic droplet excitations couple to the phonons. This will explain the universality in the heat conductivity at temperatures below $\sim$1 K.

B. The Universality of Phonon Scattering

First of all, what do we mean by "phonons" in amorphous materials? There is no periodicity, therefore one can only strictly speak of elastic *strain*, even if the structure is completely stable. In the latter case, low gradient strains $\nabla\phi$ are still described by a simple bi-linear form:

$$H_{\rm ph} \equiv \int d^3\mathbf{r} \frac{\rho c_s^2}{2} (\nabla\phi)^2. \quad (15)$$

The $\nabla\phi$ field is defined on a isotropic, translationally invariant flat metric, as in continuum mechanics (Landau and Lifshitz, 1986), and so a wave-vector k is an operational concept. It is easily seen, by dimensional analysis, that strains arising specifically due to disorder will be of higher order in k than the term in Eq.(15): The corresponding energy terms should scale with some positive power of the lattice inhomogeneity lengthscale(s), $l_{\rm inhom}^\zeta$ ($\zeta > 0$), so as to vanish upon "zooming out". The terms will subsequently go as $k^2(l_{\rm inhom}k)^\zeta$. But, as we have already seen, the amorphous lattice is not stable,

that is there are anharmonic transitions with arbitrarily small energy and barrier. Still, the regions encompassing the transitions are quite small, at most 6 lattice spacings across, which is much less than the thermal de Broglie wave-length at 1 K (about $10^3 a$ in a-silica). The unstable regions interact with the strains of the otherwise stable lattice. We conceptualize this interaction by approximating the strain with pure phonons and computing the phonon mean-free path. The latter will turn out to be about 150 times longer than the phonon wave-length, so that the phonon approximation is internally consistent in that the phonons are indeed reasonably good quasiparticles, at the plateau temperatures and below. Finally, note in Eq.(15), we have used only one phonon polarization for simplicity (it will be usually obvious how to account approximately for all three acoustic phononic branches at the end of a calculation; using this "scalar" version of the lattice dynamics, for the purposes of this paper, boils down to neglecting the difference between the longitudinal and transverse sound, except in the later discussion of the Grüneisen parameter).

The structural transitions interact with the phonons because the energy of the transition changes in the presence of a strain: To see this exlicitly, consider the elastic energy within a droplet-sized region capable of undergoing a *low* energy transition, as relevant at low T. For the sake of argument, assume there is no sheer deformation; a similar argument applies to the transverse phonon branches. The stress energy is then $\int_{V_\xi} d^3\mathbf{r} K u_{ii}^2/2$, where K is a compressibility constant on the order of ρc_s^2, which we are allowed to treat as a constant, with the error contributing in a higher order in k, as already mentioned. u_{ii} is the trace of the elastic tensor (Landau and Lifshitz, 1986), which has the same meaning as $\Delta\phi$. Since the transition energy is low, the lowest order, quadratic expansion suffices. This implies that all individual bonds within the region distort by a very small amount (already shown not to exceed d_L, even at the transition's bottle-neck). We have demonstrated that such regions do indeed exist and found their density in the previous section. We separate the total elastic tensor u_{ij} into a contribution ϕ_{ij} due to the elastic stress and d_{ij} due to the tunneling displacement. The $d_{ii}\phi_{ii}$ cross term represents the coupling between the transition and the strain. If the phonon wave-length is larger than ξ, ϕ_{ii} is constant within the integration boundaries and can be taken out of the integral. One consequently arrives at the following *energy difference* for the defect states in the presence of a phonon: $\rho c_s^2 \phi_{ii} \int_{V_\xi} d^3\mathbf{r}\, d_{ii}$. Here, d_{ii} corresponds to the transition induced displacement between two given structural states. Each tunneling center is a multilevel system. However, since we are presently interested in the coupling of the lowest energy transition to the strain, we consider here the set of d_{ii} corresponding to the *two lowest* energy states of the region. (Higher energy transitions turn out to be intimately related to the lowest energy transition, and are discussed later, in Section IV.) We therefore conclude that a tunnelling transition, active at low temperatures, is linearly coupled to a lattice strain with the strength defined as $g = \rho c_s^2 \int_{V_\xi} d^3\mathbf{r}\, d_{ii}/2$; the corresponding term in the Hamiltonian reads:

$$H_{int} \equiv \mathbf{g} \nabla\phi \sigma_z. \tag{16}$$

We present next two independent ways to estimate the coupling constant g. The first one is based on the realization that at the glass transition, purely phononic excitations and a frozen-in structural transition must coexist, that is they are are of marginal stability with respect to each other. On the one hand, a local region posed to harbor a structural transition below T_g, must not be "crumpled" by a passing phonon. On the other hand the energy of the transition can only be so high, as to be sustainable by the lattice stiffness. In other words, an atom will be part a of frozen-in transition, if that atom is roughly in equilibrium between the transition driving forces and the ambient lattice strain. This stability condition gives at the molecular scale a, by Eqs.(15) and (16): $\mathbf{g}\sigma_z = -\rho c_s^2 a^3 \nabla\phi$. The lattice strain will be distributed throughout the material in the usual manner, subject, of course, to the equipartition that fixes the variance of the strain so as to conform to the thermally availabe energy. We take advantage of this by multiplying the equilibrium condition by $\nabla\phi$ and noting that thermal averaging is also ensemble averaging. This yields that for an atom posed to be part of low energy structural transitions below T_g, it is generically true that

$$|\left\langle \mathbf{g}\nabla\phi\, \sigma_z \right\rangle| \simeq \rho c_s^2 \left\langle (\nabla\phi)^2 \right\rangle a^3 \simeq k_B T_g. \tag{17}$$

Noting that $\langle \mathbf{g}\nabla\phi\, \sigma_z \rangle \simeq \langle |\mathbf{g}\nabla\phi| \rangle$, one arrives at a simple relation:

$$g = \sqrt{\rho c_s^2 a^3 k_B T_g}, \tag{18}$$

which is the main result of this Subsection. It is understood that this estimate is accurate up to a number of order one, and g's are likely distributed. At any rate, we observe that the TLS-phonon coupling is the geometric average between the glass transition temperature and an energy parameter $\rho a^3 c_s^2$ ($\sim 10^1$eV) related to the cohesion energy of the lattice (note the quantity ρc_s^2 is a multiple of the Young's modulus). We point out the estimate above applies quantitatively to low barrier transitions only. The mechanical stability criterion is a zero frequency, static condition. However, it takes a finite time for a structural transition to respond to an external stress. In other words, a region harboring a *slow* transition will likely appear perfectly elastic to a high frequency phonon. We thus arrive at the conclusion that TLS-phonon coupling must be frequency dependent, however deviations from the result obtained above will enter in a higher order in ω, k.

Alternatively, one may attempt to estimate the integral over the derivative of the displacement field that entered in the expression for the coupling constant $g = \rho c_s^2 \int_{V_\xi} d^3\mathbf{r}\, d_{ii}/2$. Since d_{ii} is the divergence of a vector,

the integral is reduced to that over a surface within the droplet's boundary: $\int_{S_\xi} d\mathbf{s}\,\mathbf{d}(\mathbf{r})$, where $\mathbf{d}(\mathbf{r})$ is the tunneling displacement itself, near the boundary. How near? The Gauss theorem applies so long as the field $\mathbf{d}$ is continuous. This field is roughly d_L in magnitude close to the droplet's center and is zero outside of the region. A function defined on a discrete lattice is expressly discontinuous. Requiring that one be able to cast a continuous tunneling displacement field on a discrete manifold, so that the field interpolates smoothly between d_L in the middle and zero outside, imposes constraints on the $\mathbf{d}$ values at the droplet's boundary. We argue this value should generically go as $(a/\xi)d_L$, up to a constant, in order to realize the interpolation and spread evenly the tensile field of the domain wall throughout the droplet. In other words, $\sim (a/\xi)d_L$ is quite obviously the lower bound, while higher values statistically imply a higher stress, and higher transition energy. Now, since $\mathbf{d}(r)$ is randomly oriented, the integral over the droplet's border is of the order $a^2\sqrt{N^{*2/3}}(a/\xi)d_L$, where $N^{*2/3}$ is the number of molecules at the boundary. The Lindemann distance at T_g is equal to the magnitude of a thermal fluctuation, hence $d_L/a \simeq |\nabla\phi|$ [5]. As a result, the coupling to the extended defects is still about $g \simeq \sqrt{\rho c_s^2 a^3 T_g}$, again within a factor of two or so.

Note that, when considering a particular value of lattice distortion $\nabla\phi$ in the discussion above, we did not specify the wave-length(s) of the phonons that contributed to this distortion, therefore the estimate of g in Eq.(18) is correct as long as the form of the interaction term (Eq.(16)) is adequate. This surely holds for long-wave phonons relevant at the TLS temperatures.

With the knowledge of g, we can estimate the inverse mean free path of a phonon with frequency ω. As done originally within the TLS model, the quantum dynamics of the two lowest energies of each tunneling center are described by the Hamiltonian $H_{TLS} = \epsilon\sigma_z/2 + \Delta\sigma_x/2$. This expression, together with Eqs.(15) and (16), form a complete (approximate) Hamiltonian of the TLS plus the lattice vibrations. The phonon inverse mean free path is then calculated in a standard fashion (Jäckle, 1972; Phillips, 1981):

$$l_{\rm mfp}^{-1}(\omega) = \pi\frac{\bar{P}g^2}{\rho c_s^3}\omega\tanh\left(\frac{\hbar\omega}{2k_BT}\right). \qquad (19)$$

[5] For reference, $|\nabla\phi| \sim (T_g/\rho c_s^2 a^3)^{1/2}$ at T_g is about 0.05 for SiO_2, 0.06 for B_2O_3 (oxide glasses), 0.03 for PS and PMMA (polymer glasses), in agreement with the Lindemann criterion. We stress the sensitivity to the value of the molecular size a, which is somewhat arbitrary. Here, we have not calculated the bead size based on chemistry, but instead used the values of the speed of sound, as employed in the scaling procedure of Freeman and Anderson (Freeman and Anderson, 1986). According to the definition of the Debye frequency, $a = (c_s/\omega_D)(6\pi^2)^{1/3}$.

This yields

$$\lambda_{dB}/l_{\rm mfp} = \frac{2\pi^2}{3}\tanh(1/2)\left(\frac{a}{\xi}\right)^3, \qquad (20)$$

where factor 1/3 comes from the averaging with respect to different orientations of the defects and we used $\bar{P} \simeq 1/T_g\xi^3$. It follows that $l_{\rm mfp}/\lambda_{dB} \sim (\xi/a)^3 \simeq 200$ up to a constant of order one. Hence, the analysis above explains the universality of the combination of parameters $\bar{P}g^2/\rho c_s^2$, and relates it to the geometrical factor $(a/\xi)^3 \simeq 10^{-2}$, which is the relative concentration of cooperative regions in a supercooled liquid, an almost universal number within the random first order glass transition theory (Xia and Wolynes, 2000), depending only logarithmically on the speed of quenching. Strictly speaking, our argument predicts the universality in $l_{\rm mfp}/\lambda$ only within 10%-20% or so. This is a consequence of indeterminacy of ϵ vs. Δ correlation that may be system specific, or could be due to deviations of the ξ/a ratio from the universal 5.8 at T_g. Since the latter ratio depends on the glass preparation time, the corresponding experimental study seems worthwhile.

Numerically, Eq.(20) yields $l_{\rm mfp}/\lambda \simeq 70$, a factor of 2 less than the empirical 150 (Freeman and Anderson, 1986). We could not have expected much better accuracy from our estimates, that used no adjustable parameters. Although it may seem that we have slightly overestimated the number of scatterers, the size of the error is too small to reliably support this suggestion. However, this is a good place to make a few comments on the distribution of the tunneling matrix elements Δ, which will also prove useful for the discussion of the phonon scattering at higher frequencies in Chapter IV. The estimate for the phonon mean free path in Eq.(19) is not terribly sensitive to the form of tunneling amplitude distribution (Phillips, 1981) (within reasonable limits). This is because the contribution of an individual TLS to the total scattering cross-section is proportional to Δ^2/E^2, where $E \equiv \sqrt{\Delta^2+\epsilon^2}$. Two common distributions have been used in the literature. One distribution simply assumed $(\Delta^2/E^2) \sim 1$ in the absence of a more specific knowledge and a flat distribution of the total energy splitting E (this is actually the original TLS model). The earlier Standard Tunneling Model (STM) (Anderson *et al.*, 1972; Phillips, 1972), on the other hand, postulates $P(\Delta) \propto \frac{1}{\Delta}$ (approximately supported by our own conclusions too), which predicts a nearly flat E distribution as well. In the end, both models differ only in that the TLS model has to postulate the average (Δ^2/E^2) value when calculating the scattering cross-section (this number is absorbed into the TLS-phonon coupling constant g). On the other hand, the STM allows for somewhat more closed-form derivations, however it still has to introduce the cut-off values Δ_{min} and Δ_{max} as parameters (fortunately, many measured quantities depend on these parameters only logarithmically). (The distinction between the two models is described in detail in the front article by Phillips in (Phillips, 1981).) One point in favor of the STM is that it

necessarily predicts time dependence of the specific heat. While a time dependence has been observed, its specific functional form has not been unambiguously established in the experiment (see (Hunklinger and Raychaudhuri, 1986; Pohl, 1981)). We also mention, for completeness, there is a different way to parametrize the two-level system motions within the more general, soft-potential model (Buchenau *et al.*, 1992; Karpov *et al.*, 1983). At any rate, we see that while a two-level system's contribution to the total phonon scattering depends on the value of its $\Delta \sim E$ ratio, the precise form of the Δ distribution will change the answer quantitatively, but not qualitatively. We note, that in the context of the present calculation it is preferable to consider the simpler, TLS setup that does not specify the Δ distribution, because our argument has so far been only *semi*-classical. Indeed, so far the tunneling amplitudes have only interested us from the perspective of the volume *density* of *allowed* transitions. We saw that an indeterminacy of the density could not exceed a 10% or so due to a weak (logarithmic) dependence of that density on a specific Δ distribution. Therefore, we are more confident in the numerical estimates using the TLS-model setup that does not require introducing additional parameters (such as Δ_{min}) explicitly. Nevertheless, the special role of $\Delta \sim E$ defects in scattering is worth noting. These defects have low classical energy splittings $\epsilon < \Delta$ and their dynamics are mostly determined by the *quantum* energy scale. These are the "fast", or "zero-barrier" excitations discussed earlier in the literature (Black and Halperin, 1977; Geszti, 1982), whose tunneling matrix element probably can not be directly estimated by WKB, but we can still guess that it scales with ω_D. This suggests that using the same distribution function $P(\Delta)$ for *all* thermally defects may not be justified, as circumstantially supported by results of Black and Halperin (Black and Halperin, 1977) who found that the density of TLS derived from the heat capacity and conductivity measurements respectively are not exactly equal to each other. While this indeterminacy in the exact barrier distribution introduces only an error of order one in quantitative estimates (Black and Halperin, 1977) of the density of states and is not of special concern here, we note that the present theory, upon inclusion of the effects beyond the strict semi-classical picture, *does* in fact provide a mechanism for the excess of the "fast" two-level systems, as will be explained in Section V.

Strong Interaction Scenarios. By deriving the density of states of structural transitions, and their coupling to the phonons based on the known properties of the amorphous lattice, we have constructively established the microscopics of glassy excitations in excess to the purely elastic excitations. It follows from the discussion that *no other* excitations are present in glasses at 1 K and below (see also the discussion on the exhaustive classification of excitations in amorphous lattices in Subsection IV.A). Importantly, the density of states (DOS) in excess of the phonons, is due to *local* motions. This is in contrast with Strong Interaction Scenarios (SIS) (Burin and Kagan, 1996; Coppersmith, 1991; Leggett, 1991; Yu and Leggett, 1988) that posit that *any* local excitations (other than pure strain) would give rise to a "universal" density of states. Such universal density of states arises in SIS as a consequence of long range, $1/r^3$, interaction mediated by the phonons, so that the actual observed DOS is a highly renormalized entity. The corresponding excitations are expressly non-local, possibly infinite in extent. The idea is very attractive because of its generality but remains a pure abstraction, until those bare excitations are constructively shown to *exist* in the first place. Additionally, even upon assuming some bare excitations are present, demonstrating the quantitative relationship between the effective density of states and the phonon coupling that conforms to the experimental $\bar{P}g^2/\rho c_s^2 \sim 10^{-2}$ has so far proven elusive (Caruzzo, 1994; Leggett, 1999; Lubchenko and Wolynes, 2000). On the other hand, we have shown that local structural transitions, that interact with phonons with a particular strength, must indeed take place in amorphous solids. In order to determine where the current theory stands in relation to the SIS, one may inquire whether the phonon-mediated interaction leads to the emergence of some collective density of states. It should be immediately clear that no such additional, collective DOS appears at T_g, because the argument in the previous subsection has already included *all* the effects of the surrounding of a structural transition, which simply amounted to the thermal noise at T_g delivered to the transition by the elastic waves. It, of course, does not matter what the phonon source is. What happens at low temperatures should be considered separately. The effects of interaction turn out to be small in the TLS regime and are discussed in detail in the final Section of this paper. Here, we give several qualitative estimates for the sake of completeness, both at high and low temperatures. The phonon-mediated interaction goes roughly as $\frac{g^2}{\rho s_c^2}\frac{1}{r^3}$, with a numerical factor less than one (see Section VI). Ignoring the factor, the interaction is expressed, with the help of Eq.(18), via the glass transition temperature according to $k_B T_g \frac{a^3}{r^3}$. Two neighbouring domains, a distance ξ apart, would thus couple with strength $J_{\rm neigh} = T_g(a/\xi)^3$. In order to assess the effects of interaction on the effective energies of individual transitions, or whether it even makes sense to talk about on-site energies after the interaction is turned on, one must compare the interaction strength to the width of the distribution of the on-site energies as derived in the absence of interaction, exactly the same way it is done in the context of Anderson localization. According to the previous Subsection the latter width, call it ΔE, is of the order T_g. The ratio $J_{\rm neigh}/\Delta E \simeq (a/\xi)^3$ is a small number, as expected. There will be no long range effects, due to resonant interactions, at high temperatures near T_g. At very low temperatures, only tunneling centers (TC) with energy splitting $\sim k_B T$ or less are thermally active. While the relevant spread of the on-site energies $E_T \sim k_B T$ is now down by a factor T/T_g

compared to the glass transition temperature, the *concentration* of active TC is also down by the same factor, namely $(T/T_g\xi^3)$, thus increasing the mutual separation between the regions of mobile transitions. The total dipole-dipole induced static field due to all those thermally active two-level systems at a given spot is simply $\frac{g^2}{\rho c_s^2}(T/T_g\xi^3) \simeq k_BT(a/\xi)^3$, again much smaller than the relevant on-site energy range $E_T \sim k_BT$. The motions within the tunneling centers are quantum-mechanical at these low temperatures, and so one may consider possible effects of *resonant* interactions between distinct TC's, as in the Burin-Kagan scenario (Burin and Kagan, 1996). These effects have been shown to become important only at ultra-cold temperatures of μK and below (Neu *et al.*, 1997), as already mentioned in the introduction.

Besides having explained the origin of the universality of combination $\bar{P}\frac{g^2}{\rho c_s^2}$ ubiquitous in the STM, we have also seen why the value of this parameter is different from 1, suggested by the strong defect-defect interaction universality scenario. This value can be traced to the relative concentration of the domains $(a/\xi)^3 < 0.01$, as just mentioned. It is curious that the defect-phonon interaction in the long wave-length limit can be expressed as a surface integral. Besides supporting our picture of the residual excitations as motions of domain walls, it points at a connection with string theories, where the elementary particles exhibit internal structure at high enough energies, which is also true in our case. In fact, this internal structure is ultimately the cause of the phenomena observed in glasses at higher temperatures, namely the so called bump in the specific heat and the thermal conductivity plateau, which are dealt with in Chapter IV.

C. Distribution of Barriers and the Time Dependence of the Heat Capacity

The STM postulated tunneling matrix element distribution $P(\Delta) \propto 1/\Delta$ implies a weakly (logarithmically) time dependent heat capacity. This was pointed out early on by (Anderson *et al.*, 1972), while the first specific estimate appeared soon afterwards in (Jäckle, 1972). The heat capacity did indeed turn out time-dependent, however its experimental measures are indirect, and so a detailed comparison with theory is difficult. Reviews on the subject can be found in (Nittke *et al.*, 1998; Pohl, 1981). Here, we discuss the Δ distribution dictated by the present theory, in the semi-classical limit, and evaluate the resulting time dependence of the specific heat. While this limit is adequate at long times, quantum effects are important at short times (this concerns the heat condictivity as well). The latter are discussed in Subsection V.A.

In the tunneling argument from Section III.A, we have suggested a WKB type expression for the tunneling amplitude:

$$\Delta = \Delta_0 e^{-\frac{\pi V^\ddagger}{\hbar\omega^\ddagger}}, \tag{21}$$

which would be completely correct in the case of a parabolic barrier with frequency $\omega^\ddagger$ and height $V^\ddagger$ and was motivated by the necessity to maintain the proper scaling with $\hbar$ in the denominator of the exponent, given that the typical barrier height is determined by the *classical* landscape characteristics and should scale with T_g. According to Eq.(14), $P(V^\ddagger) \propto e^{\frac{V^\ddagger}{\sqrt{2}T_g}}$. It follows then that

$$P(\Delta)d\Delta = A\left(\frac{\Delta_0}{\Delta}\right)^c \frac{d\Delta}{\Delta}, \tag{22}$$

where $c = \hbar\omega^\ddagger/\sqrt{2}T_g$ should be less then 0.1 according to our estimates of $\omega^\ddagger$ (see section IV.B). A is a constant, to be commented on very shortly. The distribution in Eq.(22) becomes $P_{STM}(\Delta)d\Delta \propto d\Delta/\Delta$ postulated in the standard tunneling model, if $c \to 0$. As shown next, the non-zero c gives rise to an anomalous exponent $\alpha = c/2$ in the heat capacity $C \propto T^{1+\alpha}$ and a power law $t^{c/2}$ for the specific heat time dependence at long times, as opposed to a logarithmic one, predicted by the STM. While $c \simeq 0.1$ implies $\alpha \simeq 0.05$, experimentally, α seems to vary from 0.1 to 0.5. This larger value is consistent with quantum mixing effects that go beyond the semiclassical analysis as we will discuss later.

Scaling $\hbar\omega^\ddagger$ in the denominator of the tunneling exponent implies that $\omega^\ddagger$ must be a quantum energy scale and it is indeed shown in Section IV.B that $\omega^\ddagger$ is proportional to the Debye frequency ω_D. While the tunneling argument from Section III.A only explicitly considered the statistics of the *highest* energy state along the tunneling trajectory, the expression in Eq.(21) actually does not use such a simplified picture but considers a *finite* vicinity of the barrier top. The conclusion of Section IV.B that the barrier heights are distributed exponentially, such as in in Eq.(14), remains true in either case. The leads to a non-zero value of c, and here we explore what consequences this has for the low temperature heat capacity and conductivity. As follows from the discussions in Section III.A, constant A in Eq.(22) is of order one.

Since the temperatures in question here are so low ($1K$ and below), we will ignore the energy dependence of $n(\epsilon)$ in this section and take $n(\epsilon) = \bar{P}$. In order to see the time dependence of the heat capacity we obtain the combined distribution of the TLS energy splittings E and relaxation rates τ^{-1} - $P(E, \tau^{-1})$, much as was done in (Jäckle, 1972), - and then count in only those TLS whose relaxation time τ is shorter than a particular experimental observation time t.

The (phonon irradiation induced) relaxation rate of a TLS is (Jäckle, 1972):

$$\tau^{-1} \simeq \frac{3g^2\Delta^2 E}{2\pi\rho c_s^5}\coth(\beta E/2). \tag{23}$$

It follows from Eqs. (22) and (23) that

$$P(E,\tau^{-1}) = \bar{P}A\left(\frac{\tau}{\tau_{min}(E)}\right)^{c/2}\left(\frac{\Delta_0}{E}\right)^{c}\frac{\tau}{2\sqrt{1-\tau_{min}(E)/\tau}}, \tag{24}$$

where

$$\tau^{-1}_{min}(E) \equiv \frac{3g^2E^3}{2\pi\rho c_s^5}\coth(\beta E/2) \tag{25}$$

is the fastest relaxation rate of a TLS with energy splitting E, achieved at $\Delta = E$, of course. As follows from Eq.(25), the rate scales roughly as the cube of temperature and is empirically of order an inverse millisecond at $10^{-2}K$. The resultant sample's heat capacity per unit volume is then:

$$C(t) = \int_0^\infty dE\left(\frac{\beta E}{2\cosh(\beta E/2)}\right)^2\int_{t^{-1}}^{\tau^{-1}_{min}} d\tau^{-1}\,P(E,\tau^{-1}), \tag{26}$$

where $[\beta E/2\cosh(\beta E/2)]^2$ is the TLS heat capacity. With a change of variables, Eq.(26) reads:

$$C(t) = \int_0^\infty dE\left(\frac{\beta E}{2\cosh(\beta E/2)}\right)^2\int_0^{\log(t/\tau_{min}(E))} dz\,\frac{A}{2}\left(\frac{\Delta_0}{E}\right)^{c}\frac{e^{\frac{c}{2}z}}{\sqrt{1-e^{-z}}}. \tag{27}$$

At long times the expression Eq.(27) yields a power law for both time and temperature dependence of the specific heat:

$$\lim_{t\to\infty} C(t) \propto t^{c/2}T^{1+c/2}, \tag{28}$$

where, note, the temperature dependence also comes from the energy dependence of $\tau_{min}(E) \propto E^{-3}$ in Eq.(27). The value $c \sim 0.1$ implies the long time heat capacity should obey $C \propto T^{1+\alpha}$ at low T, where $\alpha \sim 0.05$, a smaller number than observed in amorphous materials. We must bear in mind that the issue of the exact form of the time dependence in the laboratory still appears to be unresolved, as there is no definite agreement between different experiments; for references, see (Hunklinger and Raychaudhuri, 1986; Nittke *et al.*, 1998; Pohl, 1981; Sahling *et al.*, 2002). While there is no doubt that the specific heat *is* time-dependent, some experiments agree with the logarithmic time profile, as predicted by the STM, others give a lower or higher speed of variation with time. The present semiclassical prediction with $c = 0.1$ would be hard to distinguish from a logarithmic law. Finally, even though a correction to the linear temperature heat capacity dependence with $c = 0.1$ is most likely smaller than what is experimentally observed, the value of this correction is non-universal, consistent with empirical data.

The expression in Eq.(27) can be evaluated numerically for all values of t, and the results for three different waiting times are shown in Fig.11 for $c = 0.1$. The value of $\tau_{min} = 2.0\mu sec$ at $E/T_D = 5.7\cdot 10^{-4}$, derived from the present theory (also consistent with (Goubau and Tait, 1975)) was used. The results for $t = 10\mu sec$ demonstrate that due to a lack of fast relaxing systems at low energies, short time specific heat measurements can exhibit an apparent gap in the TLS spectrum. Otherwise, it is evident that the power-law asymptotics from Eq.(28) describes well Eq.(27) at the temperatures of a typical experiment.

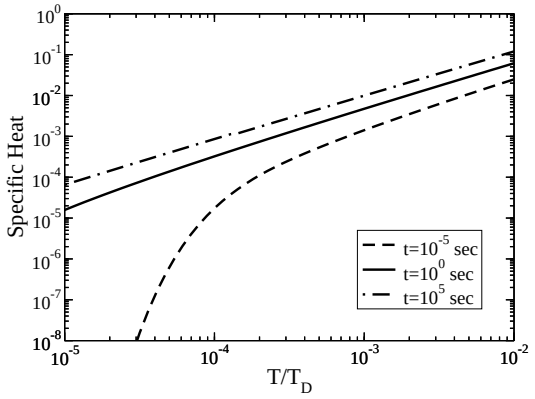


FIG. 11 Displayed are the TLS heat capacities as computed from Eq.(27) appropriate to the experiment time scales of order a few microseconds, seconds and hours. Value of $c = 0.1$ was used here. If one makes an assumption on the specific value of Δ_0, it is possible to superimpose the Debye contribution on this graph, which would serve as the lowest bound on the total heat capacity. As checked for $\Delta_0 = \omega_D$, the phonon contribution is negligible at these temperatures.

As clear from the discussion above, the long-time power law behavior of the heat capacity is determined by the "slow" two-level systems corresponding to the higher barrier end of the tunneling amplitude distribution, ar-

gued to be of the form shown in Eq.(22). If one assumes that this distribution is valid for the zero-barrier tail of the $\log(\Delta)$ distribution as well, one would expect that the heat conductivity would scale as T^{2+c} at the TLS temperatures, in contrast to an observed experimental sub-quadratic dependence $T^{2-\alpha'}$. As we shall see in Section V, other quantum effects are indeed present in the theory and we will discuss then how these contribute both to the deviation of the conductivity from the T^2 law and the way the heat capacity differs from the strict linear dependence, both contributions being in the direction observed in experiment. Finally, when there is significant time dependence of c_V, the *kinematics* of the thermal conductivity experiments are more complex and in need of attention. When the time-dependent effects are included, both phonons and two-level systems should ideally be treated by coupled kinetic equations. Such kinetic analysis, in the context of the time dependent heat capacity, has been conducted before by other workers (Strehlow and Meissner, 1999).

IV. THE PLATEAU IN THERMAL CONDUCTIVITY AND THE BOSON PEAK

In this section we continue to explore the consequences of the existence of the low temperature excitations in amorphous substances, which, as argued in Chapter III, are really resonances that arise from residual molecular motions otherwise representative of the molecular rearrangements in the material at the temperature of vitrification. We were able to see why these degrees of freedom should exist in glasses and explain their number density and the nearly flat energy spectrum, as well as the universal nature of phonon scattering off these excitations at low T (< 1 K).

At higher temperatures ($K_BT \sim 10^{-2.0}$ to $10^{-0.5}\hbar\omega_D$), an apparently different kind of excitations begins to appear, leading to the so called bump in the heat capacity and plateau in the thermal conductivity, as was discussed in the Introduction. We argue in this chapter that the transitions between the mutually accessible frozen-in minima in the amorphous lattice that give rise to the two level system behavior at the lowest T also explain the existence of the modes responsible for this "Boson Peak" and the intense phonon scattering at the corresponding frequencies. This thus removes the need to invoke theoretically any additional mechanisms, although other contributions may well be present to some extent; we will try to assess this possibility in the following Section.

A. Introduction: Classification of Excitations in Glasses

While we believe to have mostly achieved a microscopic understanding of the excitations that are specific to the amorphous solids and are not present in other types of materials, this description is rather new and, naturally, there is certain lack of established language that could be efficiently used to characterize these excitations. In this section, we will introduce some terminology that will be used in the rest of the article. At the same time, we will provide a brief general analysis of what possible qualitatively distinct types of molecular motions can exist in glasses.

Any atomic motions that take place in a frozen glass, obviously may also be present in the liquid above T_g. For example, those high T motions that correspond to shear attain stiffness (on realistic time scales) below freezing. The motions in the liquid, apart from pure volume change, corresponding to the longitudinal sound, are molecular translations, or, informally speaking, jumps. Above T_A, such jumps are not accompanied by a noticeable volume change and bond stretching, as no metastable structures form in the liquid at these temperatures. The barriers are therefore largely entropic. (It is nice to compare Feynman's discussion of the absence of energy barriers in superfluid He (Feynman, 1954) in this regard.) Below T_A, such hopping already involves moving a number of molecules from one local minimum of the free energy functional to another such minimum and thus requires structural rearrangement within a certain cooperative length owing to the formation of metastable local arrangements. Molecular translations do not conserve momentum, which subsequently must be provided by the rest of the bulk. We thus call these degrees of freedom, which are relics of the translational motions in the liquid above T_g, *inelastic* degrees of freedom. They are truly inelastic also in the macroscopic sense of the word, because the existence of alternative configurations in the solid bulk, which are also coupled to the phonons, ultimately leads to irreversible relaxation, if the sample is subjected to mechanical stress thus causing a shift in the thermal population of the alternative internal, structural states. This is the mechanism behind the so called bulk viscosity (Landau and Lifshitz, 1986) (incidentally, it also contributes to the so called relaxational phonon absorption, which we discuss in subsection IV.G). The switching from one energy minimum to another is accomplished by moving the domain wall - the interface between the two alternative configurations - through the local region. As mentioned earlier, this domain wall is something of an abstract entity, really a quasiparticle of a sort. Yet it has many ponderable attributes. For one thing, it has a mass (per unit area), which will be obtained in this section. It also has surface tension, therefore it can support surface vibrations, again, of a sort. Although these vibrations are realized through real atomic motions, it is more beneficial to think of them as vibrational modes of an imaginary membrane. In fact, as will be argued later, the oscillations of this membrane correspond to the indeterminacy in the exact boundary of the frozen-in domain that has more than one kinetically accessible internal state. Therefore, highly anharmonic atomic motions in the real space correspond to *harmonic* motions in the space where the domain walls are defined. This mental construction does the trick of enabling us to

calculate the ripplon spectrum, as demonstrated in section IV.C. Now, since it was shown in (Xia and Wolynes, 2000), that the liquid degrees of freedom below T_A consist of switching to alternative local energy minima; we can claim our assignment of different *inelastic* modes is exhaustive (but not unique, of course!). These are, again, translations and vibrations of the domain walls.

On the other hand, any purely *elastic* motions in the glassy lattice can be thought of as a sum of ordinary, affine, displacements and non-affine displacements (see e.g. (Wittmer *et al.*, 2001)). The affine component would be the only one present in a perfectly isotropic medium and would follow the stress pattern according to a Poisson equation (the situation with a non-isotropic crystal is conceptually the same). The non-affine displacements are a consequence of the absence of periodicity. They involve a small number of molecules and are characterized by a non-zero circulation of the displacement field. It is not clear at present whether the size of these non-affine "islands" could be inferred in present day computer simulations, since the amorphous structures that can be currently generated on modern computers still correspond to unrealistically rapid quenching rates. The resulting structure corresponds to a sample caught in a very high energy state with extraordinarily low barriers. As is clear by now from the random first order transition theory, such structures correspond to temperatures close to T_A and will have very small cooperative regions approaching the molecular scale a.

We conclude this subsection by repeating ourselves that one important difference between the elastic and the inelastic modes is in how they absorb the phonons. While any static disorder can only provide Rayleigh scattering with a characteristic length scale equal to the size of the heterogeneity, the inelastic (resonant) absorption's cross-section scales as the square of the phonon wave-length, it thus will considerably dominate the Rayleigh mechanism for the longer wave-length phonons (absorption saturation in the TLS's does not occur at the sound intensities typical of heat transfer).

B. The Multilevel Character of the Entropic Droplet Excitations

We hope to have convinced the reader by now that the tunneling centers in glasses are complicated objects that would have to be described using an enormously big Hilbert space, currently beyond our computational capacity. This multilevel character can be anticipated coming from the low temperature perspective in (Lubchenko and Wolynes, 2001). Indeed, if a defect has at least two alternative states between which it can tunnel, this system is at least as complex as a double well potential - clearly a multilevel system, reducing to a TLS at the lowest temperatures. Deviations from a simple two-level behavior have been seen directly in single-molecule experiments (Boiron *et al.*, 1999). In order to predict the energies at which this multilevel behavior would be exhibited we first estimate the domain wall mass. Obviously, the total mass of all the atoms in the droplet is so large that the possibility of *simultaneous* tunneling of all atoms is completely excluded. The tunneling, we argue, occurs stagewise; each individual motion encounters a nearly flat potential, implying low frequency instantaneous modes.

In addition, the effective mass of the domain wall turns out to be low, *also* owing to the collective, barrierless character of the tunneling events. This is because moving a domain wall over a molecular distance a involves displacing, at any one (imaginary!) time, individual atoms only a Lindemann length d_L. Suppose this occurs on the (imaginary) time scale τ. The resulting kinetic energy is $M_w(a/\tau)^2 = N_w m(d_L/\tau)^2$, where $N_w \simeq (\xi/a)^2$ is the number of molecules in the wall and m is the molecular mass. Thus the mass of the wall M_w is only $m(\xi/a)^2(d_L/a)^2$. Using $(\xi/a) \simeq 5.8$ and $(d_L/a)^2 \simeq 0.01$ gives $M_w \simeq m/3$. This implies the mass of the wall per *atom* is very small - about a hundredth of a molecular mass, consistent with the simulations of certain barrierless dislocation motions in copper (Vegge *et al.*, 2001). Using $(d_L/a)^2 \simeq k_B T_g/\rho c_s^2$, derived earlier, one can express the wall's mass through the material constants as $M_w \simeq (\xi/a)^2 k_B T_g/c_s^2$. The wall mass estimate above, inspired by the Feynman's argument on the effective mass in liquid helium (Feynman, 1953), is entirely analogous to the well known estimate of the soliton mass in polyacetylene, see e.g. (Heeger *et al.*, 1988). In the latter, the soliton moves a large distance, while individual atoms undergo only small displacements leading to a low soliton mass.

We can now use the typical value of the barrier curvature from our tunneling argument in section III.A (see Fig.10) to estimate the typical frequency $\omega^\ddagger$ of motion at the tunneling barrier top. We now express the barrier profile $V(N)$ as a function of the droplet's radius $r \equiv a(3N/4\pi)^{1/3}$ and obtain

$$\omega^\ddagger = -\partial^2 V/\partial r^2/M_w \simeq 1.6(a/\xi)\omega_D. \qquad (29)$$

According to the quantum transition state theory (Wolynes, 1981), and ignoring damping, at a temperature $T' \simeq \hbar\omega^\ddagger/2\pi k_B \simeq (a/\xi)T_D/2\pi$, the wall motion will typically be classically activated. This temperature lies within the plateau in thermal conductivity (Freeman and Anderson, 1986). This estimate will be lowered if damping, which becomes considerable also at these temperatures, is included in the treatment. Indeed, as shown later in this section, interaction with phonons results in the usual phenomena of frequency shift and level broadening in an internal resonance. Also, activated motion necessarily implies that the system is multi-level. While a complete characterization of *all* the states does not seem realistic at present, we can extract at least the spectrum of their important subset, namely those that correspond to the vibrational excitations of the mosaic, whose spectral/spatial density will turn out to be suf-

ficiently high to account for the existence of the Boson Peak.

C. The Vibrational Spectrum of the Domain Wall Mosaic and the Boson Peak

At low temperatures the two-level system excitations involve tunneling of the mosaic cells typically containing $N^* \simeq 200$ atoms. The tunneling path involves stagewise motion of the wall separating the distinct alternative configurations through the cell untill a near resonant state is found. At higher temperatures, other final states are possible since the exact number and identity of the atoms that tunnel can vary. These new configurations typically will be like the near resonant level but will also move a few atoms at the boundary, i.e. at the interface to another domain. This is schematically shown in Fig.12. Alternatively, due to the quantum mechanical uncertainty of the exact location of the domain wall, its shape is intrinsically subject to fluctuations (these are zero-point vibrations of the domain wall). It is thus not surprising that the ripplon's frequencies turn out to be proportional to ω_D, the basic quantum energy scale in the system. These fluctuations of the domain boundary shape can be visualized as domain wall surface modes ("ripplons"). A detailed calculation of the ripplon spectrum would require a considerable knowledge of the mosaic's geometry. At each temperature below T_A the domain wall foam is an equilibrium structure made up of flat patches of no tension (remember the renormalized $\sigma(r) \propto r^{-1/2}$; however fluctuations will give rise to finite curvature and tension). To approximate the spectrum we notice that the ripples of wave-length larger than the size of a patch will typically sense a roughly spherical surface of radius $R = \xi(3/4\pi)^{1/3}$. The surface tension of the mosaic has been calculated from the classical microscopic theory and is given by $\sigma(R) = \frac{3}{4}(k_B T_g/a^2)\,\log((a/d_L)^2/\pi e)(a/R)^{1/2}$ (Xia and Wolynes, 2000), where d_L/a is the universal Lindemann ratio. It could appear that such tension could collapse an individual fragment of the mosaic but this tension is, of course, compensated by stretching the frozen-in outside walls. We approximate the effect of this compensation by an isotropic positive pressure of a ghost (i.e. vanishing density) gas on the inside.

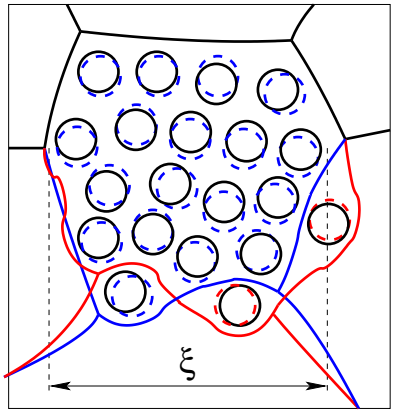


FIG. 12 Tunneling to the alternative state at energy ϵ can be accompanied by a distortion of the domain boundary and thus populating the ripplon states. The doubled circles denote atomic tunneling displacements. The blue line signifies, say, the lowest energy state of the wall, and the blue circles correspond to the respective atomic displacements. An alternative wall's state is shown in red, the corresponding alternative sets of atomic motions are coded using different colors. The domain boundary distortion is shown in an exagerated fashion. The boundary does not have to lie *in between* atoms and is drawn this way for the sake of argument; its position in fact is not tied to the atomic locations in an *à priori* obvious fashion.

The eigen-frequency spectrum of the surface modes of a hollow sphere with gas inside is well known (see e.g. (Morse and Feshbach, 1953), as well as our appendix A). If we pretend for a moment that the surface tension coefficient σ is curvature independent, the possible values of the eigen-frequency ω are found by solving the following equation:

$$\cot[\alpha_l(\omega R/c_g)] = \left(\frac{\rho_W}{\rho_g R}\right) - \frac{(l-1)(l+2)}{(\omega R)^2}\left(\frac{\sigma}{\rho_g R}\right), \tag{30}$$

where ρ_W is the membrane's mass per unit area, ρ_g and c_g are gas' mass density and sound speed respectively. As stated earlier, Eq.(30) only applies for $l \geq 2$. Finally, function $\cot[\alpha_l(z)] \equiv \left(-l + z\frac{j_{l+1}(z)}{j_l(z)}\right)^{-1}$, where $j_l(z)$ is the spherical Bessel function of l-th order, does exhibit behavior similar to that of the regular trigonometric cotangent for arguments of the order unity and larger, going however to $-1/l$ as $z \to 0$. Its graph for $l = 2$ is shown in Fig.13. An inspection shows that for each

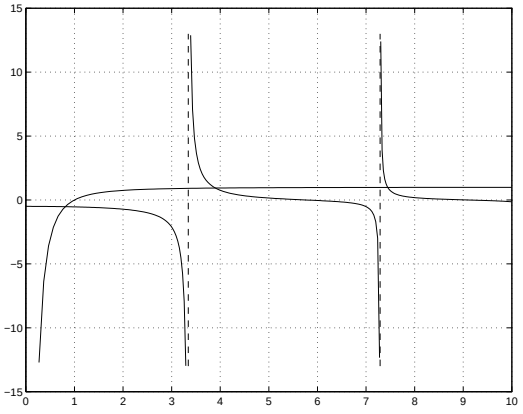


FIG. 13 The functions entering Eq.(30) are shown for some arbitrary parameter values. Here, $l = 2$.

l, the smallest solution of Eq.(30) gives the frequency of the proper eigen-mode of the shell itself (shifted due to the presence of the gas inside), whereas the rest of the solutions represent the standing acoustic waves in the gas.

This is especially clear in the $\rho_g \to 0$ limit, when the lowest frequency does not even depend on the gas' sound speed, whereas the rest of the solutions are obviously determined by the inverse time it takes the sound in the gas to traverse the sphere.

Since we are interested only in the wall's *proper* modes in the limit $\rho_g \to 0$, we get unambiguously for the frequency of an l-th harmonic:

$$\omega_l^2 = (l-1)(l+2)\left(\frac{\sigma}{\rho_W R^2}\right); \quad (l \geq 2). \tag{31}$$

Accounting for the unusual r dependence of the surface tension $\sigma(r) \propto r^{-1/2}$ modifies the standard result from Eq.(31) by a factor of 9/8. The reason is, the peculiar surface energy dependence $F_{surf}(R) = 4\pi R^2\sigma = 4\pi\sigma_0 R^{3/2}a^{1/2}$ calls for the following dependence of pressure on the curvature: $p = \frac{1}{4\pi R^2}\frac{\partial F_{surf}(R)}{\partial R} = \frac{3}{2}\frac{\sigma}{R}$ (as compared to the regular $p = 2\frac{\sigma}{R}$). The eigen-frequencies, in their turn, are determined by calculating the (frequency dependent) excess pressure due to a variation in curvature. Since now $p \propto R^{-3/2}$, varying p with respect to R brings down another factor of 3/2, thus giving 9/4 instead of the 2 of the curvature independent case. Hence the (barely significant, but curious) correction factor of 9/8 used in (Lubchenko and Wolynes, 2003a). Since we have been assuming that the amplitude is infinitesimally small, this factor is the only consequence of having a curvature dependent σ, which should have made the membrane oscillations even more non-linear (as compared to $\sigma =$ const case) in the case of *finite* displacements. Pinpointing this effect, however, is clearly beyond the accuracy attempted by the present model. Finally, one finds a spectrum with

$$\omega_l^2 = \frac{9}{8}\frac{\sigma}{\rho_W R^2}(l-1)(l+2); \quad (l \geq 2), \tag{32}$$

where each l-th mode of a sphere is $(2l+1)$-fold degenerate. Using $\rho_W = (d_L/a)^2\rho a$, obtained earlier in the chapter and $T_g \simeq \rho c_s^2 a^3 (d_L/a)^2$ (section III.B), one finds

$$\begin{aligned} \omega_l &\simeq 1.34 \;\; \omega_D (a/\xi)^{5/4}\sqrt{(l-1)(l+2)/4} \\ &\simeq \quad 0.15\,\omega_D\,\sqrt{(l-1)(l+2)/4}. \end{aligned} \tag{33}$$

Because of the universality of the (a/ξ) ratio (Lubchenko and Wolynes, 2001), ω_l is a multiple of the Debye frequency. Apart from the barely significant $(a/\xi)^{1/4}$ factor, again, due to the R dependent σ, the ubiquitous scaling $\omega_l \sim (a/\xi)\omega_D$ stresses yet another time the significance of the scale ξ. Such a scale has been previously empirically deduced by interpreting inelastic scattering experiments but has been usually ascribed to the static heterogeneity length scale, in contrast with the dynamical nature of the mosaic in the present theory. We note, again, that this "static heterogeneity" has never been unambiguously seen in X-ray diffraction. Owing to the material's discreteness, one does not expect harmonics of higher than $\pi\left(\frac{3}{4\pi}N^*\right)^{1/3}[(R-a/2)/R] \simeq 9..10$th order, a relatively large number, which justifies the tacitly assumed continuum approximation. The lowest allowed ripplon mode is $l = 2$ (corresponding frequency is $\sim$ 1THz for silica, in remarkable agreement with the inelastic neutron scatering data (Wischnewski *et al.*, 1998)).

The requirement $l \geq 2$ can be understood from the symmetry considerations. $l = 1$, the case of no restoring force, corresponds to a domain translation. Within our picture, this mode corresponds to the tunneling transition itself. The "translation" of the defects center of mass violates momentum conservation and must be thus accompanied by absorbing a phonon. Such resonant processes couple *linearly* to the lattice strain and contribute the most to the phonon absorption at the low temperatures, dominated by one-phonon processes. $l = 0$, on the other hand, corresponds to a uniform dilation of the shell. This mode is formally related to the domain growth at $T > T_g$, and is described by the theory in (Xia and Wolynes, 2000). It is thus possible, in principle, to interpret our formalism as a multi-pole expansion of the interaction of the domain with the rest of the sample. Harmonics with $l \geq 2$ correspond to pure shape modulations of the membrane.

The existence of the domain wall vibrations explains and allows us to visualize, at least in part, the multilevel character of the tunneling centers as exhibited at temperatures above the TLS regime. Curiously, the existence of TLS's, even though displayed at the lowest T, is basically of classical origin due to the non-equilibrium nature of the glassy state. Yet the ripplons, even though seen at higher T, are mostly due to quantum effects and would not be predicted by a strictly semi-classical theory, in which $\hbar \to 0$. A schematic of the resultant droplet energy levels is shown in Fig.14. The arrangement of the

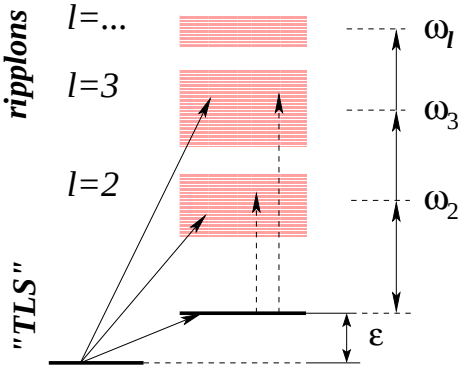


FIG. 14 Tunneling to the alternative state at energy ϵ can be accompanied by a distortion of the domain boundary and thus populatiting the ripplon states. All transitions exemplified by solid lines involve tunneling between the intrinsic states and are coupled linearly to the lattice distortion and contribute the strongest to the phonon scattering. The "vertical" transitions, denoted by the dashed line, are coupled to the higher order strain (see Appendix A) and contribute only to Rayleigh type scattering, which is much lower in strength than that due to the resonant transitions.

combined internal (configurational) and ripplonic density of states, as depicted in Fig.14, has the following motivation behind it. We include the possibility of distorting the domain wall during the tunneling transition by providing a set of vibrational states on top of the alternative internal state. The arrangement of the energy states as depicted in Fig.14 insures that only thermally active tunneling centers have mobile (and thus vibrationally excitable boundaries). The atomic motions at the *inactive* defects' sites (i.e. that cannot tunnel or cross the barrier) would be indistinguishable from the regular elastic lattice vibrations. Importantly, direct transitions to the ripplonic state can occur from one of the two lowest - "TLS" - energy states of a tunneling center. This inherent assymetry between the two structural states of a tunneling center actually reflects the thermodynamical inequivalence of the two states at the glass transition temperature. While one of the states represents the local structure in (meta-stable) equilibrium with the current liquid arrangement around it, the other state is a configuration that must only be regarded as one of the structures along the many escape routes from the current equilibrium local state. At T_g, most of those escape routes become too costly energetically.

This is a good place to remind the reader that existing explanations of the large density of states at the BP energies have to do either with purely harmonic excitations of disordered, but perfectly stable lattice (see Introduction), or by generalizing the low energy inelastic, two-level degrees of freedom to multilevel systems, as was done e.g. by the soft potential model (SPM) (Buchenau *et al.*, 1992; Karpov *et al.*, 1983). Such generalizations imply a connection between the anomalies seen in the TLS regime and at these higher energies. Such a connection is strongly suggested by experiment, most prominently by the strength of phonon scattering. The latter is *inelastic* at the BP energies, as it was at the TLS energies. We stress, the rate of increase of the ripplonic density of states is much much higher than that empirically assumed in the purely empirical SPM. Again, there is virtually no freedom to adjust the numbers in our theory.

In order to compute the heat capacity of the ripplons on top of the structural transitions we will need to consider the (classical) density of the inelastic states in more detail than in the previous section. The density of states $n(\epsilon) = \frac{1}{T_g} e^{\epsilon/T_g}$ was derived earlier taking as the reference state the generic global liquid state corresponding to the (high-energy) configuration frozen-in at T_g. It turns out that only transitions to states with $\epsilon < 0$ (relative to the liquid state!) will contribute to the TLS density of states. Indeed, as we have shown, the size of the region that permits a *low-barrier* rearrangement must be slightly (by ∼18 molecules) larger than the generic cooperative size at T_g. On the other hand, we know from the RFOT theory that larger cooperative regions correspond to lower energy liquid structures. Therefore one of the two alternative states must be lower in energy than the generic liquid state at T_g. As a result, the negative ϵ's correspond to some of the very numerous but mostly unavailable lower lying energy states, now accessed by tunneling. Now, if each of those true *local* ground states is taken as the reference one, the spectral density will be now $n(\epsilon) = \frac{1}{T_g} e^{-\epsilon/T_g}$ ($\epsilon > 0$). We consequently can let ϵ from Fig.14 take both positive and negative values by writing

$$n(\epsilon) = \frac{1}{T_g} e^{-|\epsilon|/T_g}. \tag{34}$$

We can now calculate each domain's partition function by including all possible ways to excite the system:

$$Z_\epsilon = 1 + \sum_{\{n_{lm}\}} e^{-\beta(\epsilon + \sum_{lm} n_{lm}\omega_{lm})} = 1 + e^{-\beta\epsilon} \prod_l Z_l^{2l+1}, \tag{35}$$

where $Z_l \equiv 1/(1 - e^{-\beta\omega_l})$ is the partition function of an lth order ripplon mode and we used $m = -l..1$. Here we assume each ripplon is a harmonic oscillator. Note that since the "harmonic" excitations of frequency ω_l are on top of another (structural) excitation, we must consider the issue of the zero-point energy of these "harmonic" excitations, that is no longer a matter of simply choosing a convenient reference energy. Note that this zero-point energy is actually several orders of magnitude higher than the subKelvin energies that are sufficient to excite *some* of the local structural transitions. And indeed, the energy that comprises the ripplons' ground state energy is not extracted from the thermal fluctuations of the medium, but, one may say, is simply "converted" from the zero-point energy of local elastic vibrations of the lattice. At the site of a "slow" (or, thermally inactive) structural transition, domain wall vibrations are indistinguishable from the regular lattice phonons, as already mentioned.

The specific heat corresponding to the partition function in Eq.(35) is found by computing $c_\epsilon = \beta^2 \frac{\partial^2 log Z_\epsilon}{\partial^2 \beta}$:

$$c_\epsilon = \frac{\left[\beta\epsilon + \sum_l (2l+1) \frac{\beta\omega_l}{e^{\beta\omega_l} - 1}\right]^2}{\left[2\cosh \frac{\beta\epsilon + \sum_l (2l+1)\log(1 - e^{-\beta\omega_l})}{2}\right]^2} + \frac{\sum_l (2l+1) \left(\frac{\beta\omega_l}{2\sinh \frac{\beta\omega_l}{2}}\right)^2}{e^{\beta\epsilon + \sum_l (2l+1)\log(1-e^{-\beta\omega_l})} + 1}. \tag{36}$$

Expression (36) clearly becomes the TLS specific heat $c_{TLS} = \left(\frac{\beta\epsilon}{2\cosh(\beta\epsilon/2)}\right)^2$ for $T \ll \omega_l$.

In order to obtain the amorphous heat capacity per domain, we (numerically) average c_ϵ with respect to $n(\epsilon)$; the result is shown in figure 15 with the thin solid line.

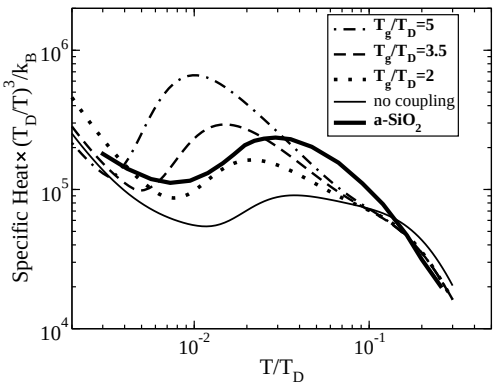


FIG. 15 The bump in the amorphous heat capacity, divided by T^3, as follows from the derived TLS + ripplon density of states. The thin curve corresponds to Eq.(36). The thick solid line is experimental data for a-SiO_2 from (Pohl, 1981). The experimental curve, originally given in J/gK^4, was brought to our scale by being multiplied by $\hbar^3\rho c_s^3(6\pi^2)(\xi/a)^3/k_B^4$, where we used $\omega_D = (c_s/a)(6\pi^2)^{1/3}$, $(\xi/a)^3 = 200$, $\rho = 2.2\text{g/cm}^3$, $c_s = 4100\text{m/sec}$ and $T_D = 342K$ (Freeman and Anderson, 1986). The other curves take into account effects of friction and frequency shift in the ripplon frequencies. They will be explained later in subsection IV.F. The Debye contribution was included in our estimate of the total specific heat; it was calculated according to (per particle) $c_D = 9(T/T_D)^3\int_0^{T/T_D} dx\frac{x^4e^x}{(e^x-1)^2}$ (Kittel, 1956). This equals to $234(T/T_D)^3$ at the low T. When multiplied by $(\xi/a)^3 \simeq 200$, this gives a value $4.6\cdot10^4$ in good agreement with the experiment (see Fig.3.10 from (Pohl, 1981)); note, however that the amorphous T_D is *lower* than the corresponding crystalline one, still it seems $T_D^{amorph} > \frac{1}{2}T_D^{cryst}$. We remind the reader that no adjustable parameters have been used so far.

D. The Density of Scatterers and the Plateau

In order to estimate the phonon scattering strength and thus the heat conductivity, we need to know the effective scattering density of states, the transition amplitudes and the coupling of these transitions to the phonons.

Any transition in the domain accompanied by a change in its internal state is coupled to the gradient of the elastic field with energy $g \sim \rho c_s^2 \int d\mathbf{s}\,\mathbf{d}(\mathbf{r})$, where $\mathbf{d}(\mathbf{r})$ is the molecular displacement at the droplet edge due to the transition (see section III.B). An additional modulation in the *domain wall* shape due to the current vibrational state cancels out due to the high symmetry ($l \geq 2$), as easily seen when computing the angular part of the surface integral. We therefore conclude that any transitions between groups marked with solid lines in Fig.14 are coupled to the phonons *with the same strength as the underlying (TLS-like) transition*. (Notice this also implies inelastic scattering off those transitions!) Incidentally, no selection rules apply for the change in the ripplon quantum numbers, being essentially a consequence of strong anharmonicity of the total transition.

We do not possess detailed information on the transition amplitudes, however they should be on the order of the transition frequencies themselves, just as is the case for those two level systems that are primarily responsible for the phonon absorption at the lower T which also have their transition amplitudes comparable to the total energy splitting. The argument is thus essentially the same as proposed earlier in section III.A. It should be noted, however, that the Hilbert spaces corresponding to the *quantum* in nature ripplons and the *classical* inelastic states are quite distinct (although overlapping); it thus should not be surprising that the matrix element beween *superpositions* of these spaces is on the order of the energy differences themselves. In what follows, we circumvent to an extent the question of what the precise distribution of the tunneling amplitudes of the TLS+ripplon transitions is and simply calculate the *enhancement* of the bare TLS induced scattering due to the presence of the ripplons. This is suggested by an earlier notion that the structural transitions in glasses couple to the phonons with the same strength even if accompanied by exciting vibrational modes of the mosaic.

We now calculate the density of the phonon scattering states. Since we have effectively isolated the transition amplitide issue, the fact of equally strong coupling of all transitions to the lattice means that the scattering density should directly follow from the partition function of a domain via the inverse Laplace transform. We will not proceed this way for purely technical reasons. In addition, we will separate the cases of positive and negative ϵ (see Fig.14), corresponding to absorption from ground and excited states respectively.

The phonon-ripplon interaction exhibits itself most explicitly through the phonon scattering, which becomes so strong by the end of the plateau as to cause complete phonon localization. This interaction also results in other observable consequences, such as dispersion (or frequency shift) of the ripplon frequencies, as well as rendering the resonances finite width. Furthermore, we will argue, this interaction suffices to account for the non-universality of the plateau. First, however, we consider a simpler situation, where we assume the ripplon spectrum itself is unaffected by coupling to the phonons.

E. Phonon scattering off frictionless ripplons

If $\epsilon > 0$, the phonon absorbing transition occurs from the ground state. The total number of ways to admit energy ω into the system is

$$\rho(\omega) = \int_0^\infty d\epsilon\, n(\epsilon) \sum_{\{n_{lm}\}} \delta(\omega - [\epsilon + \sum_{lm} n_{lm}\omega_{lm}]) = 1/T_g \sum_{\{n_{lm}\}} \theta(\omega - \sum_{lm} n_{lm}\omega_{lm}) e^{-\beta_g(\omega - \sum_{lm} n_{lm}\omega_{lm})}, \qquad (37)$$

where we sum over all occupation numbers of the ripplons with quantum numbers l, m ($m = -l..l$). Using an integral representation of the step function θ, this can be rewritten as

$$\rho(\omega) = \frac{1}{T_g} \sum_{\{n_{lm}\}} \lim_{\epsilon_1 \to 0^+} \int_{-\infty}^{\infty} \frac{dk}{2\pi(ik + \epsilon_1)} e^{ik(\omega - \sum_{lm} n_{lm}\omega_{lm})} e^{-\beta_g(\omega - \sum_{lm} n_{lm}\omega_{lm})}. \qquad (38)$$

The integral in Eq.(38) will be taken by the steepest descent method (SDM). The reason why we do not apply an analogous technique directly to the δ-function in Eq.(37) is not only because we want to get rid of the ϵ integration, but also because that the SDM proved more forgiving in terms of accuracy when used to approximate the θ-function, rather than the δ-function.

For each k on the real axis, the sum over the occupation numbers n_{lm} diverges, so each integral should be taken before the summation. However, in the vicinity of the point that will turn out to be the saddle point k_0 ($\Im k_0 < -\beta_g$) all the sums are finite, so we reverse the order of summation and integration. The integration contour is shifted as shown in see Fig.16.

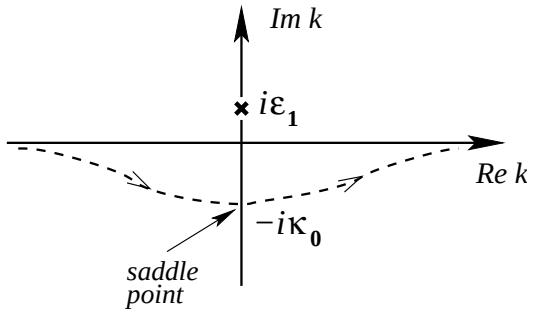


FIG. 16 The integration contour from Eq.(38) is distorted as explained in text. The pole $k = i\epsilon_1$ is shown by a cross. Note the contour does not cross the pole when being shifted off the real axis.

Hence, the saddle-point approximation yields for the value of the integral in Eq.(38) ($\kappa \equiv ik$):

$$\rho(\omega) = \frac{1}{T_g} \frac{1}{\sqrt{2\pi |f''(\kappa_0)|}} \frac{1}{\kappa_0} \exp\{(\kappa_0 - \beta_g)\omega - \sum_{lm} \log[1 - e^{-(\kappa_0 - \beta_g)\omega_{lm}}]\}, \qquad (39)$$

where the saddle point κ_0 is determined from

$$\omega = \sum_{lm} \frac{\omega_{lm}}{e^{(\kappa_0 - \beta_g)\omega_{lm}} - 1} + \frac{1}{\kappa_0} \qquad (40)$$

and the curvature at the saddle point is equal to

$$|f''(\kappa_0)| = \sum_{lm} \frac{\omega_{lm}^2}{4\sinh^2[(\kappa_0 - \beta_g)\omega_{lm}/2]} + \frac{1}{\kappa_0^2}. \qquad (41)$$

As is clear from (40), the approximation amounts to finding the effective temperature so as to populate the ripplonic states to match the excitation energy ω. The expression for the curvature (41) appropriately involves the corresponding heat capacity of the excitations.

The $\omega \to 0$ and the barely relevant $\omega \to \infty$ asymptotics are easily found. As luck has it, the $\omega \to 0$ limit of Eq.(39), apart from $1/T_g$ factor, gives $\exp(1)/\sqrt{2\pi} \simeq 1.08$, only 8% away from the correct 1. The $\omega \to \infty$ yields, on the other hand, $\rho(\omega) \propto \prod_{lm}(\omega/\omega_{lm}) \propto \omega^{96}$, as expected ($\sum_{l=2}^{9}(2l+1) = 96$). The SDM is thus reasonably accurate in this case, which could be at least

somewhat evaluated by computing the value of the fourth order term under the exponent at "one sigma" distance from the extremal action point. This turns out to be satisfactorily small, as demonstrated in Fig.17, along with the density of states itself as a function of ω.

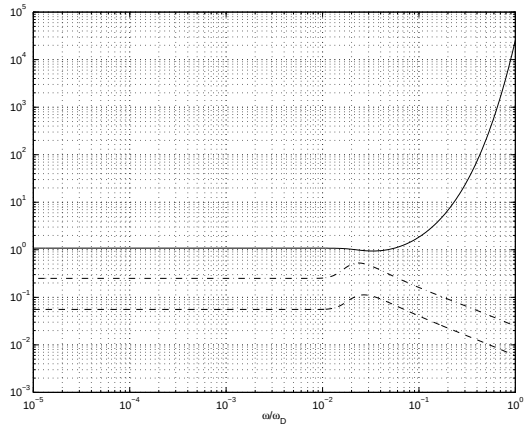


FIG. 17 The solid line shows $\rho(\omega)T_g$ from Eq.(39). The dash-dotted line shows the value of the fourth order term. The third order term, being purely imaginary, contributes only in the sixth order; it is shown as the dashed line, however there are other contributions to the 6-th order.

When estimating absorption from the ground state, we totally ignore the depletion of ground state population at finite temperatures, when the system spends some time in an excited state. This is fine because by the relevant temperatures, the excited state absorption dominates anyway (see Fig.14 and note that $\omega_l - |\epsilon| < \omega_l + |\epsilon|$). This case, i.e. $\epsilon < 0$, is somewhat less straightforward. Let us calculate

$$N_E(\omega) \equiv \int_0^E d\epsilon\, n(\epsilon) \sum_{\{n_{lm}\}} \delta(\omega - [\sum_{lm} n_{lm}\omega_{lm} - \epsilon]). \quad (42)$$

This expression gives the *cumulative* density of absorbing states between energies 0 and E (note the change of sign in front of ϵ). This expression can be used to estimate the total excited state absorption by computing

$$\rho_{exc}(\omega, T) \equiv \int_0^\infty dE\, f(E,T)\, \frac{\partial N_E(\omega)}{\partial E}, \quad (43)$$

where $f(E,T) \equiv 2/(e^{\beta E}+1)$ gives the appropriate Boltzmann weights. The factor of 2 is used in order to calibrate the excited state absorption relative to the ground state case: $f(0,T) = 1$. We now have two θ-functions and consequently two integrations. The SDM value for $N_E(\omega)$ is given by

$$N_E(\omega) = \frac{1}{T_g}\frac{1}{2\pi|\text{"Det"}|^{1/2}}\frac{1}{\lambda_0\mu_0}\exp\{(\beta_g+\lambda_0-\mu_0)\omega + \lambda_0 E - \sum_{lm}\log[1-e^{-(\beta_g+\lambda_0-\mu_0)\omega_{lm}}]\}. \quad (44)$$

The corresponding saddle points are determined from

$$\omega + E = \sum_{lm}\frac{\omega_{lm}}{e^{(\beta_g+\lambda_0-\mu_0)\omega_{lm}}-1} + \frac{1}{\lambda_0} \quad (45)$$

and

$$\omega = \sum_{lm}\frac{\omega_{lm}}{e^{(\beta_g+\lambda_0-\mu_0)\omega_{lm}}-1} - \frac{1}{\mu_0}. \quad (46)$$

Here,

$$|\text{"Det"}| \equiv \sum_{lm}\frac{\omega_{lm}^2}{4\sinh^2[(\beta_g+\lambda_0-\mu_0)\omega_{lm}/2]}\left(\frac{1}{\lambda_0^2}+\frac{1}{\mu_0^2}\right) + \frac{1}{\lambda_0^2\mu_0^2} \quad (47)$$

is the determinant of the curvature tensor in the direction (i.e. 2D subset) of the fastest descent in the 4-dimensional (complex) λ, μ space. The steepest descent approximation turns out to perform well, except at very low frequencies ($\omega < 10^{-2}\omega_D$). However, even though it overestimates the answer, it is still very small compared to the $\rho(\omega)$ calculated earlier at these frequencies, much as the complete result would be. The appropriate graph is shown in Fig.18.

An accurate calculation of the heat conductivity requires solving a kinetic equation for the phonons coupled with the multilevel systems, which would account

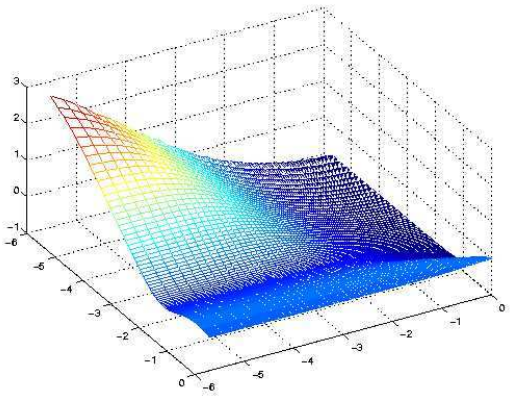


FIG. 18 The value of the fourth order correction in the exponent at the distance of one σ from the saddle point, used to evaluate the adequacy of the SDM, is shown here. Each axes is shown in the base 10 logarithm scale. The error at the low energies ($< 10^{-2}\omega_D$) is extremely large, which is a consequence of the fact that the expression in Eq.(44) gives an incorrect asymptotics as $\omega, E \to 0$. However it still gives a density of states which is less than 1, which is all that matters to us. The performance at the plateau energies, which is essential here, is good. Actually, in order to save space, we have presented here the data for the case with the phonon coupling effects on the ripplon spectrum taken into account ($T_g/\omega_D = 5$). This case is more interesting anyway, and the error here is slightly larger (but still tolerable!), we thus have covered all the cases.

for thermal saturation effects etc. We encountered one example of such saturation in the expression (19) for the scattering strength by a two-level system, where the factor of $\tanh(\beta\omega/2)$ reflected the difference between thermal populations of the two states. Neglecting these effects should lead to an error of the order unity for the thermal frequencies. Within this single relaxation time approximation for each phonon frequency, the Fermi golden rule yields for the scattering rate of a phonon with $\hbar\omega \sim k_B T$:

$$\tau_\omega^{-1} \sim \omega \frac{\pi g^2}{\rho c_s^2} \left[\rho(\omega) + \rho_{exc}(\omega, T)\right]. \qquad (48)$$

The heat conductivity then equals $\kappa = \frac{1}{3}\sum_\omega l_{\rm mfp}(\omega) C_\omega c_s$. The mean free path cannot be less than the phonon's wave-length λ (which occurs at the Ioffe-Riegel condition). Since our theory does not cover the phonon localization regime we account for multiple scattering effects by simply putting $l_{\rm mfp} = c_s\tau_\omega + \lambda$. At high T, the heat is not carried by "ballistic" phonons, but rather is transfered by a random walk from site to site, as originally anticipated by Einstein (Einstein, 1911) for homogeneous isotropic solids. The resultant heat conductivity is shown in Fig.19 We postpone further discussion of the results above until we include the effects of coupling of the resonant transitions to the phonons on the transitions' spectrum.

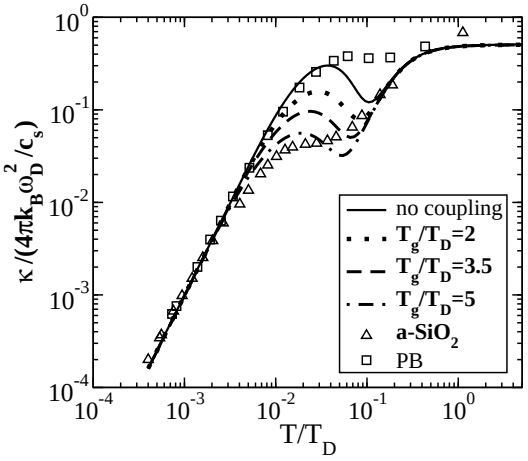


FIG. 19 The predicted low T heat conductivity. The "no coupling" case neglects phonon coupling effects on the ripplon spectrum. The (scaled) experimental data are taken from (Smith, 1974) for a-SiO_2 ($k_B T_g/\hbar\omega_D \simeq 4.4$) and (Freeman and Anderson, 1986) for polybutadiene ($k_B T_g/\hbar\omega_D \simeq 2.5$). The empirical universal lower T ratio $l_{\rm mfp}/l \simeq 150$ (Freeman and Anderson, 1986), used explicitly here to superimpose our results on the experiment, was predicted by the present theory earlier within a factor of order unity, as explained in Section III.B. The effects of "non-universality" due to the phonon coupling are explained in Section IV.F.

F. The effects of friction and dispersion

A transition linearly coupled to the phonon field gradient will experience, from the perturbation theory perspective, a frequency shift and a drag force owing to phonon emission/absorption. Here we resort to the simplest way to model these effects by assuming that our degree of freedom behaves like a localized boson with frequency ω_l. The corresponding Hamiltonian reads:

$$H = \omega_l a^\dagger a + \sum_{\mathbf{k}} \omega_k b_{\mathbf{k}}^\dagger b_{\mathbf{k}} + \sum_{\mathbf{k}} \frac{(\mathbf{gk})}{\sqrt{2\omega_k V\rho}} (a^\dagger b_{\mathbf{k}} + b_{\mathbf{k}}^\dagger a). \quad (49)$$

The ensuing equations of motion are

$$\dot{a} = -i\left[\omega_l a + \sum_{\mathbf{k}} \frac{(\mathbf{gk})}{\sqrt{2\omega_k V\rho}} b_{\mathbf{k}}\right],$$
$$\dot{b}_{\mathbf{k}} = -i\left[\omega_k b + \frac{(\mathbf{gk})}{\sqrt{2\omega_k V\rho}} a\right]. \qquad (50)$$

We next introduce the following (retarded) Green's functions $A(t) \equiv -i\theta(t)\left\langle[a(t), a^\dagger(0)]\right\rangle$ and $B(t) \equiv -i\theta(t)\left\langle[b(t), a^\dagger(0)]\right\rangle$. The fourier transforms of these Green's functions will consequently obey

$$(\omega - \omega_l)\widetilde{A} = \frac{1}{2\pi} + \sum_{\mathbf{k}} \frac{(\mathbf{gk})}{\sqrt{2\omega_k V\rho}} \widetilde{B}_{\mathbf{k}}$$
$$(\omega - \omega_k)\widetilde{B}_{\mathbf{k}} = \frac{(\mathbf{gk})}{\sqrt{2\omega_k V\rho}} \widetilde{A}. \qquad (51)$$

From Eqns.(51), one determines the real and imaginary parts of the Green's functions self-consistently. We however can disregard the phonons' dispersion and damping which introduces an error in a higher order, in so far as the shifted frequencies ω_l's are concerned. This yields

$$\widetilde{A} = \frac{1}{2\pi}\left(\omega - \omega_l - \frac{1}{3}\frac{g^2}{4\pi^2\rho c_s^2}\lim_{\epsilon_1\to 0^+}\int_0^{k_c}\frac{k^3\,dk}{\omega/c_s + i\epsilon_1 - k}\right)^{-1}, \tag{52}$$

where k_c is the cut-off wave-vector whose value will be discussed shortly (we have also replaced $\sum_{\mathbf{k}} \to V\int\frac{d^3\mathbf{k}}{(2\pi)^3}$). Eqn.(52) gives immediately for the inverse life-time of the internal resonance

$$\tau_{\omega_l}^{-1} = \frac{g^2}{4\pi\rho c_s^2}\left(\frac{\omega}{c_s}\right)^3 \simeq \frac{3\pi}{2\hbar}T_g\left(\frac{\omega}{\omega_D}\right)^3, \qquad \omega \le \omega_c \tag{53}$$

and its frequency shift

$$\begin{aligned}\omega_l(\omega) &= \omega_l - \frac{g^2}{4\pi^2\rho c_s^2}\int_0^{\omega_c}\frac{d\omega'(\omega'/\omega_c)^3}{\omega'-\omega}\\ &\simeq \omega_l - \frac{3}{2\hbar}T_g\left(\frac{\omega_c}{\omega_D}\right)^3\int_0^{\omega_c}\frac{d\omega'(\omega'/\omega_c)^3}{\omega'-\omega},\end{aligned} \tag{54}$$

where the factor of 1/3 has disappeared because we have accounted for the three phonon polarizations and also ignored the distinction between the longitudinal and transverse branches. The singularity in Eq.(54) at $\omega \to \omega_c$ is completely artificial, as the cut-off is not supposed to be sharp. In our numerical estimates, we use a cut-off smeared by $\delta\omega_c = \omega_c/\sqrt{D}$, where D is the glass' fragility (see Appendix A); this is however totally unimportant as the divergence is only logarithmic. According to Eq.(54), the frequency shift scales roughly with ω_c^3 and is thus rather sensitive to its value. Due to the dispersion, the resonance in Eq.(52) is effectively broadened because the value of the integral in Eq.(54) is positive for sufficiently small ω, but turns negative at a frequency which is a multiple of ω_c.

We approximate the phonon coupling effects by replacing in our spectral sums in Eqs.(39-41), (44-47) the discrete summation over different ripplon harmonics by integration over "lorentzian" profiles:

$$\sum_l \int d\omega\,\delta(\omega-\omega_l) \to \sum_l \int d\omega\,\frac{\gamma_\omega/\pi}{[\omega-\omega_l(\omega)]^2+\gamma_\omega^2}, \tag{55}$$

where $\gamma_\omega \equiv \tau_\omega^{-1}$ is a (frequency dependent) friction coefficient and $\omega_l(\omega)$ is the ripplon frequency shifted due to the dispersion effects. This approximation amounts to having the total inverse life-time of a transition involving more than one mode being the sum of the inverse life-times of the participating modes. This would be correct in the case of a frequency independent γ, but should be still adequate at the low T end of the plateau, where the absorption is mostly due to single ripplon mode processes.

The value of the cut-off frequency ω_c is close to but larger than $(a/\xi)\omega_D$ (see Appendix B), as the phonons whose wave-length is shorter than ξ cause an increasingly smaller effective gradient of the phonon field as sensed by a region of size ξ. These shorter wave-length phonons will still strongly interact with the droplets, however at this point we could only emulate that to some extent by increasing ω_c. This also brings us back to the radiation life-time's frequency dependence. It is now clear that for $\omega_l(\omega) > \omega_c$, γ_ω will not follow the simple cubic dependence cited above, the latter being probably still a safe lower estimate. We will thus use the above expression as it makes little difference computationally in the region of such intense damping. At the corresponding temperatures, the scattering is probably better formally described by the stochastic resonance (Gamaitoni *et al.*, 1998) methodology anyway.

We are now ready to discuss the non-universality of the plateau. It is evident from Eqs.(53)-(54) that even though the absorbers' frequencies are determined by the quantum energy scale ω_D, the overall effective frequency *shifts* scale with T_g. The ratio T_g/ω_D seems to vary within the range of between 2 and 5 among different glasses, and the non-universality in this number could have a substantial effect subject to the value of ω_c. As argued in Appendix B, a value of $\omega_c < 2.5(a/\xi)\omega_D$ is justified. $\omega_c = 1.8(a/\xi)\omega_D$ seems to yield the experimentally observed spread in the plateau's position. Our results for three values of T_g/ω_D are shown in Fig.19. Since ω_c should be regarded as an adjustable parameter we can claim to possess only circumstantial evidence that the plateau's non-universality is caused by the spread in the value of the ratio of the two main energy scales in the problem: the classical T_g and the quantum ω_D. On a speculative note, this phenomenon may be a sign of strong mixing (and thus level repulsion) between the ripplons and the phonons, as implicitly confirmed by a phonon localization transition at frequencies just above those at the plateau. Indeed, the self-energy of an internal resonance of dimensions ξ coupled with strength g to an elastic medium scales (within perturbation theory) as $g^2/\rho c_s^2\xi^3 \propto T_g$. This can be viewed as lowering of an impurity band edge due to the interaction with the phonons, yet another way to express the existence of mixing between the resonant transitions and the elastic waves. Within our theory, the non-universality of the plateau is an internally consistent proof that the degrees of freedom causing the Boson Peak are *inelastic* ones, whose coupling with the phonons then must be equal to g related to the value of T_g through the stability requirement explained in Section III.

We now comment on the plateau slopes in Fig.19 being noticeably more negative than the experimental value. The explaination is, we did not solve the full kinetic equation for the interacting system, but used a simplistic single life-time approximation. We demonstrate this issue by briefly presenting a slightly different way to estimate $\rho_{exc}(\omega,T)$ from Eq.(43). Here, we imagine we do not

exactly know the thermal weight function $f(E,T)$ due to the lack of knowledge of the life-times in the multilevel system. On general grounds, however, this function should decrease rapidly for $\omega > \alpha T$, where the α is of order unity. This yields $\rho_{exc}(\omega,T) \simeq N_{\alpha T}(\omega)$ (where $N_E(\omega)$ was defined in Eq.(42)). We show the result of this approximation for reasonable $\alpha = 1$ and $\omega_c = 2(a/\xi)\omega_D$. Even though these curves resemble the experimental data

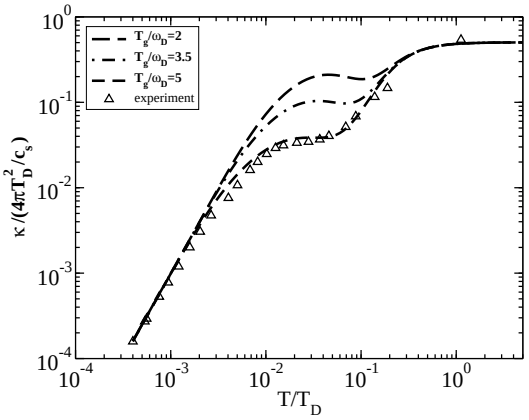


FIG. 20 The predicted low T heat conductivity for three diferent values of $T_g/\omega_D = 5, 3.5, 2$ for a simpler model of the scattering density as explained in text. The a-SiO_2 is the same as in Fig.19.

better than in the previous figure, they do not really provide more material support for the theory than the earlier method. This discussion simply demonstrates that the basic estimates are robust enough to "survive" different levels of treatment. Also, curiously, these curves reflect the experimental tendency that the higher T plateaux seem to have a more negative slope as compared to the low T ones (see Fig.1), which was less obvious in Fig.19.

Finally in this subsection, we return to the specific heat. The effects of the phonon coupling on the ripplon spectrum can be taken into account in the same fashion as in the conductivity case. Here, we replace the discrete summation in Eq.(36) by integration over the broadened resonances, as prescribed by Eq.(55). The bump, as shown in Fig.15, is also predicted to be non-universal depending on T_g/ω_D. The predicted bump for $T_g/\omega_D = 2$ seems to match the best the available data for a-SiO_2, whereas the more appropriate $T_g/\omega_D \sim 4$ is about a factor of 3 lower in temperature. It is somewhat unsatisfying that the plateau's and the bump's position can not be thus both made to exactly match the experiment at the same time say by adjusting ω_l, which is certainly allowed given the qualitative character of some of the estimates. However, since we had to employ an approximation when calculating the scattering density of states, the discrepancy does not warrant too much concern, in our opinion.

G. The Relaxational Absorption

In addition to the resonant absorption, an internal resonance will also provide a so called "relaxational" scattering mechanism. Since a cross-over to the multilevel behavior of the tunneling centers leads to an increased resonant scattering, we must check whether the relaxation mechanism is enhanced as well. This latter mechanism arises because a passing phonon modifies the energy bias of a particular pair of internal states. This causes irreversible thermal equilibration processes within each pair, resulting in energy dissipation (Jäckle *et al.*, 1976; Maynard, 1975). This phenomenon is sometimes referred to as the bulk viscosity (Landau and Lifshitz, 1987). One important difference between the relaxational and resonant absorption is that the former does not saturate and can easily exceed the latter at low enough temperature and high enough sound intensity, which is what is usually observed in ultrasonic experiments unless special care is taken (Hunklinger and Raychaudhuri, 1986) (this saturation is not an issue in heat conductance, owing to the rather low sound intensities in these experiments). Applying the notion of the relaxational absorption to the two-level systems explained well the shape of the maximum in the temperature dependence of the sound speed at very low frequencies at $\sim 1K$ (Hunklinger and Raychaudhuri, 1986), which is one of the impressive achievements of the TLS model. In (Hunklinger and Raychaudhuri, 1986), the relation between the slopes of the logarithmic temperature profiles around the maximum was explained. At higher T, the logarithmic decrease in c_s is followed by what has been viewed by others as a mysterious linear law (Belessa, 1978). At higher frequencies still, the logarithmic decrease is outweighed by the just mentioned linear T dependence. We have argued that the increase in the density of the scattering states is due to thermal activation of the vibrational states of the domain walls, or matching of the thermal phonon frequency with that of a ripplon on a mobile domain wall. Does the existence of the vibrational modes modify the relaxational scattering as compared to a bare underlying two-level system? The answer is: not significantly, for the following reason. The magnitude of the dissipation due to the bulk viscosity depends on the number of local distinct molecular configurations, populated according to the Boltzmann statistics. A shift in this population results in relaxational dissipation. While having a domain wall excited may modify the energy scale in the Boltzmann distribution, which may produce some effect, it does not change the number of the intrinsic ("inelastic") glassy states, and thus will not on average enhance the relaxational scattering. This is to be compared to the resonant scattering, which depends on the degeneracy of the ripplon states and will thus intensify at higher T, subject to the degree of the ripplon's linearity. While the relaxational mechanism thus seems to play only a minor role in the phonon absorption at the plateau temperatures, its effects are observable and can

explain, as we will argue below, the temperature independent $\log\omega$ part in the sound speed variation as measured in (Belessa, 1978). According to (Jäckle *et al.*, 1976), the variation in the speed of sound due to a collection of two-level systems is

$$\left.\frac{\delta c_s}{c_s}\right|_\omega = \left\langle\!\!\left\langle \frac{g^2}{2\rho c_s^2}\left(\frac{\epsilon_i}{E_i}\right)^2 \frac{\beta}{\cosh^2\beta E_i}\,\frac{1}{1+\omega^2\tau_i^2}\right\rangle\!\!\right\rangle, \quad (56)$$

where

$$\tau_i \simeq \frac{3g^2\Delta_i^2 E_i}{2\pi c_s^5}\coth(\beta E_i/2) \quad (57)$$

is the radiative life-time of the ith TLS (Jäckle, 1972) (see also Eq.(53)), and the double angular brackets denote averaging with respect to E_i, Δ_i and τ_i. While it would seem that detailed information on the relevant parameters' distribution is necessary to use Eq.(56), some qualitative conclusions can be made on general grounds. First, for small ω the average is dominated by the long life-time systems, i.e. those with $\Delta \ll E$ and thus $\epsilon \sim E$. As a result, the averaging over these systems is not very sensitive to the possible correlation between E_i and τ_i, and thus the summation over the two-level system (nearly flat!) spectral density $\sim \int d\epsilon(1/T_g\xi^3)$ introduces, within order unity, only a numerical factor proportional to T/T_g (and eliminates the explicit temperature dependence). As just argued, the $(\epsilon/E)^2$ factor should only give a correction factor of order unity, and we are left with averaging expression $1/(1+\omega^2\tau_i^2)$ with respect to the life-time distribution. At low frequencies ω, this averaging will be dominated by the TLS with the long life-times. Quite generally, for large τ, $P(\tau)d\tau \propto d\tau/\tau$ because τ^{-1} scales algebraically with Δ, and the distribution of $\log\Delta$ is flat (at least for small Δ), or, almost flat, up to a weak power law, as argued earlier. More specifically, for a two-level system coupled linearly to the elastic strain, $\tau^{-1} \propto \Delta^2 E$ (Eq.57). Therefore at each E (which is incidentally only weakly dependent on Δ in the relevant long life-time case $\Delta/E \ll 1$), obviously $d(\log\Delta) = const \Rightarrow d(\log\tau) = const$. Thus the averaging w.r.t. τ will produce a term of the order $\sim (g^2/\rho c_s^2)(1/T_g\xi^3)\log\omega$, which is of the right order of magnitude (and sign!). Since the dimensionless factor in front of the $\log\omega$ term has been shown to be universal ($\propto (a/\xi)^3$), the present theory predicts that it should not vary significantly among the insulating glasses; in fact, according to our argument, it is proportional to the coefficient α at the logarithmic temperature dependence of the sound speed variance in the TLS regime, a rather universal quantity indeed (Leggett, 1991). We stress however that the just predicted TLS-like property should be observed in the *plateau* regime. A deviation would be a sign of more than two inelastic states playing a role in the transition. We finally mention that the lower limit in the integral over the life-time distribution should produce a $\log T$ term, which would be however masked by the stronger linear dependence.

V. QUANTUM EFFECTS BEYOND THE STRICT SEMI-CLASSICAL PICTURE

A. Quantum Mixing of a Tunneling Center and the Black-Halperin Paradox

The preceding sections have shown that structural transitions, accompanied at high enough temperatures by vibrational excitations of the mosaic, account for the most conspicuous departures of the low temperature behavior of glasses from the prescriptions of a standard harmonic lattice theory - namely the existence of multilevel intrinsic resonances in a amorphous sample made by quenching a supecooled liquid. At the lowest temperatures these resonances behave for the most part as if they were two-level systems, while at higher T the density of states of these intrinsic excitations grows considerably and leads to the Boson Peak phenomena. While we have computed the density of states accessible by *tunneling* even at the lowest temperatures, we have assumed, within a semi-classical approach, that having a small tunneling barrier between alternative local structural states does not affect significantly the corresponding spectrum $n(\epsilon)$ of the lowest energy transitions from its classically defined value. Likewise, we have assumed that the vibrational spectrum of moving domain walls is unaffected by the presence of tunneling, that would in principle mix those vibrations quantum mechanically. Clearly, the transitions that are active at low T must have some significant (even if small) overlap between the wave-functions corresponding to the alternative structural states. This overlap would lead to the familiar effects of repulsion between the semi-classically determined energy levels. This could be described as partial quantum melting of some tunneling centers, but it is probably better to use term "quantum mixing".

In this section we estimate the magnitude of these quantum mixing effects. Even though the strictly semiclassical theory agrees well with experiment as is, making such estimates that go beyond it is useful for two distinct reasons. First, we must check to what extent the semiclassical picture, tacitly assumed earlier, is a consistent zeroth order approximation to a more complete treatment. Second, it is important to ask whether the expected corrections to the strict semiclassical theory lead to observable consequences. In what follows, we provide approximate arguments that indeed such corrections are discernible and may even potentially answer some long-standing puzzles in this field.

Quantum Mixing. As the starting point in the discusion, we consider a simplified version of the diagram of a tunneling center's energy states from Fig.14 with $\epsilon < 0$, as shown on the left hand side of Fig.21. We remind the reader that the $\epsilon < 0$ situation, explicitly depicted in Fig.21, implies lower transition energies than when the semiclassical energy difference $\epsilon > 0$ and thus dominates the low temperature onset of the Boson Peak and the plateau.

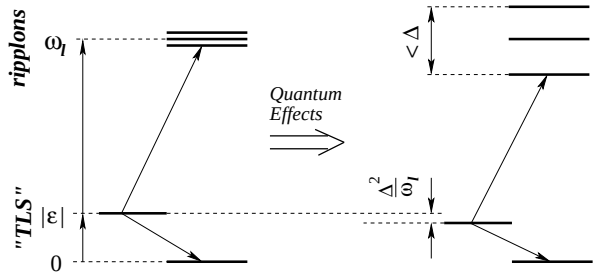


FIG. 21 A low energy portion of the energy level structure of a tunneling center is shown. Here, $\epsilon < 0$, which means that the reference, liquid, state structure is *higher* in energy than the alternative configuration available to this local region. A transition to the latter configuration may be accompanied by a distortion of the domain wall, as reflected by the band of higher energy states, denoted as "ripplon" states.

Accounting for tunneling, the low energy portion of the Hamiltonian that corresponds to Fig.21 is as follows:

$$H_i = \begin{pmatrix} 0 & \Delta/2 & 0 & 0 \\ \Delta/2 & |\epsilon| & \Delta_{i_1} & \Delta_{i_2} \\ 0 & \Delta_{i_1} & \hbar\omega_{i_1} & 0 \\ 0 & \Delta_{i_2} & 0 & \hbar\omega_{i_2} \end{pmatrix}, \tag{58}$$

where the semi-classical values of the ripplonic energies are denoted as $\hbar\omega_i$ and the transition amplitudes to those levels are Δ_i respectively (only two lowest of those ripplonic states are shown in Eq.(58)). As argued in detail in Section IV, only one of the lowest two energy levels in a tunneling center (the top one in this case) is directly coupled to the higher, ripplonic, energy states. Obviously, virtual transitions to those high energy states will result in lowering the energy of the higher level. There are no direct transitions from the bottom state of energy 0, as explained in the previous Section, and therefore its position is unaffected by the presence of the ripplons. Consequently, the effective energy splitting of the two-level system (with $\epsilon < 0$) will be lower than the classical value obtained earlier, and the smaller the original value of ϵ was, the more pronounced the effect will be. In what follows we estimate the consquences of this effect on the apparent energy spectrum of the lower excitations, i.e. the empirical two-level systems. In the limit of inifinitely small tunneling amplitude Δ, the decrease in ϵ could be estimated using a perturbative expansion:

$$|\tilde{\epsilon}| = |\epsilon| - \sum_i \frac{\Delta_i^2}{\hbar\omega_i - |\tilde{\epsilon}|}. \tag{59}$$

Here, $\tilde{\epsilon}$ is the new value of the energy splitting, ω_i's are the ripplon frequencies and Δ_i's are tunneling amplitudes of transitions that excite the corresponding vibrational mode of the domain wall. Those amplitudes will be discussed in due time; for now, we repeat, the expression above will be correct in the limit $\Delta_i/\hbar\omega_i \to 0$. Finally, the renormalized value $\tilde{\epsilon}$ was used in the denominator. While, according to Feenberg's expansion (Feenberg, 1948), including $\tilde{\epsilon}$ in the resolvent is actually more accurate, we do it here mostly for convenience.

Given that the semi-classical values of eigen-values $\hbar\omega_i$ are known, the low energy portion of the energy level structure of the tunneling center, as shown in Fig.21, gives a quantitative idea of the eigen-energies of the full Hamiltonian only in the limit of a very small tunneling splitting Δ. In a complete treatment, all transition amplitudes must be included and the Hamiltonian diagonalized. In general, such diagonalization (and, in our case, the system's "quantization") is difficult, however could still be conducted approximately in some cases of interest. Consider, for the sake of argument, the following situation, where Δ is not necessarily smaller than ϵ but $\sum_i \Delta_i^2/\hbar\omega_i$ is. In this arrangement, the energy shift due to the higher lying states can be computed using perturbation theory and yields a "renormalized" value of the classical energy difference that we have called $\tilde{\epsilon}$. This procedure also modifies the tunneling amplitude Δ of the underlying TLS by a *multiplicative* factor according to

$$\widetilde{\Delta} = \Delta \left(1 - \frac{1}{2} \sum_i \frac{\Delta_i^2}{(\hbar\omega_i)^2} \right). \tag{60}$$

Following this, the full energy splitting of the TLS tunneling transition is computed using $E = \sqrt{\Delta^2 + \tilde{\epsilon}^2}$. The important feature of the argument is that Δ (or $\widetilde{\Delta}$) is allowed to take arbitrarily large values relative to ϵ and the ratio of the two parameters is not treated perturbatively. The lowering of ϵ due to virtual transitions among the higher energy states changes somewhat the effective density of transition energies E that directly enters into the heat capacity and conductivity calculations. While Eq.(59) is perturbative, it should accurately give finite effects in the mean-field limit of infinitely many transitions $\hbar\omega_i$ coupled infinitely weakly to one of the two bottom states of the tunneling center. We will analyze the physical consequences assuming the accuracy of Eq.(59). We must, of course, bear in mind that while a tunneling center is nearly a meanfield entity, owing to the strong correlations, it is actually of finite, albeit molecularly large size. Let us plot $|\epsilon|$ as a function of $|\tilde{\epsilon}|$ (see Fig.22(a)). Clearly, the smallest allowed value of the effective classical splitting $|\tilde{\epsilon}|$ of zero corresponds to a finite value of $|\epsilon|$ equal to

$$\Sigma \equiv \sum_i \frac{\Delta_i^2}{\hbar\omega_i}. \tag{61}$$

Therefore, smaller values of $|\epsilon|$ do not correspond to physically realizable systems, according to Eq.(59). The overall excitation spectrum of the structural transitions with those (small) values of $\epsilon < \Sigma$ is strongly affected by the ease of tunneling. As a consequence, the ϵ and Δ distributions become correlated. The quantity $\sum \Delta_i^2/\hbar\omega_i$ is of central importance for this section of the article, therefore we will discuss it now in some detail. The wave-functions of the highly quantum tunneling centers

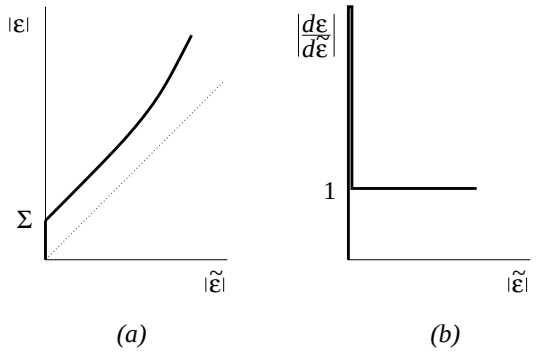


FIG. 22 Shown in panel (a) is the relation between the bare energy difference ϵ between frozen-in structural states in a glass and the effective splitting $\tilde{\epsilon}$ that is smaller due the level repulsion in the tunneling center. Panel (b) depicts schematically the derivative of ϵ with respect to $\tilde{\epsilon}$, which is used to compute the new effective distribution $P(\tilde{\epsilon})$ of the transition energies.

are heavily mixed combinations of the classical states corresponding to potential energy minima. Transitions between such states are strongly coupled to lattice vibrations and, among other things, would strongly scatter phonons. This result is expected on rather general grounds and was exploited earlier when we noted that the eigen-states of the classical potential energy are largely unrelated to the eigenstates of the vibrational modes of the domain wall, hence one expects that transition amplitudes of exciting a ripplon (which, loosely speaking, is a highly anharmonic combination of both structural and vibrational modes of the lattice) are expected to be comparable to the ripplon energy itself. If this is the case, then number Σ is actually very large relative to ϵ and one, strictly speaking, should not use a *perturbative* expression, such as in Eq.(59) in order to assess the lowering of ϵ due to quantum effects. We note, however, it is more likely that the seeming discrepancy simply stems from our "quantization" procedure being so far rather naive, so let us slow down a bit and attempt to outline briefly a more careful way to quantize the tunneling centers's dynamics. First of all, recall that we actually know the values ω_i in a strongly quantum regime, because they were computed assuming a freely moving membrane. On the other hand, we know that in the classical limit domain wall vibrations are indistinguishible from the lattice vibrations. Remarkably, the vibrational eigen-frequencies of a "box" of dimensions ξ - ω_D times a number from a/ξ to 1 - span roughly the same range of energies that the ω_i's do. Therefore, even though the quantization procedure will "reshuffle" all the ripplonic states, it will not significantly shift their position as a whole. Next, since static lattice inhomogeneities scatter phonons only elastically, the coupling of the ripplonic excitations to the phonons must scale with a positive power of Δ so as to vanish in the classical limit. Consequently, in the limit of small tunneling matrix element Δ, the transition amplitudes Δ_i's must scale with a positive power of Δ. On the other hand, as mentioned many times, in the quantum regime, the Δ_i's are of the order $\hbar\omega_i$ and are not directly related to Δ. Therefore, a careful quantization procedure of introducing quantum tunneling in the system must combine and rationalize both of those seemingly conflicting notions. It will turn out that in the quantum regime, the Δ_i's are related to the strength of the underlying tunneling transition Δ only in a certain renormalized sense. We will now outline this renormalization/quantization procedure. This procedure imposes certain restrictions on how adding the possibility of tunneling to a local structural transition can be performed, so that the structure of the energy levels of the transition, that we know from general arguments, is *preserved*. Recall that "switching on" tunneling to the higher energy states $\epsilon+\hbar\omega_i$ not only lowered ϵ, but also made Δ smaller by a factor of $[1-\sum_i \Delta_i^2/(\hbar\omega_i)^2]$. This expression is only valid if the sum is a small number, so that the whole correction factor is necessarily positive and only changes the effective *magnitude* of the matrix tunneling element, but not its sign. We must require that Δ not change its sign in the course of the "quantization", but only its absolute value, because the (ordinarily small) value Δ only reflects the (ordinarily small) *configurational* overlap between two local structural states, while the sign (or complex phase, in general) bears no special meaning here because no particular *spatial* symmetry is involved in the problem. (Such spatial symmetry is important, for instance, when computing overlaps between eigenstates, or near-eigenstates of orbital momentum centered around close locations in space.) Thus, the final answer should depend only on $|\Delta|^2$. This becomes especially evident after the following realization. Note that the expression in the brackets in Eq.(60) is a small coupling limit of what can be considered a Franck-Condon factor. The appearance of such a factor after the introduction of non-zero transition amplitudes is natural: the degrees of freedom that used to be classical and static, can now follow to some extent a selected motion in the system. The Franck-Condon (FC) factor is the overlap between the the initial and final wave-functions of these other ("ripplonic") degrees of freedom, corresponding to the initial and final configuration of that selected motion. (A well known example of a FC factor arising in an analogous, dynamical fashion is the tunneling matrix element renormalization in the spin-boson problem (Leggett *et al.*, 1987).) Let us suppose, in a simplified manner, that the effective renormalization of *all* of the newly introduced tunneling amplitudes occurs in a similar fashion. This allows one to self-consistently close Eq.(60) and rewrite it for a representative amplitude Δ_Q:

$$\widetilde{\Delta}_Q = \Delta_Q \left[1 - \frac{B}{2} \frac{\widetilde{\Delta}_Q^2}{(\hbar\omega_D)^2} \right], \qquad (62)$$

where replacing Δ_Q by $\widetilde{\Delta}_Q$ inside the brackets preserves the approximation's order. B is a numerical constant, reflecting the sum over ripplon states with their vibra-

tional frequencies ω_i, and we have replaced ω_i by the Debye frequency ω_D. The two must be related at the end of the renormalization, as we already know. Identifying the expression in brackets with a Franck-Condon factor reminds us that Δ_Q (or $\widetilde{\Delta}_Q$) is not only a (generic) tunneling amplitude but also can be considered a coupling constant, therefore only its absolute value is physically relevant in the present context, not its sign. The smallness of Δ_Q and $\widetilde{\Delta}_Q$ lets us recast Eq.(62) as

$$d\log\left(\frac{\widetilde{\Delta}_Q}{\Delta_Q}\right) = -\frac{B}{2}d\left[\frac{\widetilde{\Delta}_Q^2}{(\hbar\omega_D)^2}\right], \tag{63}$$

where the reference state is $\widetilde{\Delta}_Q = \Delta_Q = 0$, $\lim_{\Delta_Q\to 0}(\widetilde{\Delta}_Q/\Delta_Q) = 1$ (that is "no tunneling" $\Rightarrow$ "no renormalization"). Notice that the r.h.s. of Eq.(63) depends explicitly only on the effective tunneling element $\widetilde{\Delta}_Q$, but not on the original (tunable) perturbation strength Δ_Q. We therefore can use the differential relation in Eq.(63) to extend the perturbative construction from Eq.(62) into the region of arbitrarily large values of the bare coupling Δ_Q by using the outcome of the previous (infinitesimal) change in Δ_Q as the initial input in the subsequent increment $d\Delta_Q$. Each of these increments is a small perturbation around a new, self-consistently determined, value of $\widetilde{\Delta}_Q$. One gets the following self-consistent equation for the effective tunneling amplitude as a result:

$$\widetilde{\Delta}_Q = \Delta_Q e^{-\frac{B}{2}\frac{\widetilde{\Delta}_Q^2}{(\hbar\omega)^2}}. \tag{64}$$

Our renormalization procedure is internally consistent in that the physical value of the tunneling amplitude depends on the scaling variable - the bare coupling Δ_Q - only logarithmically. This bare coupling must scale with the only quantum scale in the problem - the Debye frequency, as pointed out yet in the first section.

In a more complete treatment, the Δ renormalization would not be characterized by a single "Franck-Condon" parameter, but by a distribution of Franck-Condon factors. Therefore, the exponential form in Eq.(64) might be possibly replaced by a different, perhaps a polynomial expression. In fact, one may think minimally of Eq.(64) as of one of the possible Padé extensions of the perturbative formula (62). At any rate, such a Padé approximant will retain the main feature of Eq.(64) in that the value of the observable tunneling matrix element $\widetilde{\Delta}_Q$ is bounded from above and depends strongly on the (semi-)classical energies $\hbar\omega_i$. According to the discussion above, this restriction stems from a self-consistency condition, namely that the leading term in the exponent in Eq.(64) must scale with $\widetilde{\Delta}_k^2$, if this same number $\widetilde{\Delta}_k$ is on the l.h.s. in that equation. An important corollary of this is that the perturbative term inside the brackets of Eq.(60) must scale with $\widetilde{\Delta}^2$ itself, hence the perturbation correction Σ will scale with $\widetilde{\Delta}^2$ too (from now on, we will drop tildes from the symbols denoting the physical tunneling amplitudes, but retain them for the effective ϵ's). That is, with our definition of B, it is roughly true that

$$\Sigma = B\frac{\Delta^2}{\hbar\omega_D}. \tag{65}$$

We have thus demonstrated explicitly that the magnitude of quantum effects on the classical energy splitting ϵ on a particular site should depend on the facility of tunneling at that same site. We have therefore established that the fact of quantum Δ_i being close in value to a rather large energy scale ω_i is consistent with a relatively small value of the correction in Eq.(59) and its scaling with Δ^2. As another dividend from the argument, we obtain a ballpark estimate of the constant B. A structural transition that is thermally active at a plateau temeperature $k_BT \sim \hbar\omega_i$ and being an efficient phonon scatterer, will have $\Delta \sim \hbar\omega_i$. Therefore, $B = \sum_i \omega_D/\omega_i$, will be a number on the order of several hundreds, since the total number of the ripplonic modes (at the laboratory glass transition, at which $\xi/a \simeq 5..6$) is approximately a hundred, and ω_i is proportional to, but somewhat smaller than the Debye frequency ω_D.

Eq.(65) implies that while the distributions of the classical energy splittings ϵ and the bare semiclassical tunneling amplitude Δ may be uncorrelated, quantum corrections require that $\tilde{\epsilon}$ and Δ be correlated for systems with a sufficiently low barriers and which simultaneously have small energy difference between the initial and final structural state. Conversely, the independence approximation is valid when, roughly, $|\epsilon| > B\frac{\Delta^2}{\hbar\omega_D}$. Since Δ is proportional to $\hbar\omega_D$, this criterion is a formal restatement of an earlier comment that the theory is strictly valid in the classical limit. (Note that there is also a (much stronger) $\hbar$ dependence in the exponent of the tunneling element Δ (see Eq.(21)). While, obviously, only a negligible fraction of the *total* number of structural rearrangements in the liquid at T_g would not satisfy the classicality criterion, these particularly facile transitions do actually comprise a significant portion of those transitions that are thermally active at *cryogenic* temperatures. We will now indicate what the observable consequences of this deviation for the strict semiclassical limit are. In order to do this, let us discuss first the difference between the strongly quantum and the bare "classical" structural transitions.

According to Eq.(59), for all transitions, whose diagonal energy difference would be $|\epsilon| < \Sigma$ in the classical limit, the effective diagonal splitting $\tilde{\epsilon}$ is actually zero, meaning that the full energy splitting E is entirely comprised of the originally *off-diagonal* energy scale Δ. This implies that the energy eigen-states of such highly mixed tunneling centers are heavy superpositions of the original classical structural states and would not be easily interpreted in terms of the atomic coordinates of the potential minima alone, but must include the kinetic energy term as well. This is directly related to the well known ambiguity in separating the energy of such systems into potential

and kinetic components even at conditions that are entirely classical, such as at a high temperature. Of course, in such cases *free energy* formulations must be employed that allow one to count the number of configurational states unambiguously, while using "inherent" structures based on *potential* energy stationary points alone is of limited utility. The strongly quantum case can be loosely understood by transcribing the complex multiparticle rearrangements onto a single collective "reaction" coordinate (as in the soft potential model (Galperin *et al.*, 1991)). In fact, this analogy to a single coordinate soft potential model is quite loose because of the much higher density of states of the ripplons (that give rise to the Boson Peak and correspond to the vibrations of the membrane) compared with the density of states of the soft potential model, which is one dimensional so that only one coordinate is vibrationally excited. Nevertheless, following this analogy, consider a two-well potential (with very steep outer walls) with a barrier high enough so that the physical coordinate eigen-states corresponding to the particle being in the left or the right well are unambiguously definable and the diagonal component of the transition's energy is equal to the difference in the potential energy of the two well with high accuracy. Imagine next lowering the barrier. In the limit of zero barrier the system is simply a particle in a square box, whose energy scale is determined by the quantum energy scale in the problem - that is the particle's kinetic energy alone. This analogy reminds us that just like the transition from a largely classical to quantum behavior in a double well potential, the transition at $|\epsilon| = \Sigma$ is not sharp (note, however, that unlike in a one dimensional soft-potential model, the density of excited states of a tunneling center is very high thus possibly leading to a sharper cross-over). Put another way, this "phase transition" clearly corresponds to term-crossing and therefore would be gradual in a finite system. From a mean-field perspective, the transition at $\epsilon = \Sigma$ resembles a de-localization phase transition (see e.g. (Abou-Chacra *et al.*, 1973)) which we may think of as quantum depinning of the domain wall. Alternatively, one could say that the local structure of classical energy levels melts out locally in that the energy variation on the mostly classical landscape (determined by T_g) happens locally to be smaller than the confinement kinetic energy of the domain wall motion. Of course, this is occuring for only small parts of an otherwise rigid matrix. Again, since the system is finite, one expects a soft cross-over rather than a sharp transition when such "melting" occurs. Both ways of interpreting the quantum mixing/melting described above are consistent with our view of the tunneling process leading to the expression (21) for the tunneling amplitude Δ. The action exponent in Eq.(21) scales as the height of the barrier relative to the under-barrier frequency. The former quantity, while distributed, scales with the classical energy scale in the problem - T_g, while the latter is proportional to the Debye frequency (and, most likely, is somewhat distributed too). The quantum limit of large $\hbar\omega_D$ corresponds to a narrow barrier and a short tunneling path. This would imply the relative unimportance of the classical energy landscape modulation during the tunneling process. Finally, in order to avoid ambiguity, we stress that the structural transitions of both types of tunneling centers, that we have called "classical" (in that the wave functions are well localized near minima and are well defined structurally, i.e. in position space) and "quantum" (i.e. in a superposition of structural states), at low temperature occur in a purely quantum mechanical fashion, that is by tunneling.

We now show that the presence of a somewhat distinct class of such low barrier, or "fast", two-level systems, whose effective diagonal splitting is zero, leads to additional phonon scattering in comparison with the strictly semiclassical analysis, which neglects the renormalization from quantum mixing effects. This additional scattering at low energy is consistent with the apparent subquadratic temperature dependence of the heat conductivity in the TLS regime. The mixing also leads to a superlinear addition to the heat capacity at subKelvin temperatures. These highly quantum tunneling centers in strongly mixed superpositions of structural states, therefore, give a mechanism to resolve a quantitative deviation from the standard tunneling model, which was brought up by Black and Halperin (Black and Halperin, 1977) in 1977. They noted that the short time heat capacity of a-SiO_2 is larger than would be predicted by the logarithmic dependence obtained in the STM, if one uses the TLS parameters extracted from ultra-sonic measurements. The quantitative mismatch appears to be as if there were two kinds of two-level systems: one set obeying the distribution postulated in STM, and another set of "fast" tunneling centers responsible for the short time value of the heat capacity. We can see our analysis of mode mixing leading to the existence of a finite number of two-level systems with $\tilde{\epsilon}$ very nearly 0, as suggested by Eq.(59) is quite consistent with this empirical notion[6].

To see this more explicitly we note that Eq.(59) allows one to formulate the effects of quantum mode mixing as a change in the apparent distribution of the diagonal energy splitting. Whatever the old distribution of classical energy difference $n(\epsilon)$, the new distribution of the effective classical component of the transition energy can be found using $n(\tilde{\epsilon})|d\tilde{\epsilon}| = n(\epsilon)|d\epsilon|$. For $\tilde{\epsilon}$'s not too close to $\hbar\omega_i$ (case $\tilde{\epsilon} \sim \hbar\omega_i$ will be discussed later), which is appropriate in the TLS regime, the function $|\partial\epsilon/\partial\tilde{\epsilon}|$ that describes the relative probability distribution of the two

[6] We must stress however that the Black-Halperin analysis has been conducted only for a single substance, namely amorphous silica, and systematic studies on other materials should be done. The discovered numerical inconsistency may well turn out to be within the deviations of the heat capacity and conductivity from the strict linear and quadratic laws repsectively. Finally, a controllable kinetic treatment of a time-dependent experiment would be necessary.

quantities, is given by

$$\left|\frac{\partial\epsilon}{\partial\tilde{\epsilon}}\right| = \Sigma\delta(\tilde{\epsilon}) + 1, \tag{66}$$

where the δ-function is positioned to the right of the origin: $\int_0^{0^+} d\epsilon\delta(\epsilon) = 1$ (see also Fig.22b). Consequently, the distribution of the effective diagonal splitting is:

$$n_\Delta(\tilde{\epsilon}) = \frac{1}{T_g\xi^3}\left[B\frac{\Delta^2}{\hbar\omega_D}\delta(\tilde{\epsilon}) + e^{-|\tilde{\epsilon}|/T_g}\right]. \tag{67}$$

The coefficient of the δ-function reflects the "pile-up" of the two-level systems that would have had a value of $|\epsilon| < \Sigma$ were it not for quantum effects. These fast two level systems will contribute to short time value of the heat capacity in glasses. The precise distribution in Eq.(67) was only derived within perturbation theory and so is expected to provide only a crude description of the interplay of clasical and quantum effects in forming low barrier TLS. Quantitative discrepancies from the simple perturbative distribution may be expected owing to the finite size of a tunneling mosaic cell, as mentioned earlier, and the finite life-times of each energy state due to phonon emission. These effects would also smoothen the local quantum melting transition as $\tilde{\epsilon} \to 0$. While various improvements of the functional form of $n(\tilde{\epsilon})$ might be suggested, it seems unwarranted, at present, to use any more complicated expressions for this function. Thus, to see the main consequences of the quantum mixing effect, we will proceed with the perturbative expression. Assuming a particular value of the coefficient B allows one to derive the contribution of the fast two-level systems to the heat capacity and scattering of the thermal phonons. Before we start, let us note that since we now have to deal with a specific coupled distribution of ϵ and Δ, the generic two-level system model that only specifies the distribution of the total splitting E is not sufficient. We must use the full tunneling model where the tunneling elements Δ's are distributed according to Eq.(22). The exact value of constant A in equation (22) depends (weakly!) on the (possibly ϵ-dependent) cut-off value of the $P(\Delta)$ distribution. *Both* the heat capacity and the phonon scattering strength depend on the coefficient A, therefore it is possible to check the *relative* contribution of the "quantum" centers to both of those quantities, regardless of A's value. The $n(\epsilon,\Delta)$ distribution obtained in this way is now a product of the $P(\Delta)$ distribution from Eq.(22) and the density of states from Eq.(67). The new normalization coefficient A_1 is found from the requirement that $\int d\epsilon d\Delta n(\epsilon,\Delta) = 1/\xi^3$. This gives $A_1 = \left[\frac{B}{T_g\hbar\omega_D}\Delta^{2-c} + \frac{1}{c}\left(\frac{1}{\Delta_{min}^c} - \frac{1}{\Delta_{max}^c}\right)\right]^{-1}$). In order to compute the life-time of a phonon of energy E, one averages the Golden Rule scattering rate $\frac{\pi g^2\Delta^2}{\rho c_s^2 E}\tanh\frac{\beta E}{2}$ with respect to $n(\epsilon,\Delta)$, subject to the resonance condition $E = \sqrt{\epsilon^2+\Delta^2}$ (Anderson *et al.*, 1972; Jäckle, 1972; Phillips, 1981). This yields two contributions to the decay rate:

$$\begin{aligned}\tau_E^{-1} &= \frac{\pi}{3}A_1\left(\frac{a}{\xi}\right)^3 E\left(\frac{\Delta_{max}}{E}\right)^c \\ &\times \left[\frac{BE}{\hbar\omega_D} + \int_{\Delta_{min}/E}^1 dx\frac{x^{1-c}}{\sqrt{1-x^2}}\right].\end{aligned} \tag{68}$$

The first term in the square brackets is the contribution owing to the fast, or highly quantum, two-level systems. Note that this term scales faster with E than the other term. Provided the magnitude of this first term is comparable to the other term, the fast modes will somewhat modify the overall scaling of the heat conductivity κ. Without the first term, κ scales superquadratically according to T^{2+c} (recall that the heat conductivity is *inversely* proportional to the scattering rate from Eq.(68)). If we use a numerical value of B of the order 100, this leads to a *subquadratic* T dependence of κ: Experimentally, $\kappa(T)$ scales like $T^{1.9\pm.1}$ as extracted from a decade and a half of data (see Fig.1). Without the fast TLS, one, again, would have $\kappa \propto T^{2+c}$. Using the theoretical approximation for c, this differs from the empirically observed value at least by a factor of $(10^{1.5})^{c+.1} \sim 2$ at $T \simeq 10^{-2}T_D$. Obviously, this is a very crude estimate because, first, we do not know how far down in temperature the power law scaling of κ goes; second, our correction, while going in the right direction, summed with the older result, is not strictly a power law. Since the integral in the square brackets of Eq.(68) varies between 1 and $\pi/2$ for $0 < c < 1$ ($\Delta_{min}/E \ll 1$, surely at $E \simeq 10^{-2}T_D$), we conclude that the first term must be between 10^0 and 10^1 in order to make a sizable contribution to the phonon scattering and modify its functional form. Since $E \simeq 10^{-2}T_D$, this shows that B indeed must be of the order of several hundreds, consistent with our expectations based on the number of vibrational modes in the Boson Peak.

Does this mixing induced correction to the density of states with the value of B around a hundred make an appreciable contribution to the time-dependent heat capacity? Following the calculation from subsection III.C, but now using the new distribution $n(\epsilon,\Delta)$, one finds:

$$C(t) = \frac{A_1}{T_g\xi^3}\int_0^\infty dE\left(\frac{\beta E}{2\cosh(\beta E/2)}\right)^2\left(\frac{\Delta_{max}}{E}\right)^c\left[\frac{BE}{\hbar\omega_D}\theta(t-\tau_{min}) + \int_0^{\log(t/\tau_{min}(E))} dz\frac{e^{\frac{c}{2}z}}{2\sqrt{1-e^{-z}}}\right], \tag{69}$$

where $\theta(t)$ is the usual step-function and τ_{min} is the fastest possible relaxation time of a TLS with the total energy splitting E, defined in Eq.(25). Again, the first term in the square brackets gives the contribution of the "fast" TLS. Using the same numbers as given in subsection III.C, it is straightforward to show that the second, regular, term is of the order a hundred at temperatures $T \sim 10^{-2}T_D$ when measured on the time scale of minutes. At the same time, the first term is at most of order ten. Note that at the shortest times $t \sim \tau_{min}$, when the regular two-level system only begin to contribute to the heat capacity, the theory with quantum corrections says the actual heat capacity is *finite* and is at the most one tenth of the long-time value. At the same time, the fast tunneling centers do not seem to contribute significantly to the long-time heat capacity. We note however that the result obtained $c(T) \propto T^{1+c/2}$ with $c = .1$ gives a somewhat slower rise with temperature than seen in experiment. The quantum correction again goes in the right direction of *increasing* the rate of the heat capacity growth with temperature relative to the $T^{1+c/2}$ law.

We have established that effects beyond the strict semiclassical analysis give rise to a subset of tunneling centers that undergo faster tunneling than the rest. Nevertheless, there are some quantitative issues in the heat capacity magnitude that remain to be understood, namely that the computed contribution of the "fast" centers seems somewhat lower than what is necessary to explain the deviation of the experimental T dependence from the supelinear dependence $T^{1+c/2}$ predicted by the present (approximate) argument. It is posssible that ultimately a broader view of the time-dependence of the heat capacity needs to be taken. Since, in fact, the system will clearly be aging by tunneling at those low temperatures, the notion of fixed frozen-in "defects" may no longer be adequate - essentially interactions between defects play a role. "Aging" by definition implies irreversible *structural* changes. More work on understanding the long time evolution of the tunneling centers is necessary.

We have concentrated on the quantum corrections to the low lying tunneling states with low barriers. Quantum mixing applies to the higher energy states too. Energy shifts and quantum melting occur within sub-bands of the ripplonic states of order l and respective degeneracy $(2l + 1)$, thus mixing these states. As tunneling can take place on a given time scale and the vibrationally excited levels become observable, their apparent energies can not be degenerate because the levels are coupled through those same tunneling transitions. The magnitude of energy level repulsion from the quantum mixing can be assessed qualitatively. In the limit of weak coupling, the deviation of a ripplonic frequency from its classical value scales $\sum_i \Delta_i^2/\hbar\omega_i$. The width of the ripplonic band of order l is probably limited from above by the tunneling amplitude Δ_i itself. Does this band broadening affect our previous results on the Boson Peak phenomena? Not very much. Since the observables depend mostly on the number of new excitations and the *number* of the ripplonic modes is not changed by these mixing effects, the essential core of our conclusions from Section IV remains intact. Nevertheless, some quantitative modifications are to be expected. For example, the lowest ripplonic energies may be lowered to the extent so as to cause a cross-over to a multi-level behavior in some of the internal resonances, thus possibly modifying the derived magnitude of the heat capacity and phonon scattering at sub-plateau temperatures. This effect will further contribute to the phonon interaction induced broadening of the ripplonic transitions, as estimated in Section IV.

B. Mosaic Stiffening and Temperature Evolution of the Boson Peak

Eq.(59) raises another interesting point. According to that equation, the values of both the bare and the effective classical energy bias of a transition - ϵ and $\tilde{\epsilon}$ respectively - are limited from above by the lowest ripplon frequency (ω_2). (Note that this is only realized in the $\epsilon < 0$ case, discussed in this section.) This is unimportant at low temperatures. But what happens at higher T, near this limit? Unlike in the low energy situation just discussed, one simply cannot ignore here that all the energy states have a rather short life-time. Therefore the singularity in Eq.(59) does not occur, but will be rounded. This observation does not completely answer the question that one should have asked in the first place on general grounds alone: what happens to the structure of the energy spectrum of a tunneling center, when the energy of the transition becomes comparable to a vibrational eigen-frequency of the domain wall[7]?

When attempting to answer this question, a general multi-level perspective on each tunneling center is somewhat easier to use than the very mechanical view of the wall's excitations that we have mostly employed so far, in which the ripplonic energy states are obtained by quantizing vibrations of a freely moving classical mambrane. The "singularity" at $|\tilde{\epsilon}| \sim \hbar\omega_i$ is actually a term-crossing phenomenon that, again, would not take place in the strict classical limit. Let us go back to our argument on the density of states, but consider a case when ϵ is larger than a ripplonic frequency. As mentioned many times already, vibrational excitations of a domain wall can be defined meaningfully only when a structural *transition* takes place in a given region of the material. The energy of the transition must be the *lowest* excited state of a mosaic cell. On the other hand, the values of the ripplon frequencies are determined by a (fixed) surface tension coefficient and the wall's mass density. They have fixed values. The necessary conclusion from this is that the

[7] We remind the reader that the tunneling transition energy could be also thought of as an eigen-energy of the wall's motion, but of a lower, $l = 1$ order, associated with the translational motion of the shell's center of mass

tunneling centers will not have ripplons whose frequency is lower than the transition frequency. We provide a cartoon illustrating this idea in Fig.23. We see the quantum

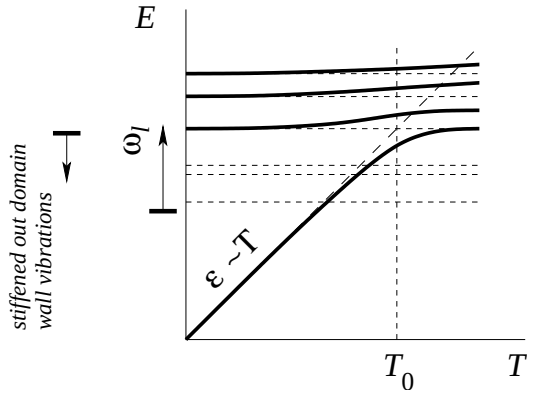


FIG. 23 This caricature demonstrates the predicted phenomena of energy level crossing in domains whose energy bias is comparable or larger than the vibronic frequency of the domain wall distortions. The vertical axis is the energy measured from the bottom state; the horisontal axis denotes temperature. The diagonal dashed line denotes roughly the thermal energies. A tunneling center, that would become thermally active at some temperature T_0 will not possess ripplons whose frequency is less than T_0.

mixing reduces the number of the lower frequency vibrational modes. The mosaic appears stiffer than expected. This effect may contribute to the temperature evolution of the Boson Peak as observed in inelastic scattering experiments. Wischnewski et al. find (Wischnewski *et al.*, 1998) that at temperatures between 51 K (numerically close to silica's $\hbar\omega_2$) and above the glass transition, the left hand side of the Boson Peak decreases in size as the temperature was raised. At the same time, the high frequency side remained relatively unchanged. Note that, as temperature is raised, the total area of the peak in Fig.2 of Ref.(Wischnewski *et al.*, 1998) does not increase. In this temperature range mosaic cell motion loses oscillating character and becomes a rather featureless activated relaxation process.

To summarize this section, we have seen that the possibility of quantum tunneling between structurally close states in glass does have a predictable effect on the spectrum and must be taken into account when computing the density of low (and not so low) energy structural excitations in these materials. At the same time, the main conclusions of the original semi-classical argument remain valid: each structural transition may be thought of as a rearrangement of about 200 molecules accompanied by distortion of the domain wall that separates the two alternative local atomic arragements.

VI. THE NEGATIVE GRÜNEISEN PARAMETER: AN ELASTIC CASIMIR EFFECT?

With the exception of the plateau's position and the quantum mixing effects, we have so far dealt with those anomalies in low temperature glasses that are more or less universal. These universal patterns are of particular interest because they cannot be easily blamed on chemical peculiarities of each substance. Indeed, given the flatness of the low energy excitation spectrum in glasses, the apparent universal ratio $l_{\rm mfp}/\lambda \simeq 150$ is the dimensionless quantity that seems to express the general, intrinsic character of those low energy excitations, as arising from the non-equilibrium nature of the glass transition. The number 150 reflects the size of nearly independent fragments into which a supecooled liquid is broken up at the laboratory glass transition. Yet, there is another dimensionless quantity, namely the Grüneisen parameter γ, that also reflects the necessity of going beyond a harmonic picture for amorphous solids. This parameter is always a positive number of order one for simple cubic crystals (at low enough T), but varies wildly among amorphous materials (Ackerman *et al.*, 1984) (see also a discussion in (Leggett, 1991)). γ in glasses has been reported to be as large as several tens and often negative in sign! A negative γ implies a negative thermal expansion coefficient $\frac{1}{V}\left(\frac{\partial V}{\partial T}\right)_p$ (the *linear* expansion coefficient $\alpha \equiv \frac{1}{L}\left(\frac{\partial L}{\partial T}\right)_p = \frac{1}{3}\frac{1}{V}\left(\frac{\partial V}{\partial T}\right)_p$ is a commonly used quantity chracterizing anharmonicity too). Contraction with heating is observed in some crystals at *not too low* temperatures, owing to the details of the anharmonic couplings in a specific substance that may result in the negativity of the Grüneisen parameter of a lattice mode of a finite frequency (see e.g. (Wei *et al.*, 1994)). Thermal contraction along a single direction in anisotropic materials is even more common. Nonetheless, as the temperature is lowered, the thermal expansion coefficient in an insulating crystal eventually becomes positive and approaches the cubic T dependence predicted by standard thermodynamics. In contrast, an isotropic negative thermal expansivity is observed in many amorphous substances even at the lowest temperatures. In addition, the expansivity is not cubic in T. The most widely known example of a substance with a negative α is rubber. Rubber owes this property to the largely entropic nature of its elasticity. Here, we will see that a distinct mechanism of thermal contraction in glasses in the TLS temperature range arises, which is a direct consequence of the existence of the spatially extended tunneling centers that give rise to the universal phenomena considered earlier.

As shown above, the excitation spectrum of the tunneling centers may be represented as a combination of the two lowest energy levels, corresponding to the structural transition and a set of higher energy states involving vibrations of the moving domain wall. By the exchange of phonons, these local (quantum) fluctuations in the elastic stress will be attracted to each other much like in the Van der Waals interaction between neutral molecules. The

elastic Casimir effect seems a more appropriate name for this phenomenon, since the moving domain walls are not point-like but, instead, resemble fluctuating membranes. While we do not claim this attraction is solely responsible for the negative expansion coefficient, it turns out to provide a large contribution to the thermal contraction in glasses. We will see how this effect arising from interaction of amorphous state excitations depends on the material constants and the preparation speed of the glass is derived and, therefore, is not universal!

We note first that not all amorphous substances actually exhibit a negative α in the experimentally probed temperature range. In such cases, it is likely that the contraction coming from those interactions in these materials is simply weaker than the regular, anharmonic lattice thermal expansion. Other contributions to the Grüneisen parameter will be discussed below as well.

Coupling the motion of the mosaic cell (TLS and Boson Peak) to phonons is necesssary to explain thermal conductivity, therefore the interaction effects discussed below follow from our identification of the origin of amorphous state excitations. The emission of a phonon followed by its absorption by another cell will give an effective interaction, in the same way that photon exchange leads to inter-particle interactions in QED. The longest range coupling between local degrees of freedom coupled linearly to the elastic stress has the form of a dipole-dipole interaction. Since the structural transitions are of finite size, the dipole assumption is only approximate for the closer centers. For the time being, we take for granted that there is no *first* order, static, interaction between the vibrating domain walls, which, if non-zero, could be *à priori* of either sign. The next, second order interaction is always negative in sign and is proportional to $-\sum_{ij}\frac{1}{r_{ij}^6} \propto -\left(1-\frac{\delta V}{V}\right)^2 \simeq -1+2\frac{\delta V}{V}$. This favors a sample's contraction (V is the volume). This attractive force, which will be temperature dependent, is balanced by the regular temperature independent elastic energy of the lattice: $F_{elast}/V = \frac{K}{2}\left(\frac{\delta V}{V}\right)^2$. Calculating the equilibrium volume from this balance allows us to estimate the thermal expansion coefficient α. More specifically, the simplest Hamiltonian describing two local resonances that interact off-diagonally is $H = \frac{\omega_i}{2}\sigma_x^i + \frac{\omega_j}{2}\sigma_x^j + J_{ij}\sigma_z^i\sigma_z^j$, where ω_i and ω_j would be the frequencies of ripplons on sites i and j and

$$J_{ij} \equiv \frac{3}{4\pi\rho c_s^2}\frac{(\mathbf{g}_i\mathbf{g}_j) - 3(\mathbf{g}_i\mathbf{r}_{ij})(\mathbf{g}_j\mathbf{r}_{ij})/r_{ij}^2}{r_{ij}^3} \qquad (70)$$

is the dipole-dipole interaction following from Eqs.(15) and (16). (Having the interaction be off-diagonal automatically removes the first order term in J_{ij}.) The factor 3 accounts in our usual simplistic way for all three acoustic phonon branches. This ignores a distinction between the longitudinal and transverse speed of sound. This simplification is however accurate enough for our purposes. Since $g \simeq \sqrt{\rho c_s^2 a^3 k_B T_g}$, the J_{ij}'s turn out to scale in a very simple way with the glass transition temperature and the molecular size a, giving $J_{ij} \sim k_B T_g \left(\frac{a}{r}\right)^3$.

Since only mobile domain walls give rise to local dynamic heterogeneities, one may conclude intuitively that only the sites of thermally active structural transitions can contribute to α. Therefore one expects that as temperature in increased, more tunneling centers will contribute to the Van der Waals attraction thus leading to negative expansivity. As already mentioned, the excitations of a tunneling centers are conveniently subdivided into a low energy TLS-like pair of states, and higher energy, "ripplonic" excitations corresponding to distortions of an active center's domain wall. Hence we may view the total Van der Waals attraction as having three somewhat distinct contributions: "TLS-TLS", "ripplon-ripplon" and "TLS-ripplon" attractions. In this section, we focus on the relatively low, subplateau temperature regime, for reasons that will be explained later. At these low temperatures, transitions to the ripplonic states are only virtual, whereas the TLS structural may well be thermally active. This, in addition to the differences in the respective spectra of these excitations, will lead to some difference in the dependence of the mutual interactions between those excitations on temperature and other parameters. In order to assess the magnitude of those interactions let us consider the following, very simple, three-level Hamiltonian that is designed to model a transition of energy ϵ_i between two different structures that may also be accompanied by a wall vibration of frequency ω_i:

$$H_i = \begin{pmatrix} 0 & 0 & 0 \\ 0 & \epsilon_i & 0 \\ 0 & 0 & \epsilon_i + \omega_i \end{pmatrix} \qquad (71)$$

Note that, even though, for simplicity's sake, we use the semiclassical energy ϵ in the Hamiltonian above, the latter is meant as (the lowest energy portion of) the full, diagonalized Hamiltonian with quantum corrections included. This corresponds to the plain two-level system formalism that does not specify a distribution of the tunneling matrix element Δ. Also, in comparison with the general case of Eq.(35), we only include an excitation by a *single* quantum of a *single* ripplon. The latter simplification is obviously justified in the lowest perturbation order, where all pairs of excitations contribute to the total in an additive fashion. Considering only single-quantum excitations is a low temperature approximation, made mostly to avoid adopting extra modelling assumptions necessary to embody the mixed spin/boson statistics on each site. This simplification is nevertheless adequate, as will become clear later in the discussion.

Since the contributions of the three constituents of the Van der Waals attraction are additive, one can consider each contribution separately. This indeed proves to be convenient not only because all the contributions exhibit distinct scaling with the parameters, but each contribution comes to dominate the expansivity at somewhat distinct temperatures. We consider first the ripplon-ripplon attraction. This contribution appears to dominate the

most studied region around 1 K. The off-diagonal (flip-flop) interaction between the ripplons has the form:

$$H_{ij}^{int} = J_{ij}|2_i 3_j\rangle\langle 3_i 2_j| + H.C., \qquad (72)$$

where the rows and columns in the unperturbed Hamiltonian from Eq.(71) are numbered in the conventional way from the upper left corner. The "ripplon-ripplon" case appears the simplest of the three because here, the issue of how many tunneling centers contribute to the effect is more or less separate from the strength of the interaction. The former is (qualitatively) determined by the number of thermally active two-level systems, that scales roughly with the heat capacity. The latter is nothing but the ground state lowering of a pair of resonances after interaction is switched on, which scales as $-J_{ij}^2/(\omega_i+\omega_j)$ and is T-independent at these low temperatures. This contribution to the negative thermal expansion is therefore expected to be roughly quadratic in temperature (this corresponds to linear *expansivity*), which is similar, if not somewhat slower than observed in amorphous silica around 1 degree K.

Calculating the correction to the system's free energy in the lowest order in J_{ij}, that corresponds to the interaction term from Eq.(72) is entirely straightforward and yields:

$$\begin{aligned}\delta F_{rr} &= -\sum_{ij} J_{ij}^2 \frac{e^{-\beta(\epsilon_i+\epsilon_j)}(1+e^{-\beta\omega_i})(1+e^{-\beta\omega_j})}{Z_i Z_j} \\ &\times \frac{\omega_i \tanh(\beta\omega_i/2) - \omega_j \tanh(\beta\omega_j/2)}{\omega_i^2-\omega_j^2}, \qquad (73)\end{aligned}$$

Here, $Z_i \equiv 1+e^{-\beta\epsilon_i}+e^{-\beta(\epsilon_i+\omega_i)}$ is the unperturbed on-site partition function, corresponding to Eq.(71). Here, subscript "rr" signifies the "ripplon-ripplon" contribution.

At low - subplateau - temperatures $T<\omega_i$, that we are primarily interested in here, the expression above reduces to the following Van der Waals energy:

$$\delta F_{rr} = -\sum_{ij}\sum_{l_1 l_2} \frac{J_{ij}^2}{\omega_{l_1}^i+\omega_{l_2}^j} \frac{1}{(1+e^{\beta\epsilon_i})(1+e^{\beta\epsilon_j})}, \qquad (74)$$

where we have explicitly written out summation over distinct ripplon harmonics l_1 and l_2 at sites i and j.

A few intermediate calculations are needed to compute the sum in Eq.(74). First, averaging of J_{ij}^2 with respect to different mutual orientations of $\mathbf{g}_i$, $\mathbf{g}_j$ and $\mathbf{r}_{ij}$ yields an effective isotropic attractive interaction $\frac{2}{3}\left(\frac{3}{4\pi}\right)^2 T_g^2 \left(\frac{a}{r}\right)^6$. Second, the sum over all harmonics amounts to $\sum_{l_1,l_2=2}^{l_{max}} \frac{(2l_1+1)(2l_2+1)}{\omega_{l_1}+\omega_{l_2}}$, where ω_l is found using the dispersion relation from Eq.(33). Here we assume that ω_i's are not correlated with J_{ij} and ϵ_i. As we already know from the discussion in the previous section, the latter assumption is adequate for values ϵ smaller than the Boson Peak frequency. Now, recall that l_{max} actually depends on the droplet's perimeter, thus introducing an additional (cubic!) scaling with ξ/a. In the end, the sum over the l's is equal, within sufficient accuracy, to $1.5\omega_D^{-1}(3/4\pi)\pi^3(\xi/a)^{5/4}(\xi/a)^3$. Finally, assuming J_{ij}'s and ϵ's to be uncorrelated enables one to present the double sum over ϵ_i as a product of two identical sums: $\left(\sum_i (1+\beta\epsilon_i)^{-1}\right)^2$. Each sum is the effective concentration of thermally active tunneling centers: $k_B(\ln 2)\frac{T}{T_g\xi^3}$ as computed by integrating $1/(1+e^{\beta\epsilon})$ with the density of states from Eq.(34). Note that here we use the simple $1/T_g\xi^3$ expression for density of the tunneling transitions, in keeping with the assumption $E\sim\epsilon_i$ of the plain two-level system model adopted in this section. This is reasonable, given the qualitative character of this calculation. Finally, the summation over the ripplon sites can now be reduced to an integration with the lower limit equal to $\xi(3/4\pi)^{1/3}$.

As a result of the previous discussion, one recovers the following expression for the energy gain (per volume) due to a volume change δV: $\delta F_{rr}/V \simeq 1.5\,(\ln 2)^2\,\pi^2 \frac{k_B T^2}{\xi^3 T_D}\left(\frac{a}{\xi}\right)^{7/4}\left(\frac{\delta V}{V}\right)$. This works against the regular elastic energy $\delta F_{elast}/V = \frac{K}{2}\left(\frac{\delta V}{V}\right)^2$, introduced earlier. The equilibrium relative change $\delta V/V$ as a function of T is obtained by setting $\partial F/\partial V = 0$. Differentiating the equilibrium value of δV with respect to temperature yields the following estimate for the thermal (volume) expansion coefficient:

$$\frac{1}{V}\left(\frac{\partial V}{\partial T}\right)_p \simeq -3.0\,(\ln 2)^2\,\pi^2 \frac{1}{K}\frac{k_B T}{\xi^3 T_D}\left(\frac{a}{\xi}\right)^{7/4}. \qquad (75)$$

This can already be used to estimate the magnitude of the ripplon-ripplon contribution to the "Casimir" effect numerically. One can do it in several ways. The simplest thing to do that does not require knowing K, is simply to use Eq.(75) to calculate the Grüneisen parameter γ itself according to $\gamma = (\partial p/\partial T)_V/c_V$ (Kittel, 1956), also using $(\partial p/\partial T)_V = -(\partial p/\partial V)_T/(\partial T/\partial V)_p$. This yields a temperature independent Grüneisen parameter:

$$\gamma_{rr} \simeq -3.0\,(\ln 2)^2\,\pi^2 \frac{T_g}{T_D}\left(\frac{a}{\xi}\right)^{7/4}. \qquad (76)$$

Using $(\xi/a)^3 \simeq 200$ and silica's $T_g/T_D \simeq 1500/350$ one obtains $\gamma \simeq -3.$, within an order of magnitude of what is observed in amorphous silica at low temperatures (that experimental number varies between -5 and -20 among different kinds of silica at 1 K and seems to grow larger with lowering the temperature, see Fig.3 from (Ackerman *et al.*, 1984)). We will argue shortly that this growth may be explained by other contributions to the attraction between local resonances.

We can also directly compare the conribution in Eq.(75) to the *linear* thermal expansion coefficient $\alpha = \frac{1}{3V}\left(\frac{\partial V}{\partial T}\right)_p$ for silica as measured in (Ackerman *et al.*, 1984). According to the Fig.2 from (Ackerman *et al.*, 1984), the α of silica is linear (possibly slightly sublinear) in temperature and equals $-1.0\cdot 10^{-9}K^{-1}$ at 1K.

The compressibility K was obtained in (Ackerman *et al.*, 1984) from measured speed of sound and density. For internal consistency, we use the scalar elasticity to estimate K in this way. Summing up three single polarization phonon Hamiltonians from Eq.(15) yields $K \simeq \rho c_s^2/3$ (remember, $\Delta V/V = 3\Delta\phi$). Using silica's constants, given in Fig.15 and the earlier obtained $\xi = 20\mathring{A}$ and recalling that $\delta l/l = \delta V/3V$, Eq.(75) gives linear expansion coefficient $\alpha \simeq -0.4 \cdot 10^{-9} K^{-1}$ at 1K, indeed strongly suggesting that attraction between the tunneling centers is a significant contributor to the negativity of the expansion coefficient. The numbers just obtained are also a convenient benchmark in assessing other contributions to the negative thermal expansivity.

Next, we estimate the magnitude of the attraction between virtual transition and the direct, lowest energy transitions on different sites. The corresponding coupling term - $J_{ij}|2_i 2_j\rangle\langle 3_i 1_j| + H.C.$ - leads to the following contribution to the free energy in the lowest order:

$$\delta F_{rT} = -\sum_{ij} J_{ij}^2 \frac{e^{-\beta\epsilon_i}(1+e^{-\beta\omega_i})}{Z_i} \times \frac{\omega_i \tanh(\beta\omega_i/2) - \epsilon_j \tanh(\beta\epsilon_j/2)}{\omega_i^2 - \epsilon_j^2}, \quad (77)$$

At subplateau temperatures, when $\beta\omega_i \gg 1$, $\tanh(\beta\omega_i/2)$ can replaced by unity. Furthemore, the summation with respect to ϵ_j is no longer cut off by the temperature and the respective integral (weighted by $n(\epsilon) = \frac{1}{T_g} e^{-|\epsilon|/T_g}$) picks up most of its value at $\epsilon \gg T$. Therefore $\tanh(\beta\epsilon_j/2)$ may be replaced by unity as well. (Actually, both of those replacements must be made simultaneously lest the sum becomes potentially ill-behaved when $\omega_i \sim \epsilon$.) As a result, the expression in Eq.(77) simplifies:

$$\delta F_{rT} = -\sum_{ij} J_{ij}^2 \frac{1}{1+e^{\beta\epsilon_i}} \frac{1}{\omega_i + \epsilon_j}. \quad (78)$$

The ϵ_j integral is related to an exponential integral E_1 and yields in the two lowest orders: $(\ln(T_g/\omega_i) - \gamma_E)$, where $\gamma_E = 0.577...$ is the Euler constant. As in the previous calculation, we regard ϵ_i, ω_i and J_{ij} as uncorrelated. The summation over ω_i can be approximately represented as a continuous integral between 0 and l_{max} and leads to a quantity that scales as the area of the domain wall with a logarithmic correction. The final result is $\delta F_{rT}/V = 0.5\frac{T}{\xi^3}(a/\xi)^4 \ln\left[2.0\frac{T_g}{\omega_D}\left(\frac{\xi}{a}\right)^{1/4}\right](-1+2\frac{\delta V}{V})$. Up to a logarithmic correction, the expression is independent of the energy parameters in the problem and thus must scale linearly in T. Note that we have written out the full expression of $\delta F_{rT}/V$ that includes the bigger, δV independent term "-1", for the following reason: This larger negative term is linear in temperature, which apparently would lead to a non-zero (positive) entropy at $T = 0$. This observation signals a breakdown of a perturbative picture of largely non-interacting two-level systems. For the sake of argument, let us estimate at what temperature this breakdown occurs we compare the magnitude of the $\delta F_{rT}/V$ term, *assuming* it is correct, to the free energy of non-interacting two-level systems per unit volume: $\int \frac{d\epsilon}{T_g\xi^3} e^{-\epsilon/T_g}[-T\ln(1+e^{-\beta\epsilon})]$, where we have appropriately chosen $E = 0$ as the reference energy. The latter expression is equal to $(\pi^2/12)T^2/T_g\xi^3$ and becomes smaller (in absolute value) than the $\delta F_{rT}/V$ term at temperatures below $10^{-3}T_g$. This temperature is actually less, but still within an order of magnitude from the lower end of the plateau, which is well within the *empirical* validity of the non-interacting two-level systems regime. Let us recall, however, that a perturbative expansion is an asymptotic one and therefore always *over*estimates the *magnitude* of a correction (we suspect that most of the error comes from the low ϵ two-level systems). Therefore, a more accurate estimate would probably yield a break-down temperature lower in value than the estimate above. There is a reason to believe the "break-down" temperature is just at the edge of the lowest temperatures routinely accessed in the experiments. This is suggested by several experiments such as on internal friction where deviations from the standard non-interacting two-level system picture have been seen (see, for example, a recent review by Pohl et al. (Pohl *et al.*, 2002)). In general, the effect of interaction between two-level systems could exhibit itself under several guises. One of those is an apparent gap in the excitation spectrum of the effective individual TLS. Such effects may have in fact been observed (Lasjaunas *et al.*, 1978; Thompson *et al.*, 2000). The estimates above show thise effects are more likely to be observed in substances with a higher glass transition temperature, such amorphous silica, or, germania (GeO_2). Note, however, that the effects of interaction on the apparent TLS spectrum must be separated from quantum effects of level repulsion on each sites, that we have considered in Section V. At any rate, the volume expansion coefficient, corresponding to the computed value of the ripplon-TLS term, is approximately equal to

$$\frac{1}{V}\left(\frac{\partial V}{\partial T}\right)_p \simeq -1.0\frac{1}{\xi^3 K}\left(\frac{a}{\xi}\right)^4 \ln\left[2.0\frac{T_g}{\omega_D}\left(\frac{\xi}{a}\right)^{1/4}\right]. \quad (79)$$

Substituting the numerical values for a-SiO_2 in Eqs.(79) and (75) shows that at 1 K, the ratio of the ripplon-TLS contribution to the ripplon-ripplon term is about 1.2 - that is they contribute comparably to the "contraction" free energy at this temperature. However, since the ripplon-TLS α is temperature independent, it will dominate at *sub*Kelvin temperatures. The Grüneisen parameter's value corresponding to Eq.(79) is

$$\gamma_{rT} \simeq -1.0\frac{T_g}{T}\left(\frac{a}{\xi}\right)^4 \ln\left[2.0\frac{T_g}{\omega_D}\left(\frac{\xi}{a}\right)^{1/4}\right]. \quad (80)$$

The ripplon-TLS term, as estimated here, therefore seems somewhat larger relative to the ripplon-ripplon term than seen in experiment, consistent with our earlier notion that it is somewhat overestimated. Still, qual-

itatively our estimates are consistent with the observed tendency of γ to increase in magnitude, when the temperature is lowered. We point out that the results obtained above disregard possible effects of a specific distribution of Δ that will influence the precise value of the coupling between phonons and tunneling centers.

Note that the heat capacity like expression reflecting the number of thermally active sites i enters into the expressions from Eqs.(79) and (80) in a linear fashion. Therefore, in contrast to Eq.(76), the temperature dependence of expression (80) is expected to be largely independent of the exact T-scaling of the heat capacity. Therefore, according to Eq.(80), the Grüneisen parameter should eventually scale as $1/T$ at low enough temperatures in all substances (however, unrealistically long observation times may be required to verify this prediction; see the discussion at the end of this section). And again, the apparent density of states of the tunneling centers may be modified at those low temperatures due to interaction effects (such as the Burin-Kagan (Burin and Kagan, 1996) effect).

According to Eqs.(76) and (80), the *dimensionless* contribution of the attractive forces between the tunneling centers can be expressed in a simple manner through the T_g/T_D and T_g/T ratios, as well as the relative size of the mosaic. Note that the effects of varying the quenching speed of the liquid on the number in Eqs.(76) and (80) add up. For instance, making the quenching faster will increase T_g and decrease ξ. The ripplon-TLS term is especially convenient with regard to testing our results, because it is nearly insensitive to changes in the Debye temperature potentially induced by altering the speed of glass preparation.

Finally, we show that the second order coupling between direct tunneling transitions is subdominant to the already computed quantities. Consider an interaction of the form $J_{ij}|1_i 2_j\rangle\langle 2_i 1_j| + H.C.$. If one repeats simple-mindedly the steps leading to Eq.(73), one obtains the following simple expression for the free energy correction due to interaction between the underlying structural transitions:

$$\delta F_{TT} = -\sum_{ij} J_{ij}^2 \frac{\epsilon_i \tanh(\beta\epsilon_i/2) - \epsilon_j \tanh(\beta\epsilon_j/2)}{\epsilon_i^2 - \epsilon_j^2}. \quad (81)$$

Assuming, again, that J_{ij} and ϵ_i's are uncorrelated, the ϵ summation can be performed via averaging with respect to the distribution from Eq.(34). One can show that the low temperature expansion of the expression above yields, within two leading terms, $\delta F_{TT}/V = -(2T_g/3\xi^3)\left(\frac{a}{\xi}\right)^6 [1 + (\pi T/T_g)^2 \ln(T_g/T)/3]$. The T-independent term in itself is curious in that it is a contribution to the "vacuum energy" of the lattice that is of purely glassy origin and is entirely due to the locality of the free energy landscape of a liquid. Indeed, as attested by its scaling with T_g/ξ^3, this "vacuum energy" contribution would disappear at the *ideal* glass transition at which the whole space is occupied by a *non-extensive* number of distinct aperiodic solutions of the free energy functional. However, this constant term will have no effect on the *thermal* expansion. The lowest order T-dependent term - $T^2 \ln T$ - actually has a slightly stronger temperature dependence than the ripplon-ripplon contribution, however the latter is larger by at least three orders of magnitude, mostly owing to the large number of ripplon modes. Apropos, we would like to stress again that the presence of vibrational modes of the (extended) mosaic walls is essential to the existence of the negative thermal expansivity effect that we just estimated. Therefore, while the present theory predicts that many (and most conspicuous) effects that distinguish amorphous lattices from crystals should be described well by a set of non-interacting two-level-like entities at cryogenic temperatures, the intrinsic *multilevel* character of the structural transitions, that follows from the present theory, in glasses exhibits itself even at these low energies in higher order perturbation theory.

To complete the discussion of the second order interaction between tunneling centers we note that the corresponding contribution to the heat capacity in the leading low T term comes from the "ripplon-TLS" term and scales as $T^{1+2\alpha}$, where α is the anomalous exponent of the specific law. Within the approximation adopted in this section, $\alpha = 0$. However it is easily seen that the magnitude of the interaction induced specific heat is down from the two-level system value by a factor of $10.(a/\xi)^5(d_L/a)^2 \sim 10^{-4..5}$ and therefore may be safely neglected.

We have so far considered the second order part of the induced interactions (square in J_{ij}^2, but forth order in g). There could be also, *à priori*, lower order contributions - first order in g, and first order in J_{ij}. First, let us consider the term linear in J_{ij}, which *also* has to do with interaction, mediated by the phonons. If non-zero, it could be of either sign. In our case, it is identically zero for the following reason. It is known (Neu *et al.*, 1997; Yu and Leggett, 1988), that the apparent TLS's are only weakly interacting (one could also infer this implicitly from the smallness of the second order term that we have already estimated. The first order term, if non-zero, is comparable to the second order in a mean-field disordered system. The dipole-dipole $1/r^3$ interaction is long range and is indeed well described by the mean field). But we are dealing here with a non-polarized state, for which the first order term, linear in the average on-site magnetization, vanishes. In any case, even if the system were in a "ferromagnetic" state, the first order term would still be only very weakly temperature dependent and thus would not contribute to the thermal contraction. Whether to consider such first order term non-zero or not is, to some degree, a matter of choice. If non-zero, it must be simply thought of as the effective Weiss-like field that is part of molecular field at each site. That field implies a *hard* gap of the order T_g and indeed is negligible at low T. Yet, at low enough temperatures - microKelvins or so (Neu *et al.*, 1997), the *phonon-mediated*

first order interaction between the tunneling centers may become important and one can no longer use the bare frozen-in values of the on-site TLS energies, but those determined by the interaction. In this regime an independent two-level system picture breaks down and more complicated renormalized excitations may begin to play a role (Burin and Kagan, 1996).

On the other hand, the other possible contribution to α, a term linear in g does not have to do with interactions between the anharmonic amorphous solid excitations but is due to the direct coupling of the tunneling centers with the phonons. This direct TLS-phonon interaction has so far been the main suspect (Galperin *et al.*, 1985; Papoular, 1972; Phillips, 1973) behind the anomalous thermal expansion properties of the glassses. This mechanism requires however the existence of a correlation (Phillips, 1973) (in our notation) between the on-site values g and ϵ, or else between Δ and $\partial\Delta/\partial\phi_{ii}$. In other words, the value of either classical or quantum splitting of a two-level system must be correlated with the way its energy changes when elastic stress is applied locally. The Δ with $\partial\Delta/\partial\phi_{ii}$ correlation has been argued to make a small contribution relative to the g versus ϵ correlation because of the smallness of the value of the Δ's for the majority of the thermally active TLS (Phillips, 1973). On the other hand, a correlation between g and ϵ could produce, in principle, both a negative or positive Grüneisen parameter and therefore could explain, by itself, the observed variety of expansion anomalies in the low T glasses. However, the degree of correlation between g and ϵ and its temperature dependence is not really known and has to be parametrized. The soft-potential model offers enough richness in behavior to accomodate two possible contributions - one dilating and the other contracting - to the sample's volume. In fact, Galperin et al. (Galperin *et al.*, 1985) suggest that those two types of the TLS may well be the two types of the tunneling centers that were postulated early on by Black and Halperin (Black and Halperin, 1977) in order to resolve the apparent discrepancy between the value of the TLS density $\bar{P}$ as deduced from the phonon scattering experiments and the equilibrium and time dependent heat capacity measurements. This, of course, could be checked experimentally by comparing the degree of the discrepancy in $\bar{P}$ and the sign of the thermal expansion coefficient in different substances. (We have shown in the previous section how the Black-Halperin paradox is, at least partially, explained by quantum corrections to the semi-classical landscape picture of structural transitions in glass.) With regard to the linear in g effect, we suggest here a modification to the original argument of Phillips from (Phillips, 1973). According to Phillips (note some notational differences), $|\gamma| = 12g\alpha_0 \ln 2/\pi^2 k_B T$ (he *also* assumed a linear heat capacity linear in T). Here, $|\alpha_0| \leq 1$ is an (unknown) coefficient that reflects the degree of correlation between g and ϵ: $\langle\!\langle \epsilon_i g_i(\epsilon_i) \rangle\!\rangle = \alpha_0 \epsilon_i g$. $\alpha_0 = \pm 1$ means complete correlation and $\alpha_0 = 0$ means no correlation. Now, due to symmetry, α_0 must be odd power in ϵ, the dominant term being therefore linear (see the form of $\alpha_0(\epsilon)$, somewhat cryptically mentioned as a remark of B. Halperin, at the end of Phillips' article). We must note, that although we have pretended, within our one-polarization phonon theory, that g is a vector quantity, it is in reality a tensor, if the phonons are treated properly. The off-diagonal terms, corresponding to interaction with shear, will indeed be uncorrelated with ϵ due to symmetry. However, the *trace* of the tensor, corresponding to coupling of the TLS to a uniform volume change could be, in principle, correlated with the energy of the transition. For example, it may happen that when the sample is locally dilated, the structural transitions in that region will require less energy to occur. At present, we do not have an argument in favor of or against such a correlation. Note, however that at the glass transition temperature, when the current arrangement of the defects freezes in, most structural transitions involve a thermal energy around T_g. On the other hand, the energy spliting ϵ of the tunneling centers relevant at the cryogenic temperatures is significantly smaller. Informally speaking, relative to the thermal energy scale at T_g all two-level systems with low splitting will feel the same to the phonons. Therefore, qualitatively, the correlation factor α_0 should be at least a factor of ϵ/T_g down from the largest value of one. Note, this coincides with the form $\alpha_0(\epsilon) \propto \epsilon$, suggested by Halperin. Therefore, the contribution of TLS-phonon coupling to the thermal expansivity of Phillips (who left the issue of the degree of correlation open at the time) should be multiplied by a factor of T/T_g. This takes into account, in a very naive way, both the symmetry and our knowledge of the energy scales relevant at the moment of the tunneling centers formation. This modifies Phillips' result to yield

$$|\gamma| < 12g \ln 2/\pi^2 k_B T_g = \frac{12 \ln 2}{\pi^2} \sqrt{\frac{\rho c_s^2 a^3}{T_g}} = \frac{12 \ln 2}{\pi^2} \frac{a}{d_L}. \tag{82}$$

The temperature independence of this contribution to the Grüneisen constant is the main difference between Eq.(82) and the original calculation of Phillips. The numerical value of the expression should be nearly the same for all substances and is about 8. This suggests that the direct coupling to phonons is a potential contributor to the elastic Casimir effect at temperatures around 1 K. Remember, however, the sign of the expression in Eq.(82) is unknown and its numerical value of 10^1 only provides an estimate from the above.

From the qualitative analysis in this section, we conclude, tentatively, that there are several contributions of comparable magnitude to the thermal expansion at low temperatures. Higher order effects may also be present. In this case, it may be more straightforward to estimate the interaction between ripplons as extended membranes without using a multipole expansion, as indeed is done when computing the regular Casimir force between extended plates.

The qualitative treatment above of the second-order

interaction between the ripplons on different sites can be extended to higher temperatures as well. It is easily seen from Eq.(73) that an excitation of energy ω_l will contribute only βJ_{ij}^2 at temperatures comparable to ω_l and above. Therefore one might expect that at the temperatures near the end of the plateau the ripplonic transitions become thermally saturated and this attractive mechanism becomes increasingly less important. The expression in Eq.(77), in contrast, is subject to thermal saturation to a lesser degree. Still, we have seen that its scaling with temperature is subdominant to the ripplon-ripplon term at temperatures above 1 K. Finally, we remind the reader about the effect of mosaic stiffening explained in the previous sections. This should also diminish the attraction between the tunneling centers, owing to a smaller number of resonant modes at the sites of centers thermally active at these higher temperatures. On the other hand, the usual anharmonic effects also become more significant at a higher T leading to a turn-over in the temperatrure dependence of α, as circumstantially supported by the old data on several materials cited in Ref.(Krause and Kurkjian, 1968). However, in order to assess this "cross-over" temperature, one needs to know the magnitude of the regular thermal expansion due to the non-linearities of the lattice. This is something that would be extremely difficult to measure independently, because even a crystal with the same stoichiometry as the respective glass, is not guaranteed to have the same non-linearity. Direct computer simulation estimates of the Grüneisen parameter, on the other hand, may be problematic due to the current difficulty of generating amorphous structures corresponding to realistic quenching rates. This is the main reason we have confined ourselves here to sub-plateau temperatures.

Finally, we note again that even at the low temperatures we have been discussing, not all glasses have been shown to exhibit a negative α. According to our theory, however, the "Casimir" contribution to α is negative and sub-linear in T, whereas the regular non-linear expansion coefficient is positive but only cubic in temperature. Therefore, there should be a (perhaps very low) temperature at which the Casimir force should dominate. Data for many substances, although still positive at the achieved degree of cooling, do extrapolate to negative values of α at finite temperatures. This is not the case, however, for all substances (Ackerman *et al.*, 1984). Even excluding the possibility of error in these difficult experiments, this is not necessarily inconsistent with our theory for the following reasons. As the temperature is lowered, it takes a long time (proportional to T^{-3}) for the tunneling transitions to occur and appear thermally activated. For these same reasons, like the amorphous heat capacity, the direct interaction effect is time dependent at low temperatures. It may therefore take an excessively long time to actually observe the effects, discussed in this section, at very low temperatures, thus making it difficult to see a sign change in α for lattices with relatively large anharmonicity. Incidentally, this analysis predicts that the response of the length of an amorphous sample to a temperature change at sub-plateau temperatures must be time dependent (such time-dependence, acompanied by heat release, has been observed in polycrystalline NbTi (Escher *et al.*, 2000)). Since the interaction effect is quadratic in concentration, one expects qualitatively that the relative rate of the expansion's time dependence should be twice that of the specific heat.

VII. CONCLUSIONS

In summary, this work elucidates the origin of the thermal phenomena observed in the amorphous materials at temperatures $\sim T_D/3$ and below, down to the so far reached milliKelvins. The nature of these phenomena can be boiled down to the existence of excitations other than elastic strains of a stable lattice. The peculiarity of these excitations is exhibited most conspicuously in the following phenomena: The specific heat obeys a nearly linear dependence on the temperature at the lowest T, greatly exceeding the Debye contribution. At the same temperatures, the heat conductivity is nearly quadratic in T and is universal if scaled in terms of the elastic constants. At higher temperatures ($\sim T_D/30$), the density of these mysterious excitations grows considerably leading to enhanced phonon scattering and thus a plateau in the temperature dependence of the heat conductance. This increase in the density of states is also directly observed as the so called Boson Peak in the heat capacity data, as well as inelastic scattering experiments.

We have argued that the origin of these excitations is a necessary consequence of the non-equilibrium nature of the structural glass transition. This transition, not strictly being a phase transition at all in a regular equilibrium sense, occurs if the barriers for molecular motions in a supercooled liquid become so high as to prohibit any macroscopic shape changes in the material on the scales of hours and longer (Xia and Wolynes, 2000). The origin of these high barriers lies in a cooperative character of the molecular motions, which involve around 200 molecules at the glass transition temperature. Unlike regular crystals, where the correlation between the molecular motions is rather long range, thus leading to the emergence of translational symmetry below solidification, the motions within the cooperative regions in a supercooled liquid, or entropic droplets, are only weakly correlated with their surrounding. In the language of the energy landscape paradigm, a crystal is a (possibly non-unique) ground state of the sample (thus the long-range correlation!), whereas a glass is caught in a high energy state, not being able to reach the true ground state for kinetic reasons. The respective dense energy spectrum at these energies exhibits itself in the existence of alternative mutually accessible conformational states of regions, or domains, of about 200 molecules in size. It was argued that quantum transitions between these alternative states are the additional excitations observed in glasses

at low temperatures. The knowledge of the spectral and spatial density of these excitations allowed us to estimate from first principles the magnitude of the observed linear specific heat. The relevant energy scale here is the glass transition temperature T_g itself.

Stability requirements for the existence of these alternative conformational states at T_g allowed us also to estimate the strength of their coupling to the regular lattice vibrations, which is determined by T_g, the material mass density and the speed of sound. This enabled us to understand the universality of the phonon scattering at the low temperatures.

The novelty of this picture is that we have established rather generally a *multiparticle* character of the tunneling events. This is counter-intuitive because, naively, the larger the number of particles involved in a tunneling event, the larger the tunneling mass is, and the harder the tunneling becomes. This is indeed the case for systems like disordered crystals or crystals with substitutional impurities, where the tunneling mass is that of an atom, and the barrier heights are determined by the energy of stretching a chemical bond by a molecular distance; this virtually excludes the possibility of tunneling. The existence of structural rearrangements in a macroscopically rigid system is a sign of the system being in a high energy state in which the available phase space is potentially macroscopically large. However, a decrease in this density of states for glass transitions occuring at a slower pace of quenching would result in the necessity to engage a larger number of atoms in these structural rearrangements. Transitions between the internal states of a domain involve only a very minor length change of each individual bond and atomic displacements not exceeding the Lindemann length, which is of the order one-tenth of the atomic length scale. It is not particularly beneficial to picture the tunneling events as individual atomic motions but rather as the motion of an interface between the alternative states of the domain. This domain wall is a quasi-particle of a sort, which has a low mass indeed: per molecule in the domain, it is only about *one-hundredth* of the atomic mass. The contributes to the ease of the tunneling events that are thermally relevant at cryogenic temperatures: These events are subject to only very *mild* potential variations and are possible, again, because the lattice is frozen-in in a high energy state.

The spatially extended character of the domain wall excitations along with their strongly anharmonic nature explains also higher temperature phenomena, such as the Boson peak and the plateau in the heat conductivity. By using our knowledge of the surface tension and the mass density of the domain wall we were able to calculate the energy spectrum of vibrational excitations of the active domain walls, or ripplons. This spectrum is in good agreement with the observed frequency of the Boson peak. The ripplonic excitations accompany the transitions between the domain's internal states and thus are strongly coupled to the phonons. This has enabled us to understand the experimentally observed rapid drop in the phonon mean free path at the plateau temperatures. In addition, we have investigated the effects of phonon coupling on the spectrum of the ripplons. These spectral shifts scale with T_g and seem to be the cause of the non-universal position of the plateau.

We have carrried out an analysis of the multi-level structure of the tunneling centers that goes beyond a semi-classical picture of the formation of those centers at the glass transition, that was primarily employed in this work. These effects exhibit themselves in a deviation of the heat capacity and conductivity from the nearly linear and quadratic laws respectively, that are predicted by the semi-classical theory.

A Van der Waals attraction between the domain walls undergoing tunneling motions was argued to contribute to the puzzling negative expansivity, observed in a number of low T glasses.

Finally, we note that the conclusions of this work strictly apply only to glasses made by quenching a supercooled liquid. One may ask, nevertheless, to what extent the present results are pertinent to *other* types of disordered solids, such as "amorphous" films made chemically or by vapor depositions, or, say, disordered crystals. Indeed, phenomena, reminiscent of real glasses, such as an excess density of states, are observed in many types of disordered materials, although they do not appear to be as universal as in true glasses (see, for example (Pohl *et al.*, 2002)). In this regard, we note that most of the phenomena discussed in the present work should indeed take place in other types of aperiodic structures. What makes quenched glasses special is the *intrinsic* character of their additional degrees of freedom that stems from the non-equilibrium nature of the glass transition. Since the characteristics of this transition (while not being a transition in a strict thermodynamic sense!) are nearly universal from substance to substance, many low (and not so low) temperature properties of all those substances can be understood within a unified approach.

Acknowledgments

We thank J.Schmalian, A.Leggett and A.C.Anderson for helpful discussions. This work was supported by NSF grant CHE 0317017.

APPENDIX A: Rayleigh Scattering of the Phonons due to the Elastic Component of Ripplon-Phonon Interaction

In this Appendix, we present an argument on the strength of the phonon scattering due to the direct coupling with the ripplons via lattice distortions, but not due to the inelastic momentum absorbing transition in which the internal state of the domain changes. We thus consider phonon scattering processes which do obey selection rules and couple to the lattice strain only in the second and higher order. This scattering is of the Rayleigh type

(and higher order) and occurs off the domain walls as localized modes. Importantly, we will use only derived quantities and no adjustable parameters in this estimate. We show here that, indeed, this absorption mechanism is not significant compared to the resonant scattering by the inelastic transitions between the internal states of a thermally active domain.

First, it proves handy to rederive the ripplon spectrum from Eq.(32) in the less general case $\rho_g = 0$ (but non-zero pressure!). As argued in Section IV, the droplet wall is at equilibrium pressure $p = \frac{3}{2}\frac{\sigma}{R} = \frac{3}{2}\frac{\sigma_0 a^{1/2}}{R^{3/2}}$. If the surface is distorted locally by Ω, this results in an extra force on this portion of the wall due to a changed curvature (Morse and Feshbach, 1953). The second Newton's law (as applied per unit area) yields then:

$$\frac{9}{8}\frac{\sigma}{R^2}\left[2+\frac{1}{\sin\theta}\frac{\partial}{\partial\theta}\left(\sin\theta\frac{\partial\Omega}{\partial\theta}\right)+\frac{1}{\sin^2\theta}\frac{\partial^2\Omega}{\partial\phi^2}\right]=\rho_W\frac{\partial^2\Omega}{\partial^2 t}, \tag{A1}$$

where θ and ϕ are the usual polar and asimuth angular coordinates on the surface and we took into account the r dependence of pressure. The equation above can be solved by a linear combination of the eigen-functions of angular momentum in 3D:

$$\chi \equiv \sum_{lm}\Omega_{lm}(t)Y_{lm}(\theta,\phi), \tag{A2}$$

$Y_{lm}(\theta,\phi)$ are the spherical Laplace functions ($m=-l..1$). Substituting a harmonic of l-th order in Eq.(A1) yields the equation for ω_l derived in text as Eq.(32). We will absorb the 9/8 factor into the definition of σ in the rest of the Appendix.

A (fake) potential energy, yielding the equation of motion (A1), is (c.f. the discussion of surface waves on a spherical liquid droplet in (Landau and Lifshitz, 1987)):

$$f_{surf}=\sigma\int d\phi\int d(\cos\theta)\left\{(R+\Omega)^2+\frac{1}{2}\left[\left(\frac{\partial\Omega}{\partial\theta}\right)^2+\frac{1}{\sin^2\theta}\left(\frac{\partial\Omega}{\partial\phi}\right)^2\right]\right\}. \tag{A3}$$

Although varying Eq.(A3) w.r.t. Ω does produce the Eq.(A1), note that it differs (by a factor of 9/8!) from the original surface energy $\sigma 4\pi r^2$. The resulting error is sufficiently small for our purposes, however this subtlety may be worth thinking about as this could reveal an extra friction mechanism due to the wetting phenomenon and surface tension renormalization mentioned in our discussion of the random first order transition in Section II.

While the domain wall positions are not strictly tied to the atomic locations, they *are* tied to the lattice as a continuum and follow the lattice distortions. Let us employ our usual "scalar" phonons descibed by Hamiltonian

$$H_{\rm ph}=\int d^3\mathbf{r}\left[\frac{\pi^2}{2\rho}+\frac{\rho c_s^2(\nabla\psi)^2}{2}\right], \tag{A4}$$

where $[\psi(\mathbf{r}_1),\pi(\mathbf{r}_2)]=i\hbar\delta(\mathbf{r}_1-\mathbf{r}_2)$. The surface energy due to the presence of both Ω and ψ is:

$$H_{surf}=\sigma\int d\phi\int d(\cos\theta)\left\{(R+[\psi-\psi(r_i)]+\Omega)^2+\frac{1}{2}\left[\left(\frac{\partial(\psi+\Omega)}{\partial\theta}\right)^2+\frac{1}{\sin^2\theta}\left(\frac{\partial(\psi+\Omega)}{\partial\phi}\right)^2\right]\right\}, \tag{A5}$$

where ψ is taken on the sphere of radius R with the center located at $\mathbf{r}_i$. The potential energy in Eq.(A5) thus provides an explicit form of phonon-ripplon interaction due to the liquid free energy functional solutions being imbedded in the real space.

If we expand the value of the displacement field ϕ in terms of spherical harmonics according to $\psi_{lm} \equiv \int d\phi d(\cos\theta)\psi(r=R)Y^*_{lm}(\phi,\theta)$, it is then possible to write down equations of motion for the (l,m)-components of both ripplon and phonon displacements:

$$\frac{\partial^2\Omega_{lm}}{\partial t^2}+\omega_l^2\left(\Omega_{lm}+\psi_{lm}\right)=0. \tag{A6}$$

The equation of motion for the phonon field can be obtained e.g. from $\ddot{\psi}=i[H_{\rm ph}+H_{surf},\pi/\rho]$ to yield:

$$\ddot{\psi} - c_s^2 \Delta\psi = -\frac{\sigma}{\rho}\int_0^{2\pi} d\phi' \int_{-1}^{1} d(\cos\theta') \int dr' \delta(r'-R) \left\{ 2(R + [\psi(\mathbf{r}') - \psi(\mathbf{r}_i)]) - \frac{1}{\sin\theta'}\left(\sin\theta' \frac{\partial\psi}{\partial\theta'}\right) \right.$$
$$\left. - \frac{1}{\sin^2\theta'}\left(\frac{\partial^2\psi}{\partial\phi'^2}\right) + \sum_{lm} \Omega_{lm}[2 + l(l+1)] Y_{lm}(\theta', \phi') \right\} \delta(\mathbf{r} - \mathbf{r}'). \quad \text{(A7)}$$

The terms with ψ on the r.h.s. serve only to modify the local elastic constants, and therefore give rise to the regular Rayleigh scattering, so we will ignore them from now on.

Equations (A6-A7) can be used to write down equations of motion for the retarded Green's functions, which are preferable due to their convenient analytical properties (see (Zubarev, 1960) for our conventions). We are interested in the system's response to "plucking" the latice at site $\mathbf{r} = \mathbf{0}$ at time zero, hence the choice of the Green's function corresponding to an operator X: $-i\theta(t-t')\,\langle[X(t), \psi(\mathbf{r}=\mathbf{0}, t'=0)]\rangle$. Eqs.(A6-A7), if rewritten for the corresponding Green's functions, will preserve except there will be an additional term $-\frac{1}{\rho}\,\delta(t)\delta^3(\mathbf{r})$, corresponding to the "plucking" event, in the r.h.s. of Eq.(A7) (note also a change in units). Thus obtained equations are possible to rewrite in the Fourier space:

$$-\omega^2 \widetilde{\Omega}^i_{lm} + \omega_l^2 \left[\widetilde{\Omega}^i_{lm} + \widetilde{\psi}^i_{lm}\right] = 0 \quad \text{(A8)}$$

and

$$-\omega^2\widetilde{\psi}_{\mathbf{k}} + c_s^2 k^2 \widetilde{\psi}_{\mathbf{k}} = -\sum_i \frac{\sigma}{\rho} \sum_{lm} \widetilde{\Omega}^i_{lm}[2 + l(l+1)] \frac{e^{-i\mathbf{k}\mathbf{r}_i}}{2\pi^2} Y_{lm}(-\mathbf{k}/k) i^l j_l(kR) - \frac{1}{(2\pi)^4\rho}, \quad \text{(A9)}$$

where $\widetilde{\psi}^i_{lm} \equiv \int d^3\mathbf{k}\, \widetilde{\psi}_{\mathbf{k}} e^{i\mathbf{k}\mathbf{r}_i} (4\pi) i^l j_l(kR) Y^*_{lm}(\mathbf{k}/k)$ and we used the expansion of a plane wave in terms of the spherical harmonics: $e^{i\mathbf{k}\mathbf{r}} = 4\pi \sum_{l=0}^{\infty} \sum_{m=-l}^{l} i^l j_l(kr) Y^*_{lm}(\mathbf{k}/k) Y_{lm}(\mathbf{r}/r)$. Here, $j_l(x) \equiv \sqrt{\pi/2x}\, J_{l+1/2}(x)$ is the spherical Bessel function, which scales as x^l for small x, hence we see that the ripplons' coupling with the phonons is quadratic or higher order in $\mathbf{k}$ as the second harmonic is the lowest order term allowed. Modes $l = 0$ and $l = 1$ have the meaning of the droplet's growth and translation respectively, as was discussed in Section IV.C. These modes are not covered by this Section's formalism. Even though the theory as a whole could be thought of as a multipole expansion of a molecular cluster interacting with the rest of the lattice, the modes of different orders end up being described by different theories.

The system of Eqs. (A8) and (A9) can now be used to determine the sound dissipation due to the interaction with the ripplons. Since the system is infinite and has a continuous spectrum, all excitations will have finite life-times, which can be, in principle, obtained self-consistently by using e.g. the Feenberg's perturbative expansion (Abou-Chacra *et al.*, 1973; Feenberg, 1948) (one in the end arrives at Green's functions that are well behaved at infinity, as implied in the thus greatly simplified derivation). We do not have to do this self-consistent self-energy determination as long as we are interested in the lowest order estimate, as justified in the end by the smallness of the obtained value of the perturbation. Substituting Eq.(A8) into Eq.(A9) yields

$$-\omega^2\widetilde{\psi}_{\mathbf{k}} + c_s^2 k^2 \widetilde{\psi}_{\mathbf{k}} = (4\pi)^2 \frac{\sigma}{\rho} \sum_i \sum_{lm} \frac{[2 + l(l+1)]\omega_l^2}{\omega_l^2 - \omega^2}$$
$$\times \int \frac{d^3\mathbf{k}_1}{(2\pi)^3} e^{i(\mathbf{k}_1 - \mathbf{k})\mathbf{r}_i} (-1)^l j_l(k_1 R) j_l(kR) Y_{lm}(-\mathbf{k}/k) Y^*_{lm}(\mathbf{k}_1/k_1) \widetilde{\psi}_{\mathbf{k}_1}. \quad \text{(A10)}$$

Since the spatial locations $\mathbf{r}_i$ of active droplets are not

correlated [8], we can replace the summation over the droplets by a continuous integral, assuming at the same time that the ripplon frequency corresponding to ω_l varies from droplet to droplet within a (normalized) distribution $\mathcal{P}_l(\omega)$ centered around ω_l and having a characteristic width $\delta\omega_l$, whose value will be discussed shortly. There is no reason to believe that the frequency and location of the tunneling centers are correlated, therefore one obtains

[8] This is not strictly true - they, of course, can not be on top of each other.

$$-\omega^2\widetilde{\psi}_{\mathbf{k}} + c_s^2k^2\widetilde{\psi}_{\mathbf{k}} \;=\; n\frac{\sigma}{\rho}\sum_l\int d\omega'\mathcal{P}_l(\omega')\frac{4\pi[2+l(l+1)](2l+1)\omega'^2}{\omega'^2-(\omega+i\epsilon)^2}j_l^2(kR)\widetilde{\psi}_{\mathbf{k}}, \tag{A11}$$

where n is the concentration of the active domain walls to be estimated shortly and we have displaced ω by ϵ into the upper half-plane because we are looking for the *retarded* Green's function. Also, in order to derive Eq.(A11), we have used the summation theorem for the spherical functions $P_l(\mathbf{nn}') = \frac{4\pi}{2l+1}\sum_{m=-1}^{l}Y_{lm}^*(\mathbf{n}')Y_{lm}(\mathbf{n})$, as well as $P_l(-1) = (-1)^l$, where P_l is the Legendre polynomial. If we ignore the real part of the r.h.s. of Eq.(A11), responsible only for the dispersion, the poles of the resultant phonon Green's function are found by solving $\omega^2 - c_s^2k^2 + i\,2\omega\tau_\omega^{-1} = 0$, where τ_ω^{-1} clearly has the meaning of the inverse life-time of a phonon of frequency ω and is given by

$$\tau_\omega^{-1} = n\frac{\sigma}{\rho}\sum_{l=2}^{9}\pi^2[2+l(l+1)](2l+1)j_l^2(kR)\mathcal{P}_l(\omega), \tag{A12}$$

where we have ignored the contribution of the peaks centered around $(-\omega_l)$. We remind the reader that $l_{max} \simeq 9$ is dictated by the finite size of a droplet.

One can find the value of $\delta\omega_l$ from an argument identical to the one used in (Xia and Wolynes, 2001a) to obtain the width of the distribution of the barriers for the droplet growth free energy profile. At the glass transition, a liquid breaks up into dynamically cooperative regions, so that a translation of one atom involves moving about 200 atoms around it, which involves overcoming a large (on average) barrier. This barrier's height is determined, together with the domain surface tension coefficient, by the configurational entropy density, which in its turn reflects the number of metastable states available to a particular volume of liquid at this temperature. Even though a good description of freezing is achieved by assuming that this number of available states does not strongly depend on where exactly on the free energy surface a particular molecular cluster is (Xia and Wolynes, 2000), it should vary from domain to domain. The size of the variation can be estimated from the known magnitude of the entropy fluctuations at constant energy, so that the ratio of the variance to the mean is related to the jump in the heat capacity at T_g and subsequently turns out to be $1/2\sqrt{D}$ (Xia and Wolynes, 2001a), where D is the liquid's fragility, entering the Vogel-Fulcher law for relaxation times in a supercooled liquid $\tau_{relaxation} \propto e^{\frac{DT_K}{T-T_K}}$. We conclude then that the lower bound on the fluctuations of the ripplon frequency ω_l is given by $\delta\omega_l \simeq \omega_l/2\sqrt{D}$.

Lastly, in order to use Eq.(A12) to compute the phonon absorption due to this particular mechanism, we need to estimate the density of the active domain walls. It will suffice for our purposes here to consider as active the defects that contribute to the specific heat, that is, roughly, $n \simeq \frac{1}{\xi^3}T/T_g$. A more accurate estimate would be similar to the one we made when calculating the bump in the heat capacity in Section IV.C.

We are now ready to give a numerical estimate of the expression in Eq.(A12). We will compute here the contribution of the $l = 2$ term in the plateau region. It is convenient to represent kR from Eq.(A12) as $kR \sim \frac{\omega}{0.4\,(a/\xi)\omega_D}$. For the reference, $(a/\xi)T_D \sim 0.2T_D$ is at the high temperature end of the plateau, whereas its middle is about an order of magnitude lower depending on the substance (see κ vs. T/T_D plot in Fig.1). We can now use our usual expressions connecting $\sigma, T_g, \omega_D, c_s, \rho, a$ etc to obtain a numerical estimate of Eq.(A12) at the plateau frequencies $\omega_{plateau} \sim 10^{-1.5}\omega_D$. Even if one favorably assumes that $\omega_2 \sim \omega_{plateau}$ (it is somewhat larger according to Section IV.D), one still gets $l_{\rm mfp}/\lambda >\sim 10^4$ at the plateau frequency, whereas the *resonant* absorption by the TLS would give $l_{\rm mfp}/\lambda \sim 10^2$. The amplitude of this type of absorption is small due to the weakness of direct coupling to the ripplons for the processes not accompanied by a change in the domain's internal state.

APPENDIX B: Frequency Cutoff in the Interaction Between the Tunneling Centers and the Linear Strain

As argued in Section III.B, the coupling of the tunneling transition to a phonon can be found from an additional energy cost of moving the molecules within the domain in the presence of a strain and is given by an integral over the droplet's volume (we consider only lon-

gitudinal strain for simplicity):

$$g = \rho c_s^2 \int_V d^3\mathbf{r} (\nabla\vec{\phi})(\nabla\mathbf{d}), \qquad \text{(B1)}$$

where ρc_s^2 is basically the elastic modulus, $\vec{\phi}$ and $\mathbf{d}$ are elastic and inelastic components of the atomic displacements respectively. If the phonon's wave-length is much larger than ξ, the elastic component is constant throughout the integration region and the integral reduces to one over the droplet's surface and thus the g estimate obtained in text. Otherwise, one obtains:

$$g = \rho c_s^2 \left\{ \int_S d\mathbf{S}\,\mathbf{d}\,(\nabla\vec{\phi}) - \int_V d^3\mathbf{r}\,(\mathbf{d}\nabla)(\nabla\vec{\phi}) \right\}. \qquad \text{(B2)}$$

The volume integral will give a higher order term in k, so for now, we focus on the surface integral. The displacement due to the phonon is conveniently expanded it terms of the spherical waves: $e^{i\mathbf{kr}} = 4\pi \sum_{l=0}^{\infty} \sum_{m=-l}^{l} i^l j_l(kr) Y_{lm}^*(\mathbf{k}/k) Y_{lm}(\mathbf{r}/r)$. Since it is the first derivative with respect to $\mathbf{r}$ that we are interested in, we only need the $l = 1$ term from this expansion. The angular part contributes only to the overall constant, but it is the spherical function $j_1(kr)$ that sets the cut-off value of the wave-vector, above which the phonons do not produce significant linear uniform stress on the domain. In Fig.24, we plot the derivative $\partial j_1(x)/\partial x$ (or, rather, we plot the square of it, which enters into all the final expressions).

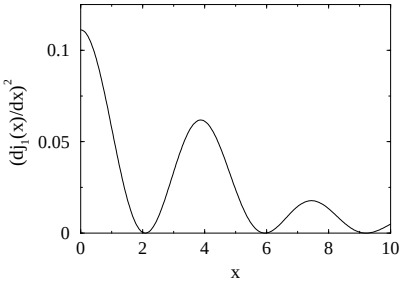


FIG. 24 Shown is the derivative of the 1st order spherical Bessel function determining the effective decrease in the elastic field gradient produced by a phonon of wave-length k ($x = kR$).

We see that it is not unreasonable to assume that only the phonons with $kR <\sim 6$ will exert an appreciable linear strain on the domain. $kR = 6$ translates into $\omega_c \sim 2.5(a/\xi)\omega_D$.

While we are at it, we estimate the interaction of the domain with the higher order strain, at least due to the term (B1), in the frequency region of interest. The next order term in the k expansion in the surface integral from Eq.(B2) has the same structure, but is scaled down from the linear term by a factor of kR. At the plateau frequencies $\sim \omega_D/30$, $kR < 0.5$ as immediately follows from the previous paragraph. While this is not a large number, it is not very small either. Therefore, this interaction term is of potential importance.

The volume integral in Eq.(B2) produces a quadratic term, which is roughly equal to $(\nabla\vec{\phi}) \int_V d^3\mathbf{r}\,(\mathbf{d}\,\mathbf{k})$. We then proceed in a completely identical fashion to our earlier estimate of g. Assuming the diplacements within the droplet are random, one gets for the integral $\frac{1}{4}\sqrt{N^*}\,a^3\,d_L k$, where factor of $1/4$ comes about because the displacement is assumed do decrease from d_L in the center of the droplet to zero at the edge (Lubchenko and Wolynes, 2001). This yields that this term becomes comparable to the linear one at frequencies $\omega \simeq \omega_D \sqrt{(a/\xi)}\, 4/(6\pi^2)^{1/2} \simeq 0.4\,\omega_D$ - well beyond the high T end of the plateu.

We must note, there are other sources of non-linearity in the system, such as the intrinsic anharmonicity of the molecular interactions present also in the corresponding crystals. While these issues are of potential importance to other problems, such as the Grüneisen parameter, expression (B1) only considers the lowest order harmonic interactions and thus does not account for this non-linear effect. We must note that if this non-linearity is significant, it could contribute to the non-univrsality of the plateau, in addition to the variation in T_g/ω_D ratio. It would be thus helpful to conduct an experiment comparing the thermal expansion of different glasses and see whether there is any correlation with the plateau's location.

References

Abou-Chacra, R., P. W. Anderson, and D. J. Thouless, 1973, J. Phys. C **6**, 1734.

Ackerman, D. A., A. C. Anderson, E. J. Cotts, J. N. Dobbs, W. M. MacDonald, and F. J. Walker, 1984, Phys. Rev. B **29**, 966.

Adam, G., and J. H. Gibbs, 1965, J. Chem. Phys. **43**, 139.

Anderson, A. C., 1981, in *Amorphous Solids: Low-Temperature Properties,* W.A.Phillips (ed.) (Springer-Verlag, Berlin, Heidelberg, New York).

Anderson, A. C., 1999, private communication.

Anderson, P. W., B. I. Halperin, and C. M. Varma, 1972, Philos. Mag. **25**, 1.

Angell, C. A., 1985, J. Non-Cryst. Solids. **73**, 1.

Angell, C. A., K. L. Ngai, G. B. McKenna, P. F. Millan, and S. W. Martin, 2000, Appl. Phys. **88**, 3113.

Belanger, D. P., 1998, in *Spin Glasses and Random Fields* (ed.) A. P. Young (World Scientific, Singapore), p. 251.

Belessa, G., 1978, Phys. Rev. Lett. **40**, 1456.

Benassi, P., M. Krisch, C. Masciovecchio, G. Monaco, G. Ruocco, F. Sette, and R. Verbeni, 1996, Phys. Rev. Lett. **77**, 3835.

Bengtzelius, U., W. Gotze, and A. Sjolander, 1984, J. Phys. C: Solid State Physics **17**, 5915.

Black, J. L., and B. I. Halperin, 1977, Phys. Rev. B **16**, 2879.

Böhmer, B., K. L. Ngai, C. A. Angell, and D. J. Plazek, 1993, J. Chem. Phys. **99**, 4201.

Boiron, A.-M., P. Tamarat, B. Lounis, R. Brown, and M. Orrit, 1999, Chem. Phys. **247**, 119.

Bouchaud, J.-P., and G. Biroli, 2004, J. Chem. Phys. **121**, 7347.

Bouchaud, J.-P., and M. Mézard, 1997, J. Phys. A **30**, 7997.

Buchenau, U., V. L. Gurevich, D. A. Parshin, M. A. Ramos, and H. R. Schober, 1992, Phys. Rev. B **46**, 2798.

Burin, A. L., and Y. Kagan, 1996, Sov. Phys. JETP **82**, 159.

Caruzzo, H. M., 1994, *On the Collective Model of Glasses at Low Temperature*, Ph.D. thesis, University of Illinois.

Coppersmith, S. N., 1991, Phys. Rev. Lett. **67**, 2315.

Derrida, B., 1981, Phys. Rev. B **24**, 2613.

Eastwood, M. P., and P. G. Wolynes, 2002, Europhys. Lett. **60**, 587.

Einstein, A., 1911, Ann. Phys. **35**, 679.

Escher, U., S. Abens, A. Gladun, C. Koeckert, S. Sahling, and M. Schneider, 2000, Physica B **284**, 1159.

Feenberg, E., 1948, Phys. Rev. **74**, 206.

Feynman, R. P., 1953, Phys. Rev. **91**, 1291.

Feynman, R. P., 1954, Phys. Rev. **94**, 262.

Foret, M., E. Courtens, R. Vacher, and J.-B. Suck, 1996, Phys. Rev. Lett. **77**, 3831.

Freeman, J. J., and A. C. Anderson, 1986, Phys. Rev. B **34**, 5684.

Galperin, Y. M., V. L. Gurevich, and D. A. Parshin, 1985, Phys. Rev. B **32**, 6873.

Galperin, Y. M., V. G. Karpov, and V. I. Kozub, 1991, Adv. Phys. **38**, 669.

Gamaitoni, L., P. Hanggi, P. Jung, and F. Marchesoni, 1998, Rev. Mod. Phys. **70**, 223.

Geszti, T., 1982, J. Physique **C9**, 481.

Golding, B., and J. E. Graebner, 1976, Phys. Rev. Lett. **37**, 853.

Goubau, W. M., and R. A. Tait, 1975, Phys. Rev. Lett. **34**, 1220.

Graebner, J. E., B. Golding, and L. C. Allen, 1986, Phys. Rev. B **34**, 5696.

Grigera, T. S., V. Martín-Mayor, G. Parisi, and P. Verocchio, 2001, eprint cond-mat/0110129.

Gross, D. J., I. Kanter, and H. Sompolinsky, 1985, Phys. Rev. Lett. **55**, 304.

Gross, D. J., and M. Mézard, 1984, Nucl. Phys. B **240**, 431.

Guttman, L., and S. M. Rahman, 1986, Phys. Rev. B **33**, 1506.

Hall, R. W., and P. G. Wolynes, 2003, Phys. Rev. Lett. **90**, 085505.

Hansen, J. P., and I. R. McDonald, 1976, *Theory of Simple Liquids* (Academic Press, New York).

Heeger, A. J., S. Kivelson, J. R. Schrieffer, and W. P. Su, 1988, Rev. Mod. Phys. **60**, 781.

Heuer, A., and R. J. Silbey, 1993, Phys. Rev. Lett. **70**, 3911.

Horbach, J., W. Kob, and K. Binder, 1999, J. Phys. Chem. **103**, 4104.

Hunklinger, S., W. Arnold, S. Stein, R. Nava, and K.Dransfeld, 1976, Phys. Lett. **42A**, 253.

Hunklinger, S., and A. K. Raychaudhuri, 1986, in *Progress in Low Temperature Physics,* D. F. Brewer (ed.) (Elsevier), volume 9.

Jäckle, J., 1972, Z. Phyzik **257**, 212.

Jäckle, J., L. Piché, W. Arnold, and S. Hunklinger, 1976, J. Non-Cryst. Sol. **20**, 365.

Joshi, Y. P., 1979, Phys. Stat. Sol. (b) **95**, 317.

Karpov, V. G., M. I. Klinger, and F. N. Ignat'ev, 1983, Sov. Phys. JETP **57**, 439.

Kauzmann, W., 1948, Chem. Rev. **43**, 219.

Kirkpatrick, T. R., and D. Thirumalai, 1987a, Phys. Rev. Lett. **58**, 2091.

Kirkpatrick, T. R., and D. Thirumalai, 1987b, Phys. Rev. B **36**, 5388.

Kirkpatrick, T. R., D. Thirumalai, and P. G. Wolynes, 1989, Phys. Rev. A **40**, 1045.

Kirkpatrick, T. R., and P. G. Wolynes, 1987a, Phys. Rev. A **35**, 3072.

Kirkpatrick, T. R., and P. G. Wolynes, 1987b, Phys. Rev. B **36**, 8552.

Kittel, C., 1956, *Introduction to Solid State Physics* (John Wiley & Sons, *Inc.*).

Krause, J. T., and C. R. Kurkjian, 1968, J. Am. Ceram. Soc. **51**, 226.

Landau, L. D., and E. M. Lifshitz, 1980, *Statistical Mechanics* (Pergamon Press).

Landau, L. D., and E. M. Lifshitz, 1986, *Theory of Elasticity* (Pergamon Press).

Landau, L. D., and E. M. Lifshitz, 1987, *Fluid Mechanics* (Pergamon Press).

Lasjaunas, J. C., R. Maynard, and M. Vandorpe, 1978, J. Physique C6 **39**, 973.

Leggett, A., 1999, private communication.

Leggett, A. J., 1991, Physica B **169**, 322.

Leggett, A. J., S. Chakravarty, A. T. Dorsey, M. P. A. Fisher, A. Garg, and W. Zwerger, 1987, Rev. Mod. Phys. **59**, 1.

Lindemann, F. A., 1910, Phys. Z. **11**, 609.

Lubchenko, V., 2002, *Quantum Theory of Glasses*, Ph.D. thesis, University of Illinois.

Lubchenko, V., and P. G. Wolynes, 2000, unpublished.

Lubchenko, V., and P. G. Wolynes, 2001, Phys. Rev. Lett. **87**, 195901.

Lubchenko, V., and P. G. Wolynes, 2003a, Proc. Natl. Acad. Sci. **100**, 1515.

Lubchenko, V., and P. G. Wolynes, 2003b, J. Chem. Phys. **119**, 9088.

Lubchenko, V., and P. G. Wolynes, 2004, J. Chem. Phys. **121**, 2852.

Maynard, R., 1975, in *Phonon Scattering in Solids,* L. J. Challis, V. W. Rampton, and A. F. G. Wyatt (eds.) (Plenum Press).

Meissner, M., and K. Spitzmann, 1981, Phys. Rev. Lett. **46**, 265.

Mézard, M., and G. Parisi, 1999, Phys. Rev. Lett. **82**, 747.

Mézard, M., G. Parisi, and M. A. Virasoro, 1985, J. Physique Lett. **46**, L217.

Mezei, F., 1991, *Liquids, Freezing and the Glass Transition* (Nort-Holland, Amsterdam), p. 629.

Mon, K. K., and N. W. Ashcroft, 1978, Solied State Comm. **27**, 609.

Morse, P. M., and H. Feshbach, 1953, *Methods of Theoretical Physics* (McGraw-Hill), volume 2, p. 1469.

Moynihan, C. T., A. J. Easteal, M. A. Debolt, and J. Tucker, 1976, J. Am. Ceram. Soc. **59**, 12.

Narayanaswamy, O. S., 1971, J. Am. Ceram. Soc. **54**, 491.

Nattermann, T., 1998, in *Spin Glasses and Random Fields* (ed.) A. P. Young (World Scientific, Singapore), p. 277.

Neu, P., D. R. Reichman, and R. J. Silbey, 1997, Phys. Rev. B **56**, 5250.

Nittke, A., S. Sahling, and P. Esquinazi, 1998, Heat Release in Solids, in *Tunneling Systems in Amorphous and Crystalline Solids,* (ed.) P. Esquinazi (Springer-Verlag, Heidelberg).

Novikov, V. N., and A. P. Sokolov, 2004, Nature **431**, 961.

Papoular, M., 1972, J. Phys. C **5**, 1943.

Perry, S., 2004, private communication.

Pfaender, H. G., 1996, *Schott Guide to Glass* (Chapman & Hall).
Phillips, W. A., 1972, J. Low Temp. Phys. **7**, 351.
Phillips, W. A., 1973, J. Low Temp. Phys. **11**, 757.
Phillips, W. A. (ed.), 1981, *Amorphous Solids: Low-Temperature Properties* (Springer-Verlag, Berlin, Heidelberg, New York).
Pilla, O., A. Cunsol, A. Fontana, C. Masciovecchio, G. Monaco, M. Montagna, G. Ruocco, T. Scopigno, and F. Sette, 2000, Phys. Rev. Lett. **85**, 2136.
Plazek, D. J., and J. H. Magill, 1968, J. Chem. Phys. **49**, 3678.
Pohl, R. O., 1981, in *Amorphous Solids: Low-Temperature Properties,* W.A.Phillips (ed.) (Springer-Verlag, Berlin, Heidelberg, New York).
Pohl, R. O., X. Liu, and E. Thompson, 2002, Rev. Mod. Phys. **74**, 991.
Raychaudhuri, A. K., and R. O. Pohl, 1981, Phys. Rev. B **25**, 1310.
Reynolds, Jr., C. L., 1979, J. Non-Cryst. Sol. **30**, 371.
Reynolds, Jr., C. L., 1980, J. Non-Cryst. Sol. **37**, 125.
Richert, R., and C. A. Angell, 1998, J. Chem. Phys. **108**, 9016.
Russel, E. V., and N. E. Israeloff, 2000, Nature **408**, 695.
Sahling, S., S. Abens, and T. Eggert, 2002, J. Low Temp. Phys. **127**, 215.
Schmalian, J., and P. G. Wolynes, 2000, unpublished.
Silescu, H., 1999, J. Non-Cryst. Sol. **243**, 81.
Simon, F., 1937, Trans. Faraday Soc. **33**, 65.
Singh, Y., J. P. Stoessel, and P. G. Wolynes, 1985, Phys. Rev. Lett. **54**, 1059.
Smith, T. L., 1974, Ph.D. thesis, University of Illinois.
Stevenson, J., and P. G. Wolynes, 2004, unpublished.
Stillinger, F. H., 1988, J. Chem. Phys. **88**, 7818.
Stoessel, J. P., and P. G. Wolynes, 1984, J. Chem. Phys. **80**, 4502.
Strehlow, P., and M. Meissner, 1999, Physica B **263-264**, 273.
Thompson, E., G. Lawes, J. M. Parpia, and R. O. Pohl, 2000, Phys. Rev. Lett. **84**, 4601.
Tool, A. Q., 1946, J. Am. Ceram. Soc. **29**, 240.
Trachenko, K., M. T. Dove, M. J. Harris, and V. Heine, 2000, J. Phys.: Condens. Matter **12**, 8041.
Tracht, U., M. Wilhelm, A. Heuer, H. Feng, K. Schmidt-Rohr, and H. W. Spiess, 1998, Phys. Rev. Lett. **81**, 2727.
Vegge, T., J. P. Sethna, S.-A. Cheong, K. W. Jacobsen, C. R. Myers, and D. C. Ralph, 2001, Phys. Rev. Lett. **86**, 1546.
Villain, J., 1985, J. Physique **46**, 1843.
Wei, S., C. Li, and M. Y. Chou, 1994, Phys. Rev. B **50**, 14587.
Wischnewski, A., U. Buchenau, A. J. Dianoux, W. A. Kamitakahara, and J. L. Zarestky, 1998, Phys. Rev. B **57**, 2663.
Wittmer, J. P., A. Tanguy, J.-L. Barrat, and L. Lewis, 2001, eprint cond-mat/0104509.
Wolynes, P. G., 1981, Phys. Rev. Lett. **47**, 968.
Wolynes, P. G., 1992, Acc. Chem. Res. **25**, 513.
Xia, X., and P. G. Wolynes, 2000, Proc. Natl. Acad. Sci. **97**, 2990.
Xia, X., and P. G. Wolynes, 2001a, Phys. Rev. Lett. **86**, 5526.
Xia, X., and P. G. Wolynes, 2001b, J. Phys. Chem. **105**, 6570.
Yu, C. C., and A. J. Leggett, 1988, Comments Cond. Mat. Phys. **14**, 231.
Zaitlin, M. P., and A. C. Anderson, 1975, Phys. Rev. B **12**, 4475.
Zeller, R. C., and R. O. Pohl, 1971, Phys. Rev. B **4**, 2029.
Zubarev, D. N., 1960, Sov. Phys. Uspekhi **3**, 320.